2003

# Influence of Stress Relaxation on Watertight Integrity of Hybrid Bolted Joints

Keith N. Pelletier

# INFLUENCE OF STRESS RELAXATION ON WATERTIGHT INTEGRITY OF

# HYBRID BOLTED JOINTS

By

Keith N. Pelletier

B.S. University of Maine, 1998

A THESIS

Submitted in Partial Fulfillment of the

Requirements for the Degree of

Master of Science

(in Mechanical Engineering)

The Graduate School

The University of Maine

December, 2003

Advisory Committee:

Vincent Caccese, Associate Professor of Mechanical engineering

Donald Grant, Richard C. Hill Professor and Chair of Mechanical Engineering

Senthil Vel, Assistant Professor of Mechanical Engineering

# INFLUENCE OF STRESS RELAXATION ON WATERTIGHT INTEGRITY OF

# HYBRID BOLTED JOINTS

By Keith N. Pelletier

Thesis Advisor: Dr. Vincent Caccese

An Abstract of the Thesis Presented
in Partial Fulfillment of the Requirements for the
Degree of Master of Science
(in Mechanical Engineering)
December, 2003

Stress relaxation and creep are major concerns when loading composite materials. Due to the viscoelactic nature of the matrix material, composite materials tend to lose initial loads at a decreasing rate. This is especially true through the thickness of the material, where the behavior of the material is dominated by the matrix.

Of particular interest to the current study presented in this thesis is the investigation of stress relaxation in bolted composite/metal hybrid connections. It is ultimately desired to be able to use bolted composite/metal hybrid connections for naval applications, where it is important to maintain as much of the initial preload in the connection as possible in order to maintain watertight integrity. In order to quantify the stress relaxation in bolted hybrid connections, it was decided to study the connections at a sub-component level. Several different effects were studied in the connections, including reloading effects, possible advantages of using tapered head bolts, and environmental effects. All tests were run for a time period of at least 3-month in order to get an estimate

of long-term stress relaxation effects in the bolted connections. Test results showed that the load curves could be fit to a power law equation using the method of least squares. Reloading tests showed that some of the preload in the connections could be maintained with periodic retightening of the bolts. The tests also showed a large temperature dependence in the connections that were reloaded multiple times. Connections that are reloaded can maintain more of their initial preload, but are extremely sensitive to temperature shift, even small shifts of only 5 degrees Fahrenheit. Temperature shifts cause the connections to move at a much greater stress relaxation rate. In general, reloading the connections will help the connections to maintain their initial preloads, but great care has to be taken to avoid any temperature changes in the connections.

Tapered head bolts were tested in some connections and compared to results obtained from non-tapered head bolts. Little to no advantage was seen when using tapered head bolts over non-tapered head bolts. The connections using tapered head bolts had roughly the same stress relaxation rate as the connections using non-tapered head bolts.

Environmental testing has recently been started on the hybrid connections, and results are not yet available. Pilot tests were inconclusive, as they were run at 150 degrees Fahrenheit, and thus thermal expansion effects are indistinguishable from stress relaxation effects. Moisture also may have gotten into the gaged bolts and effected the pilot test results. The environmental tests should provide an accurate description of what happens to the bolted hybrid connections in naval applications. Once completed, environmental test results will be presented to the project sponsor.

# ACKNOWLEDGMENTS

I would like to thank Dr. Vincent Caccese for involving me in this project. I would also like to thank him for helping me prepare this thesis.

I would like to thank the other members of my committee, Dr. Donald Grant and Dr. Senthil Vel, for taking the time to read my thesis and for helping me to further my education.

I would like to thank research assistant Keith Berube, former graduate student Michael Boone, and former research assistant Randy Bragg for helping me during various stages of the project.

I would also like to thank the various undergraduates who have worked on the project manufacturing and cutting panels, and various other minor tasks.

Most of all, I would like to thank my family who have continued to support me throughout my life and have driven me to further my education. This would not have been possible without them.

# TABLE OF CONTENTS

iv

# LIST OF TABLES

# LIST OF FIGURES

# Chapter 1

## 1. INTRODUCTION

The main objective of the MACH (Modular Advanced Composite Hull-form) project is to develop and test hybrid metal/composite connections to be used for Naval applications. The primary motivation for this project is to challenge conventional hull construction techniques and conventional hull forms. Current hull construction techniques have made it difficult to build and maintain complex shapes for military vessels in a cost efficient manner. Current construction techniques have also limited submarines to cylindrical shapes that are costly to reconfigure for new roles.

The major effort of the MACH project is to develop a metallic supporting structure connected to composite structural sections. In addition to enabling advanced hull shapes, MACH is also expected to decrease system weight. Decreased weight should lead to faster and more efficient vessels. Also, due to the modularity of the system, access to the hull would be greatly improved. If the panels are designed to be removable, this would enable easier access for maintenance of weapons and exchanging equipment for mission specific tasks. Several different connection methods have been and are currently being examined for the project, including adhesive bonding, embedded metallic inserts, and bolted connections. Bolted connections, in particular would provide easily removable panels.

Bolted connections present a problem, however, in that composites tend to creep over time, due to the viscoelastic nature of the matrix material. This creep leads to stress

relaxation and potential loss of preload in bolted connections. In order to maintain watertight integrity in the bolted connections, it is desired to minimize the amount of stress and load relaxation in the bolts, and to maintain as much of the initial preload as possible. It is the goal of this thesis to study the important parameters that govern stress relaxation in bolted composite/metal hybrid connections. In this way, cost effective reliable connections can be designed.

## 1.1. Objectives

The objective of this effort is to quantify the stress relaxation of transversely compressed composites in bolted aluminum/vinylester hybrid connections, when used where watertight seals are required. It is proposed to study bolted hybrid connections at a sub-component level, so as to isolate the effects of viscoelastic creep on the stress relaxation of the bolt. Research is proposed to study the effects of the following:

1. Effects of stress distribution,

2. Effects of re-applying torque to the bolted connections,

3. Varying thickness on the constituents,

4. Temperature/Moisture Effects,

5. Varying bolt size, and

6. Effects of tapered vs. standard bolts.

2

## 1.2. Literature Review

Composite materials offer several advantages over metals; for example, they weigh less and have improved corrosion resistance. There are however some disadvantages to using composites as well. One disadvantage is the viscoelastic creep of the material, which can lead to stress relaxation in bolted connections. The purpose of this literature review is to investigate research on the creep response of composite laminates, stress relaxation in general, and stress relaxation in bolted connections.

### 1.2.1. General Creep Response

Creep in a material is defined as a slow continuous deformation of the material under a constant stress. Creep can be separated into 3 different stages. These three stages are shown in Figure 1.1.
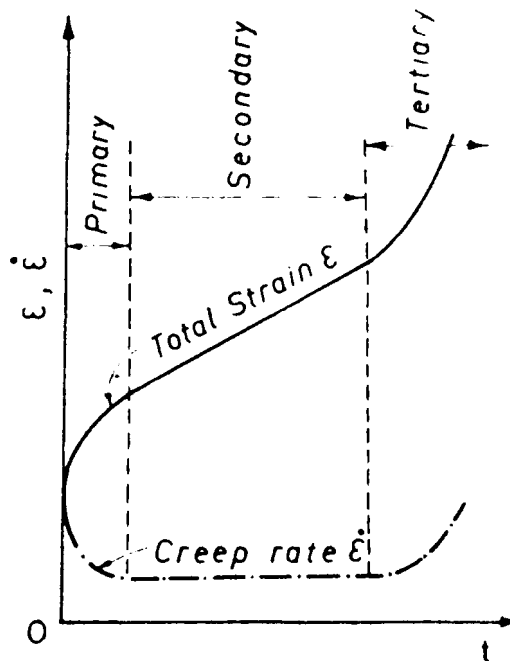


**Figure 1.1 – Three Stages of Creep [Findley et al, 1976]**

3

The first stage, primary creep, is where creep starts out rapid and decreases over time. The second stage proceeds at a nearly constant rate, and is known as secondary creep. The third and final stage, called tertiary creep, occurs at an increasing level, and ends in fracture.

Creep in composites is due primarily to the viscoelasctic nature of the resin used in infusing the composite. While not the sole factor responsible for the creep in composites, the matrix of the material is the largest contributing factor. Factors to consider when determining the creep in a composite are the fibers used, temperature, and humidity.

Shen et al [1998] made observations of viscoelastic creep at a marred polymer surface by utilizing a scanning probe microscope. The material utilized was an Acrylic Polyol/HDI Timer coating deposited on an aluminum substrate. The marring on the surface was done with a diamond tip, at five different normal force levels, 68, 133, 190, 257, and 325 micro Newtons. Utilizing the scanning probe microscope, they were able to observe the surface of this material either partially or completely recover due to creep effects. Images of the surface were taken starting at 15 minutes after the marring, and then taken continuously at increasing periods of 10 minutes, 20 minutes, and 30 minutes for a time frame of 6 hours.

It was discovered that there was a recoverable and unrecoverable aspect of the surface marring. The recoverable part was dominated by the viscoelastic creep rate, and was constant throughout the range of forces used to mar the surface, i.e. the depth of the marring. This creep rate is determined by several factors such as the components of the polymer, temperature, and humidity. The unrecoverable plastic deformation was

dependent on the forces used during marring. The surface became more and more

permanently deformed as the marring force was increased.

Another interesting find from these tests was that the viscoelastic creep in this

composite is extremely sensitive to water. Immersion in water greatly accelerated the

recovery of the surface due to creep. A test was run where the results were looked at

after 5 minutes, and the marred surface had recovered dramatically vs. a test that was

done out of water.

The orthotropic rate independent behavior of polymeric composites was described

by Sun and Chen using a plasticity model based on a one-parameter potential function.

This is given by:

$$2f(\sigma_{ij}) = \sigma_{22}^2 + 2a_{66}\sigma_{12}^2, \qquad (1.1)$$

where the $\sigma$'s are stresses, the subscripts 1 and 2 refer to the fiber and transverse

directions, and $a_{66}$ is an unknown parameter determined from experimental results [Kim

and Sun, 2002]. This lead to the rate dependent non-linear behavior in polymeric

composites being modeled using viscoplasticity models. Zhu and Sun studied the loading

and unloading of IM7/5260 carbon-epoxy composite under different rates of loading and

unloading. It was discovered that stress decreased with time during the loading cycle

when loading was kept at a constant strain level, while stress increased over time during

the unloading cycle at a constant strain rate [Kim and Sun, 2002].

Kim and Sun [2002] used this information to study and model stress-relaxation

and stress recovery in thermoplastic composite AS4/PEEK. The tests were performed at

room temperature using an MTS machine in displacement control mode controlled by an Instron 8500 digital controller. Specimens were loaded at a given strain rate to the desired strain level and held at that level for 1,000 seconds. Stress relaxation data was recorded during this period. Stress recovery tests during the unloading were performed in a similar manner at the same strain levels. The strain rates used were 0.00001/s, 0.0001/s, and 0.01/s. Off-axis coupons were used during these tests of 20, 30, and 45 degrees. Accordingly, they were able to show that the equilibrium stress-strain curves for both loading and unloading were basically the same. A one-parameter plastic potential function was very accurate in describing the behavior of the composite during loading and unloading. It was also found that the relaxation behavior in the composite during the loading and unloading are similar. At a given strain rate, the relaxation curve during loading was almost identical to the recovery curve during unloading.

### 1.2.2. Creep Response in the Fiber Direction

Creep response in the fiber direction of composites is dependent on several factors. Creep in this direction is primarily dictated by the matrix of the material, and its viscoelastic properties. The type of fiber used, and the volume fraction of the fibers also contribute to the creep properties of a composite material.

Kim and McMeeking [1994] performed testing on creep in composite materials in the fiber direction. They found that the matrix followed the following power law creep:

$$\dot{\varepsilon}_{ij} = \frac{3}{2}\dot{\varepsilon}_0 \left(\frac{\bar{\sigma}}{\sigma_0}\right)^{n-1} \frac{s_{ij}}{\sigma_0}, \qquad (1.2)$$

where $\dot{\varepsilon}_{ij}$ is the strain rate, $s_{ij}$ is the deviatoric stress, denoted by:

$$s_{ij} = \sigma_{ij} - \sigma \delta_{ij},$$  (1.3)

$\bar{\sigma}$ is the effective stress, given by

$$\bar{\sigma} = \sqrt{\frac{3}{2} s_{ij} s_{ij}},$$  (1.4)

and $\sigma_0$ and $\varepsilon_0$ are material constants. These tests were based on previous work done by McMeeking [Kim and McMeeking, 1994]. Kelly and Street [Kim and McMeeking, 1994] developed a power law creep model of composites in the fiber direction. McMeeking further developed this model by analyzing the matrix flow field in much greater depth [Kim and McMeeking, 1994]. Kim and McMeeking [1994] showed that when there is no slip or interface mass transport, the composite will have a high creep strength compared to the matrix material alone. The creep strength, $S$, is defined as the ratio of the stress in the composite material divided by the stress in the pure matrix at the same strain rate.

$$S = \frac{\sigma_a}{\sigma_0} \left( \frac{\varepsilon_0}{\varepsilon} \right)^{1/n}.$$  (1.5)

Once slipping or interface mass transfer occurs, however, either separately or together, they can greatly reduce the creep strength of the composite. If either or both occur

rapidly, it can reduce the effective creep strength to below that of the matrix material alone.

Raghazan and Meshii [1997] performed studies on the long-term deformation and strength of carbon-composites using short–term test data obtained for accelerated testing conditions such as higher temperature, stress, and humidity. Continuous carbon fiber reinforced polymer composite (AS4/3501-6) and the epoxy (3501-6) were used to test creep. Five different fiber orientations of the composite were tested, [0], [10], [30], [60], and [90]. The [0], [10], [30], and [60] orientations are made from eight plies each, while the [90] laminate was made from 16 layers. They found that the creep in the composite and its epoxy matrix increases with increases in stress, temperature, and time. The composite was discovered to be highly non-linear in behavior, and that this non-linearity increased with increases in temperature. Results also show that the slope of the compliance curves changes with changes in stress and temperature. This indicates that the non-linearity in the composite may increase with time as well. Their results indicate that the composite is a non-linear material, or is thermo-rheologically complex in behavior.

By comparing the results from creep test on the epoxy with that of the different composite lay-ups, it was found that the creep acceleration and magnitude of strain is reduced by the fibers of the composites. It was also shown, through a comparison of the tensile and shear creep, that the creep of the composite subjected to in-plane shear loading in higher than that subjected to tensile loading.

Maksimov and Plume [2001] researched creep effects as it pertains to using different fiber material in the composite. This study involved examining the creep in the

fiber direction of both Aramid and glass FPR (fiber-reinforced plastics). Since the creep was studied in the fiber direction, it was influenced more by the fibers than creep in the transverse direction. They kept the volume fraction of fibers in the composite plates the same, 0.5, and then varied the ratio between the aramid and glass fibers. The following ratios of aramid fibers to glass fibers were used: 0.5/0, 0.4/0.1, 0.29/0.21, 0.18/0.32, 0.1/0.4, and 0/0.5. These tests were run for a period of 5.7 years and all began at a stress level of 700 MPa. What they discovered was that the pure glass FPR showed very little creep, while the pure aramid FPR showed a much greater creep over the same time period. The plates that were made from mixtures of glass and aramid fibers showed increased creep as the volume fraction of aramid fibers increased. It can thus be concluded that the partial replacement of aramid fibers with glass ones makes it possible to reduce the creep behavior of the composites.

### 1.2.3. Creep Response in E-glass/Vinylester Composites

Scott and Zureick [1998] performed long-term testing on pultruded e-glass/vinylester composite under longitudinal compressive loading. These experiments were conducted at three different stress levels for a time period of up to 10000 hours. The three stress levels used were 65 MPa, 129 MPa, and 194 MPa. These levels corresponded to 20 %, 40 %, and 60 %, respectively, of the average value of ultimate compressive stress of short term tests performed using ASTM D3410 compression testing.

Scott and Zureick modeled their experimental results using the power law developed by Findley. The simplest form of power law creep is given as:

9

$$\varepsilon(t) = \varepsilon_0 + mt^n, \qquad (1.6)$$

where $\varepsilon(t)$ is the total time-dependent creep strain, $\varepsilon_0$ is the stress-dependent and

temperature-dependent initial elastic strain, $m$ is a stress-dependent and temperature-

dependent coefficient, $n$ is a stress-independent material constant, and $t$ is the time after

loading [Scott and Zurieck, 1998]. The constants, m and n, are found from the

experimental data by rearranging equation (1.6) and taking the natural log of both sides:

$$\log[\varepsilon(t) - \varepsilon_0] = \log(m) + n\log(t). \qquad (1.7)$$

Plotting the data on logarithmic scales results in a straight line, where the intercept at $t =$

1 hour yields the value of $m$, while the slope of the line is the value of $n$. From the

experimental data, they were able to develop a design equation for estimating the long-

term longitudinal elastic modulus $E_L(t)$ for FRP composite materials manufactured using

the pultrusion process with glass fiber reinforcement primarily in the longitudinal

direction and a matrix similar to Derakane 411™. They found $E_L(t)$ to be as follows:

$$E_L(t) = \frac{E_L^0}{1 + \dfrac{E_L^0}{E_t}(8760t)^n}, \qquad (1.8)$$

where $E_L^0$ is an initial longitudinal elastic modulus, $E_t$ is the time dependent component,

and $t$ is in hours.

### 1.2.4. Stress Relaxation due to Creep in Bolted Connections

Creep response in the direction perpendicular to the fibers is almost entirely dictated by the matrix of the composite. In bolted connections, this will cause a phenomenon called stress relaxation. Since, in bi-directional laminates, the matrix is not reinforced in this direction, its creep resistance is not greatly increased by the superior E-glass fiber properties. The creep in the through the thickness direction is what is typically experienced by bolted composite connections.

A composite bolted in the thickness direction is highly susceptible to preload loss, due to the viscoelastic nature of the resin, which dominates the transverse direction. If there is significant loss of preload due to creep, then the extent of total preload loss during the life of the joint must be established to determine whether the connection is adequate for the desired use.

Weerth and Ortloff [1986] did extensive studies of bolted composite connections for use in military vehicles. In their tests, they sandwiched an E-glass/Vinylester hollow cylinder composite between 2 washers. Figure 1.2 shows the experimental setup that they used. The loss in preload over time was read through the use of washer load cells and a computer controlled data acquisition system.

Tests were run for periods of 1 day, 1 month, 1 year, 5 years, and 10 years. Preload losses for those time periods were 15, 28, 36, 41, and 43 %, respectively. They found the resulting load data fit a power law form, and were able to predict the preload loss with using a power law equation as follows:

$$P_{ir} = P_i t^{(1.482 \cdot 10^{-11} P_i^{2.244} - 0.0497)}, \qquad (1.9)$$
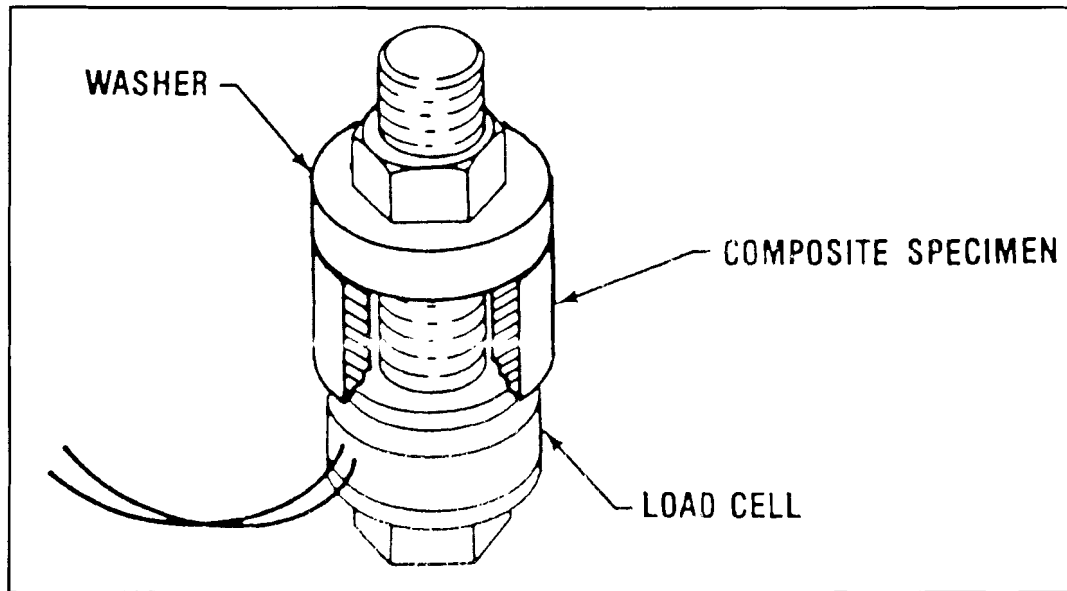
**Figure 1.2 – Bolted Composite Connection used by Weerth and Ortloff [1986]**

where $P_{ir}$ is the load in the connection at any time, $P_i$ is the initial preload, and $t$ is the time in hours.

Adding stitching through the thickness of a composite can used in bolted connections improve its creep resistance. Pang and Wang [1999] studied the effects of through the thickness stitching on the creep resistance of a carbon/glass fiber/epoxy composite material. The composite was made up of 5 layers of bi-directional carbon fiber cloth sandwiched between two layers of bi-directional E-glass cloth. The matrix used was an epoxy resin under the designation of EPOCAST 50-A/946. Three types of threads were tested to determine whether low strength thread has the same effect as high strength thread. The thread used in the tests was a cotton yarn (Tex = 300), a carbon yarn 9Tex = 200), and a thick carbon yarn (Tex = 800). In addition, two stitch densities were considered. Spacing the stitching rows at 5 mm pitch produced high density stitching.

Low density stitching was achieved using a row pitch of 10 mm. The composite was

fabricated using a standard wet lay-up. This involves working the resin into the fiber

manually using a stiff bristle brush, placing peel ply on the preform, and pressing it

between two steel plates. Pang and Wang [1999] came to several conclusions based on

their results. They found that stitching in the loading direction was very effective in

reducing the creep rate. Out of the three fibers, the 800 Tex carbon fiber was the most

efficient in reducing the creep response, followed by the 200 Tex carbon, and the 300

Tex cotton. They also found that the density of the stitching plays effects the creep rate,

with the smaller stitch pitch resulting in more effective stitching and lowered creep

response.


### 1.2.5. Temperature, Humidity, and Environment Effects on Creep

Chen and Kung [2002] evaluated the hygrothermal sensitivity of bolted composite

joints. A double-lap T300/5205 composite joint with steel bolt, a lay-up of $[\pm45/0_2]_{2s}$,

and a thickness of 6.7 mm was used for the numerical approach. This was compared to

experimental results from IM7/8552 specimens. The bolted connection was studied

through the matrix dominated thickness direction. Both the numerical results and the

experimental results showed that the clamp-up torque on the bolted connection was

extremely sensitive to changes in temperature and humidity.

In order to simplify the model, only a single bolted composite joint was

considered. The connection consisted of a plate of composite bolted through the center

of the plate. Washers of varying thicknesses were used on either side to sandwich the

composite and provide a relatively uniform loading condition. The following 5 assumptions were made in order to simplify the model.

1. Linear theory is applied to the bolt axial 1-D case,

2. The washers enable stress between them and the laminate to be treated as uniform,

3. The stress in each layer of the composite is considered uniform through the thickness,

4. Stress relaxation/creep is ignored, and

5. Temperature and humidity effects act independently of each other.

From this analysis, Chen and Kung [2002] concluded that hygrothermal sensitivity was a large factor when dealing with bolt clamping force. They also found that the washer to bolt diameter ratio was the major geometrical factor when designing a composite joint. They went on to say that long-term effects such as stress relaxation and creep could be studied to provide further design guidelines as they pertain to the hygrothermal sensitivity of bolted composite connections.

Guedes et al [2000] investigated the long-term behavior of composite materials. The long-term behavior of composites can be influence by both physical and chemical aging. The resin and the interface between the fiber and resin are the elements that influence the time dependant properties of the composite the most. They performed creep and creep recovery, relaxation and ramp loading tests on a T300/5208 laminate at room temperatures. A time period of about 14 months was used in the testing.

Guedes et al [2000] also further investigated the environmental factors coupled with the mechanical loading of a composite. They used a quasi-unidirectional glass/epoxy composite for these groups of tests. The material was tested at 75 degrees Celsius, at several different humidity levels (0 %, 24 %, 34 %, 73 %, and 92 % relative humidity). Two different exposure times were used, 1600 hours and 3100 hours. They found that the stress-strain response was completely reversible after the absorption/desorption cycle, suggesting no microstructural damage was done. They further found that the quasi-static mechanical response was very dependent on exposure time.

### 1.2.6. Methods of Measuring Creep and Stress Relaxation

ASTM standards contain a few methods of measuring both creep and stress relaxation. Testing can be performed in tension, compression, bending, and torsion, depending on which load case is closest to actual application. Of particular note are ASTM F1276-99, ASTM D2990-01, and ASTM E 328-02.

ASTM F 1276-99 describes a method to test the creep relaxation of laminated composite gasket material. A compressive stress is applied to the material between two platens. The stress is applied using a nut and bolt. The relaxation is measured using a dial indicator. The dial indicator is set to zero when no load is applied to the bolt. The bolt is then tightened to the desired stress level and a reading is taken $(D_0)$. The dial indicator is then removed, and the specimen fixture is then placed in an oven for 22 hours at $100 \pm 2$ °C. The fixture is then cooled to room temperature, and the dial indicator is

reattached and zeroed. The nut is loosened and a reading is taken with the dial $(D_f)$. The percent relaxation is then calculated by:

$$relaxation, \% = [(D_0 - D_f)/D_0] \times 100. \qquad (1.10)$$

ASTM D 2990-01 Gives methods for testing tensile, compressive, and flexural creep and creep-rupture of plastics. The method consists of applying the desired load , and then measuring the extension or compression of the specimen at specific time intervals of 1, 2, 12, and 30 minutes, 1, 2, 5, 20, 50, 100, 200, 500, 700, and 1000 hours. Temperature and relative humidity is also recorded during testing to monitor environmental factors. Strain is reported for tension or compression tests by dividing the extension or compression at given times by the initial gage length. Maximum strain at the midspan is calculated for flexural tests.

ASTM E 328-86 provides methods of testing stress relaxation in materials under tension, compression, bending, and torsion loads. The testing requires the specimens to be subjected to an increasing load till the desired initial strain is attained. Once the initial load is reached, the specimen is constrained, and the initial stress can be calculated from the initial load. Load readings are continuously taken for the duration of the test. Plots are then made of the stress over time.

Stain gages may be used to measure the strain in the specimen over time during experimentation, but they present problems when working with plastics. The major concerns are local heating due to the current in the gage, and the difficulty in aligning the axis of the gage so that different components of the strain are completely separated. Strain gages are also a concern in long-term testing due to creep of the adhesive used to

bond the gage to the specimen. For these reasons, using an extensometer is usually the best way to measure the strain during creep tests.

### 1.2.7. Analytical Creep Models

Several methods have been used over the years to model the creep behavior of materials. Andrade [Findley et al, 1976] studied the creep of lead wires under constant load, and developed the first creep law as follows:

$$l = l_0(1 + \beta t^{1/3})e^{kt}, \qquad (1.11)$$

where $l_0$ and $l$ are initial and current lengths of the specimen, $t$ is the time under load, and $\beta$ and $k$ are stress dependent constants.

Steady state creep, in particular, has been studied in great detail. Bailey and Norton [Findley et al, 1976]developed an empirical equation to describe steady state creep under low stresses,

$$\dot{\varepsilon} = k\sigma^p, \qquad (1.12)$$

where $\dot{\varepsilon}$ is the steady state creep, $\sigma$ is the applied stress, and $k$ and $p$ are material constants. This equation is known as the power law or Norton creep law. Ludwik [Findely et al, 1976] proposed an exponential law to describe the steady state creep, given by

$$\dot{\varepsilon} = ke^{\sigma/\sigma^+}, \qquad (1.13)$$

where $k$ and $\sigma^+$ are both material constants. This equation, however predicts a finite strain rate when the stresses vanish, whereas equation (1.12) predicts it to be zero. To resolve this, Soderberg [Findley et al, 1976] proposed the following equation

$$\dot{\varepsilon} = c(e^{\sigma/\sigma^+} - 1), \qquad (1.14)$$

where $c$ and $\sigma^+$ are material constants.

Creep in polymers has also been examined at great length. Leaderman [Findley et al, 1976] found the following relationship for the creep of bakelite under constant torque:

$$\varepsilon = \varepsilon^0 + A\log t + Bt, \qquad (1.15)$$

where $\varepsilon^0$, $A$, and $B$ are functions of stress, temperature, and material. Phillips [Findley et al, 1976] found that creep could be described by:

$$\varepsilon = \varepsilon^0 + A\log t, \qquad (1.16)$$

if the strain rate goes to zero as $t$ approaches infinity. The power law found by Findley[Findley et al, 1976], and given in equation (1.6) yields very good agreement to experimental results, over most other models. This is due in part to the fact that the creep

18

of polymers starts at a very rapid rate after loading, and then proceeds at a decreasing rate. Findley's model accurately describes this behavior, whereas equations (1.15) and (1.16) do not. For this reason, Findley's creep model is often used to describe creep of most plastics.

**Chapter 2**

## 2. TEST OVERVIEW AND FIXTURES

Discussed in this section are a series of tests conducted to study the effects of

stress relaxation on E-Glass/Vinylester composite/aluminum hybrid connections. One

group of tests is performed utilizing a compression block fixture to quantify the stress

relaxation of the composite laminate in the transverse direction while being subjected to a

relatively uniform stress state through the thickness of the composite material. Another

group of tests is performed to study the effects of stress concentrations and retorquing of

bolts on stress relaxation response using a single bolt test article. A third group of tests is

done to study effects of tapered bolts versus non-tapered bolts, also on a single bolt test

article. A fourth group of tests is performed to study the effects of temperature and

humidity on a single bolt aluminum/composite hybrid connection. All test specimens

were cut from E-glass/Vinylester composite panels, fabricated at the University of Maine

Crosby Laboratory, using a VARTM (Vacuum Assisted Resin Transfer Molding)

process. All tests were run for a period of at least 3 months to study initial stress

relaxation effects.

### 2.1. Test Methodology

A summary of the tests performed in this study is given in the test matrix shown

in Table 2.1. Tests include a compression series, where the composite material alone is

studied at two different preload levels of 10,000 and 5,000 pounds, as summarized in

## Table 2.1 - Test Matrix

2.1a

|  | 1/2 inch | | |
|---|---|---|---|
| Compression Block | Preload (lbs) | Stress (psi) | # of Tests |
|  | 10000 | 2500 | 1 |
|  | 5000 | 1250 | 1 |

2.1b

|  |  | Panel Thickness | | | | | | | | | |
|---|---|---|---|---|---|---|---|---|---|---|---|
|  |  | 1/2 inch | | | | 3/4 inch | | 1 inch | | | |
|  | tightening cycle | Preload (lbs) | # of tests | Preload (lbs) | # of tests | Preload (lbs) | # of tests | Preload (lbs) | # of tests | Preload (lbs) | # of tests |
| Single Bolt, Reloading, caphead bolt test | no reloading | 5000 | 2 | 2500 | 1 | 10000 | 2 | 15000 | 1 | 7500 | 1 |
|  | 3 days | 5000 | 2 | 2500 | 1 | 10000 | 2 | 15000 | 1 | 7500 | 1 |
|  | 1 week | 5000 | 2 | 2500 | 1 | 10000 | 2 | 15000 | 1 | 7500 | 1 |
|  | 2 weeks | 5000 | 2 | 2500 | 1 | 10000 | 2 | 15000 | 1 | 7500 | 1 |
|  | 3 days twice | 5000 | 2 | 2500 | 1 | 10000 | 2 | 15000 | 1 | 7500 | 1 |
|  | 3 days thrice | 5000 | 2 | 2500 | 1 | 10000 | 2 | 15000 | 1 | 7500 | 1 |

2.1c

|  |  | 3/4 inch | |
|---|---|---|---|
| Single Bolt, tapered vs. caphead bolts | Preload (lbs) | tapered | caphead |
|  | 10000 | 3 | 1 |
|  | 5000 | 2 | 2 |

2.1d

|  |  | 3/4 inch | |
|---|---|---|---|
| Environmental Tests using caphead bolts | Conditioning Cycle | Preload (lbs) | # of tests |
|  | Control at C3 | 10000 | 1 |
|  | C1, tighten, C2 | 10000 | 1 |
|  | C1, tighten, C3 | 10000 | 1 |
|  | Tighten, creep for 1 week at C3, then C2 | 10000 | 1 |
|  | Tighten, C2 for 1 month, C3 for 1 month, then repeat | 10000 | 1 |
|  | Temperature Study | 10000 | 1 |

Table 2.1a. A series of reloading tests are done on single, isolated bolt composite/aluminum hybrid connections. Six different tests are run for this group, each with a different reloading cycle, as presented in Table 2.1b. In addition, a several load levels are examined for this group of tests. Another series of tests, summarized in Table 2.1c are done on single, isolated bolt composite/aluminum hybrid connections using tapered headed bolts at two different preload levels, so as to compare their response to non-tapered bolts. Single bolt composite/aluminum hybrid connections are also examined under various temperature and humidity conditions (see Table 2.1d). Three different humidity conditions were used, as shown in the test matrix, where C1 is at 150 °F, 90 % RH, C2 submerged in water, and C3 is at room temperature and 50 % RH. The temperature study involves heating and cooling a specimen at certain intervals, both at 50 % RH and submerged. These environmental tests are discussed in greater detail in Section 2.5.

All tests are run, in general, for 3 months, and test data is collected and analyzed periodically. All four groups of tests are run at the same time through the use of a data acquisition system. Analysis of the data from the reloading test is used to determine if reloading the bolts helps to lower the stress relaxation in the composite over time. Analysis of the tapered versus non-tapered tests is used to ascertain the effect tapered bolts have on the stress relaxation, as compared to non-tapered bolts. Environmental tests were performed to assess the effect of temperature and moisture content on the stress relaxation.

## 2.2. Compression Block Tests and Fixture

Compression block tests are used to quantify the transverse stress relaxation of the E-glass/Vinylester composite under relatively uniform stress. The test fixture consists of two large steel blocks, with a composite sample being compressed between the two, as shown in Figure 2.1. A photograph of the fixture and various components is shown in Figure 2.2. The fixture has a square cross-sectional area, with dimensions of 6" by 6". The bottom half is 2.9375 inches high, while the top half is 1.8125 inches high. The fixture has bolts at its four sides to provide the compression load. Load washers of ½" diameter (Omega, LC900 series) are used on each of the four bolts to read the applied load. A Blackhawk dial torque wrench with a maximum of 175 ft lb, is used to tighten the bolts to the desired preload, so as to make comparisons between the bolt load and the applied torque. The dial torque wrench is used so that the torque can be read when the desired preload is reached. A snap torque wrench will not work for this application, as it allows the user to set a desired torque, but the load resulting from that torque may vary slightly.

### 2.2.1. Compression Block Test Article

The test article for the compression block test is a square two-inch by two-inch specimen with constant thickness, t, of ½ inch. It is made as a panel of E-glass/vinylester that has a quasi-isotropic lay-up; $([(\pm 45),(0/90)]_4)_s$. The 2 x 2 inch specimens were cut from the ½ inch thick panels. More details regarding material constituents are presented in Section 2.5.2.

**BK Precision Model 1651 Triple Output DC Power Supply**

**Signal to Iotech DaqBoard/2000 and Data Acquisition System**

**Omega LC900 Sreies Load Washers**

1.8125"

**2" x 2" x ½" E-Glass/Vinylester Composite Specimen**

2.9375"

**½" diameter Grade 8 bolts.**

6"
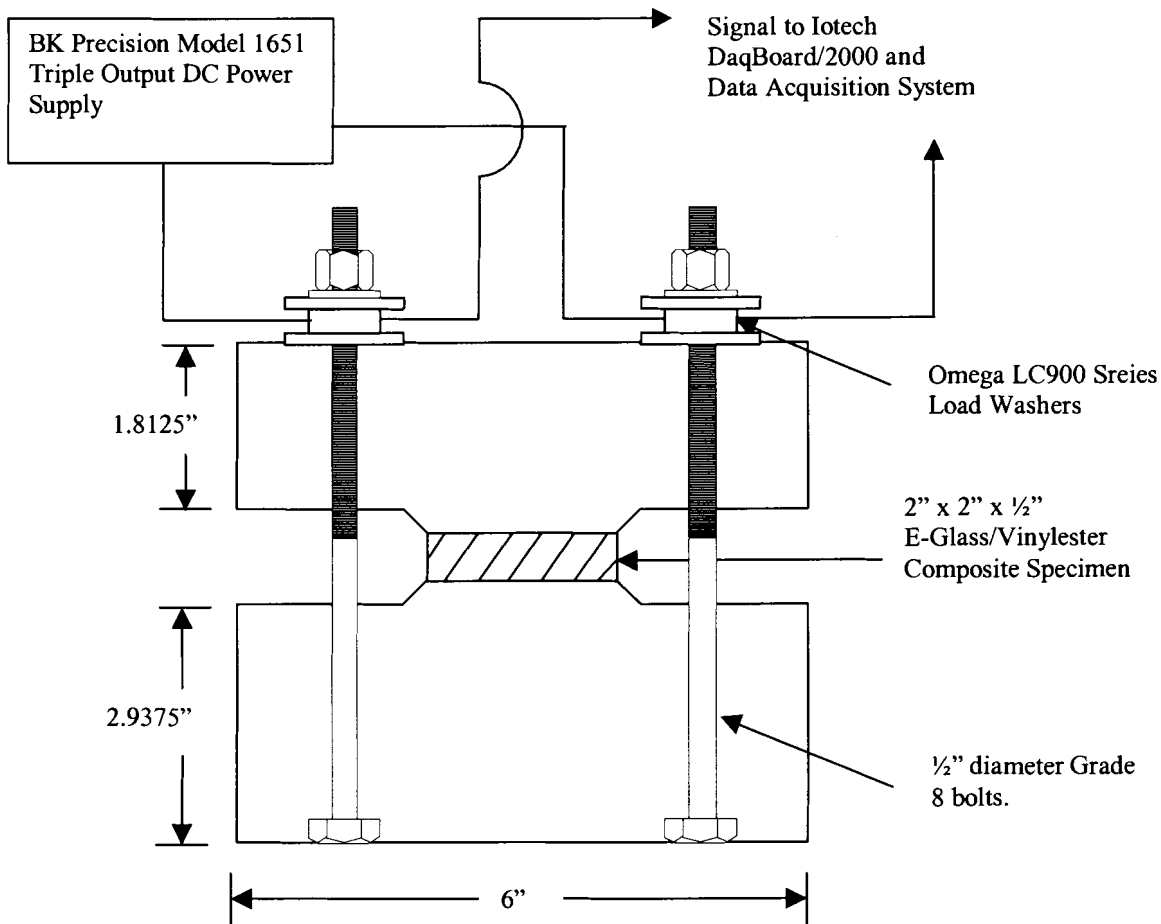
**Figure 2.1 - Compression Block Test Schematic**

Omega Series
LC900 Load
Washers

Compression
Block Fixture

Omega Series
LC900 Load
Washer

Compression
Block Fixture

2" x 2" x ½"
E-Glass/Vinylester
Test Sample

SAMPLE
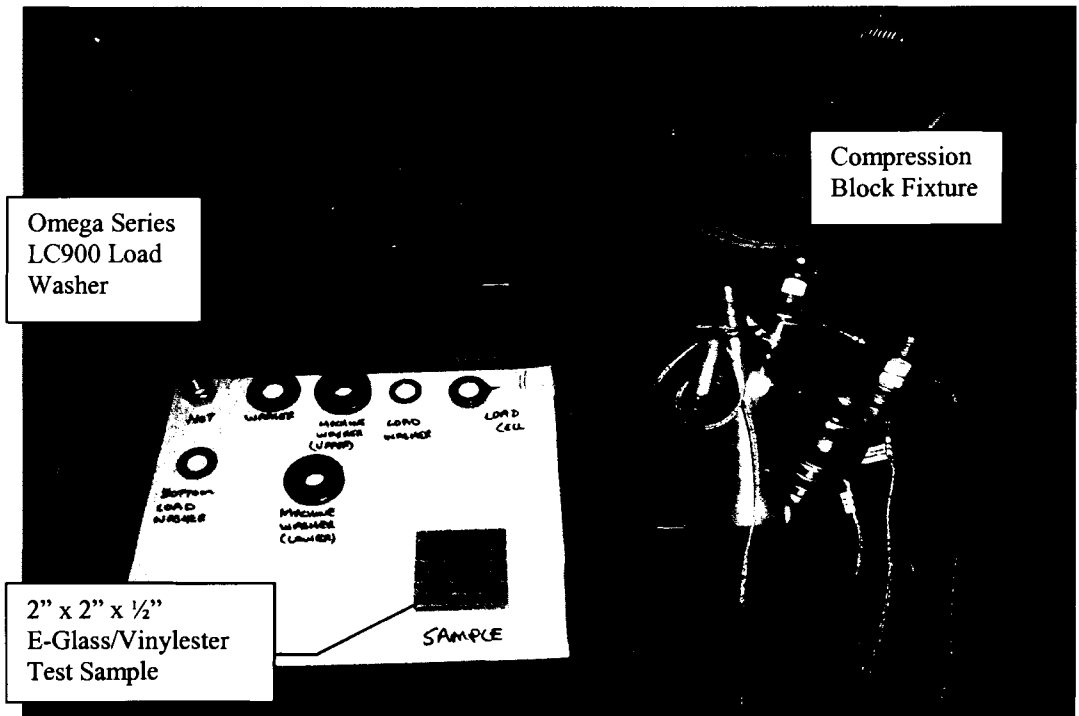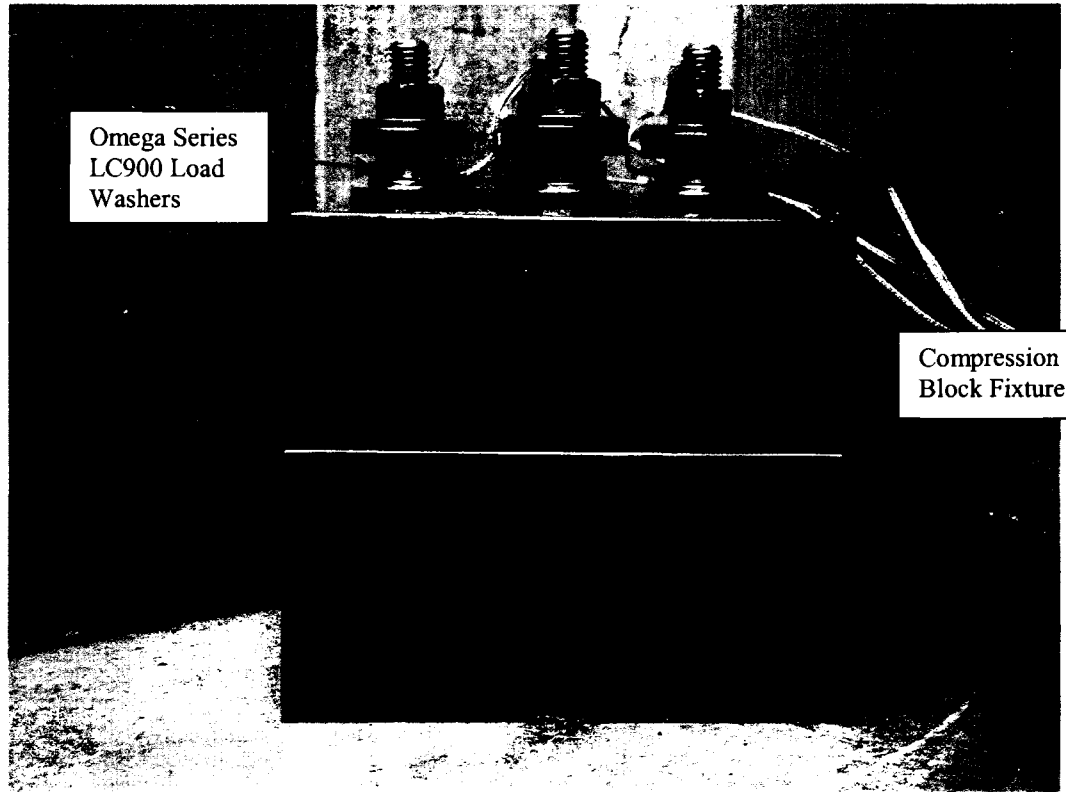
**Figure 2.2 - Photographs of the Compression Block Fixture and Various**

**Components**

### 2.2.2. Compression Block Test Procedures

Compression block tests are automated using an IOTech data acquisition system with a 16-bit resolution and a computer code called DAQFI. The DAQFI program was created at UMaine, and a module was written specifically to run the stress relaxation tests. The procedure starts by initially recording a single data point to quantify the bias voltage at zero load for each load washer. This is done before any of the bolts are loaded. Each load washer typically has a slight voltage at zero load due to fabrication techniques and the electronics. This voltage is used as a zero point for that load washer. The starting voltage is input into the voltage offset section in the configuration file for the DAQFI program. The configuration part of the program is described in more detail in Section 2.8.7.2. The voltage bias is subtracted from the output voltage recorded after loading. This allows the DAQFI program to determine the unbiased voltage and report the actual load.

The 2-inch by 2-inch composite specimen is placed between the two steel plates of the compression block, and the bolts are tightened using a dial torque wrench. All four bolts are loaded to the same value, as much as practically possible. Precise loading is difficult, however, due to the geometry of the fixture, and as one bolt is tightened it affects those around it, either increasing or decreasing the load in the other bolts. The bolts are therefore tightened in a systematic manner to minimize this difficulty. The tightening procedure starts as one bolt is tightened to approximately ¼ of the desired preload. The bolt on the opposite side from the first bolt is then tightened to approximately ¼ of the preload. After this, the two remaining bolts are tightened to ¼ of the preload. This process is repeated by tightening each bolt incrementally until all bolts

read the desired load within a few percent. A single data point indicating the starting

load in each bolt is logged into the data file, and the data acquisition program is started

and left to record the data over the 3 month time period. The data acquisition program is

set to take data according to the schedule given in Table 2.2.

**Table 2.2 – Data Acquisition Recording Schedule**

| Data Acquisition Schedule | |
| --- | --- |
| Start to 1 hr. | every minute |
| 1 hr. to 24 hrs. | every 10 minutes |
| 24 hrs. to 30 days | every 30 minutes |
| 30 days to 4 weeks | every 7 days |
| 4 weeks to end | every 14 days |

**2.3. Single Bolt, Reloading Hybrid Connection Test**

Single bolt hybrid connection tests are used to study the effects of reloading the

composite/aluminum connection on the stress relaxation of a hybrid connection. Figure

2.3 shows an overview of the test specimen, as well as a schematic of the fixture used for

testing. The maximum pressure distribution encountered during the life of the test is

determined using pressure paper. This data is used to assess the stress relaxation in an

isolated single bolt and can be used to evaluate the watertight integrity of a seal in the

connection for applications on ship hulls.

27

Schedule for
d, t, and w

| d | t | w |
|---|---|---|
| 1/2" | 1/2" | 5" |
| 3/4" | 3/4" | 7.5" |
| 1" | 1" | 10" |

Signal to Iotech
Daqboard/2000 and Data
Acquisition System

A.L. Design
Internally Gaged
Bolt, Grade 8

5t x 5t x t
E-Glass/Vinylester
Composite Specimen

t

Fujifilm
Prescale

5t x 5t x t
6061 Aluminum
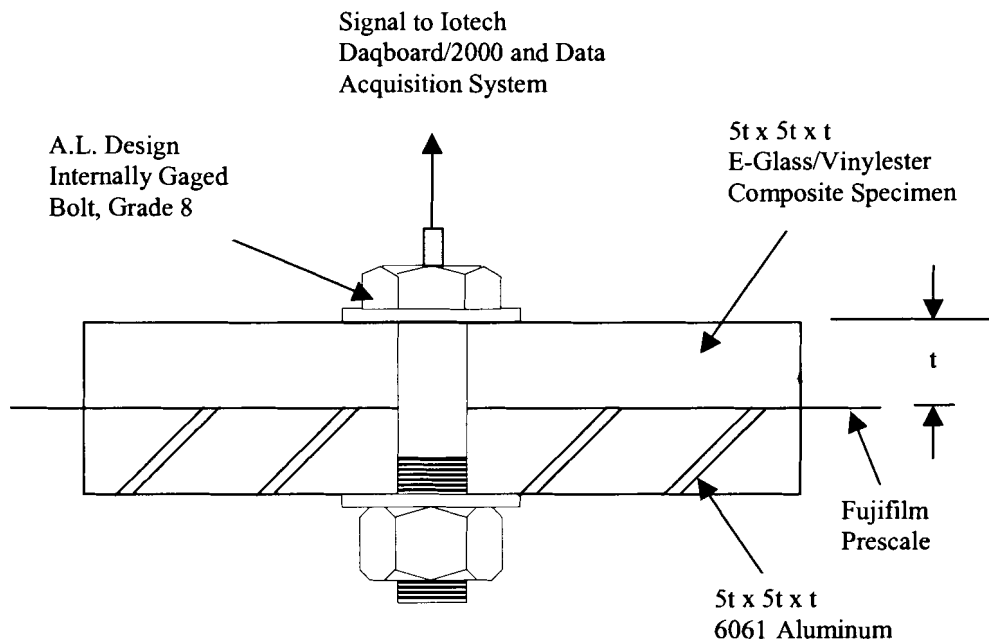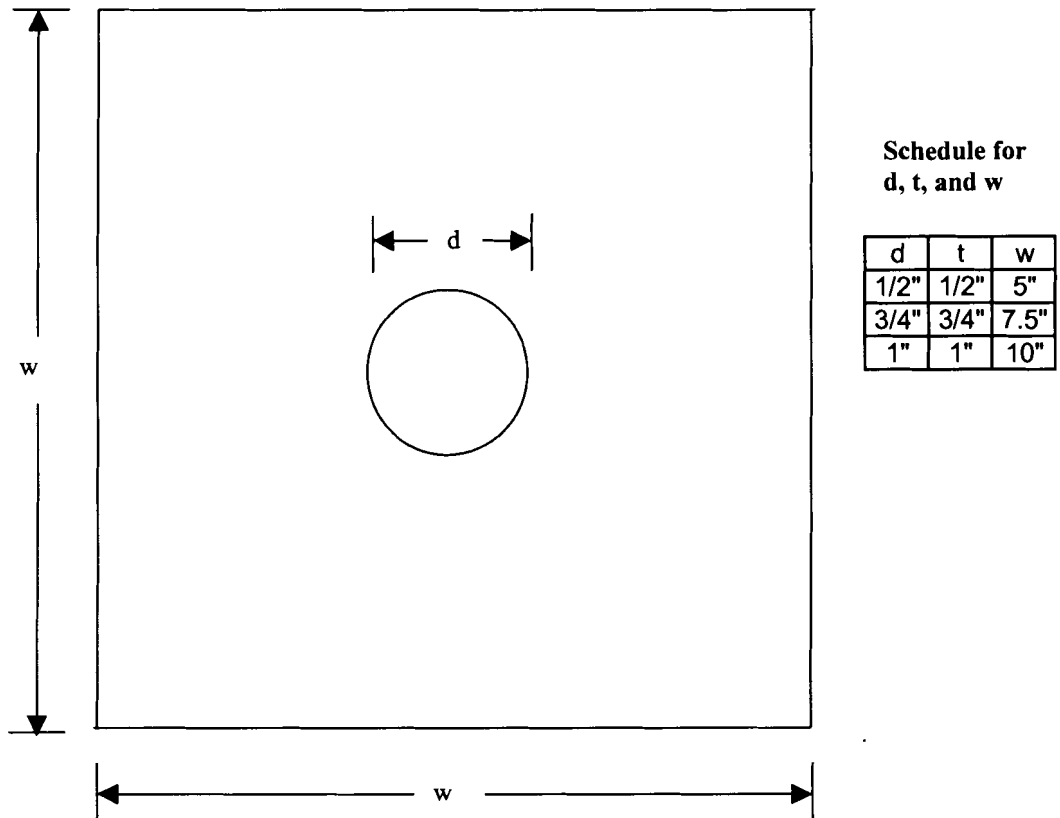
**Figure 2.3 - Single Bolt Test Specimen and Fixture Schematic**

28

The test article geometry is the same for both the reloading tests, and the tapered bolts vs. non-tapered bolts tests. A photograph of this test fixture is shown in Figure 2.4. Three different specimen thicknesses are tested during this group of tests, ½, ¾, and 1 inch thick. The composite specimens have a quasi-isotropic lay-up, a length equal to 5 times the thickness, and have a hole in the center equal to the bolt diameter, d. The lay-up for the ½", ¾", and 1" thick panels are (*), (*), and (*) respectively. The plates are bolted together using internally gaged bolts (AL Design Models ALD-BOLT-.5" X 2" LONG, ALD-BOLT-.75" X 2.5" LONG, and ALD-BOLT-1" X 3.5" LONG), used to read the load in the connection.
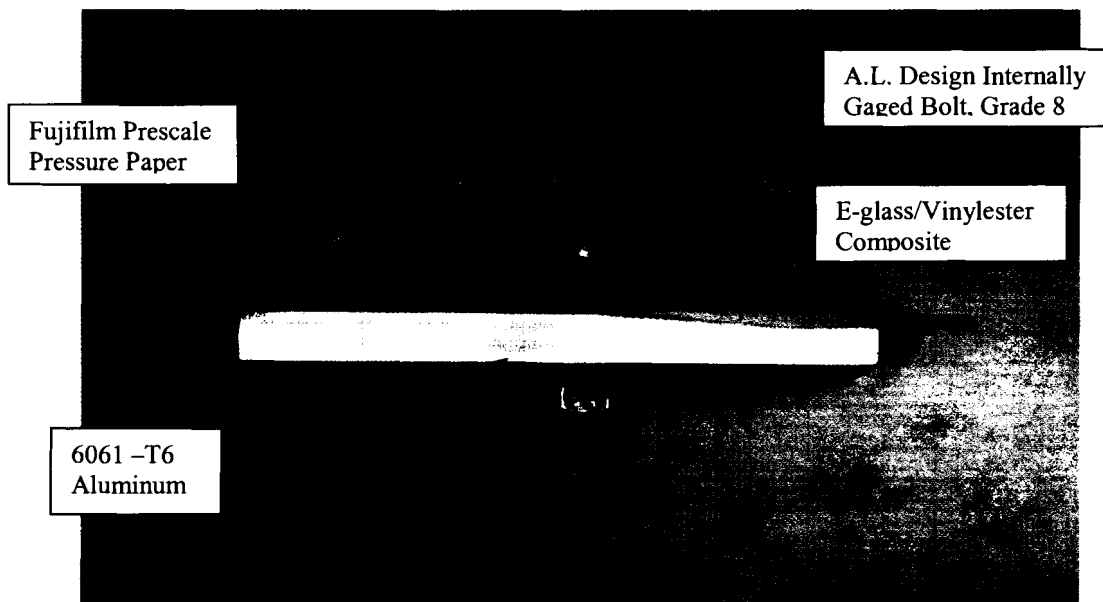


**Figure 2.4 - Single Bolt Hybrid Connection Fixture**

Six separate fixtures are run for panel thickness of ½", ¾", and 1" simultaneously. One fixture is used as a control test, with no reloading of the connection. The other five fixtures are loaded, and then reloaded according to the schedule given in Table 2.3.

**Table 2.3 - Bolt Reloading Schedule**

| Re-torquing Schedule |
| --- |
| 1: control, no reload |
| 1:reload after 3 days |
| 1:reload after 3 days twice |
| 1:reload after 3 days thrice |
| 1:reload after 1 week |
| 1:reload after 2 weeks |

The internally gaged bolts, supplied by A.L. Design Inc., are used to measure load during the retorquing tests. Three sizes of bolts are used in these tests, ½ inch diameter, ¾ inch diameter, and 1-inch diameter. The bolts are described in more detail in Section 2.8.1.2. Prescale pressure paper, supplied by Fujiflim, is inserted between the aluminum plate and the E-glass/vinylester composite. The pressure paper has a center hole cut out that is the same diameter as the bolt being used. More details regarding the pressure paper can be found in Section 2.8.2.

The bolts are tightened using the Blackhawk dial torque wrench. The 1 inch thick specimens use a torque multiplier with the torque wrench to load the bolts to torques over 175 ft lbs. The torque multiplier used is a Williams No. Tm-750 LW x 4. It is capable of a maximum torque output of 1000 ft. lbs. And a maximum torque input of 275 ft. lbs. The load relaxation data is collected through the DAQFI data acquisition system similar to the procedure described in the compression block tests.

### 2.3.1. Single Bolt, Reloading, Test Articles

The geometry of the single bolt was chosen to insure that the plate was wide enough to observe the entire pressure distribution at the composite/metal interface of the bolts due to the stress intensification below the bolt head. It was determined using finite element models of the geometry used in these tests, that pressure effects can be seen at a radial distance of, at most, 3 times the bolt diameter from the center of the bolt line. Choosing a test article that is 10 times the bolt diameter along its length enables the entire pressure distribution to be seen with the use of pressure paper. 6061-T6 aluminum plates are bolted to the composite specimens, and have the same width and nominal thickness as the E-glass/vinylester plate. The material properties of the metal and composite are discussed in detail in the material section, Section 2.6.

Parameters in this group of tests include varying preload, composite thickness, and the time between retightening bolts, as given in the test matrix, Table 2.1b. All 6 specimens for one series of these tests are cut, using a wet saw, from the same panel of E-glass/vinylester composite. Once the 6 specimens are cut from the panel, the center of each specimen is marked so that the hole can be drilled using a diamond tipped drill bit from Accurate Diamond Tool Corporation. The holes are drilled very slowly, and water is sprayed on the drill bit and the composite several times during drilling. This is to keep the drill bit cool, minimize delaminations, provide a better cut, and reduce the amount of composite dust spread during drilling.

### 2.3.2. Single Bolt, Reloading Test Procedures

Similar to the load washers, the internally gaged bolts also contain full bridge strain gages that are used to read the applied load. They are connected in the same manner as the load washers so that the data can be read through the DAQFI data acquisition system. Details of the instrumentation are given in Section 2.8.

As with the compression block test, the initial bias voltage value is taken with no load applied to the connections. Again, this voltage offset is input into its appropriate place in the program configuration file. Pressure paper is then cut to the approximate dimensions of the specimens. A hole is cut in the center the same size as the bolt hole in the composite. The pressure paper is inserted between the E-glass/vinylester composite and the aluminum in the connection.

Once the specimens have been cut, holes drilled, pressure paper cut, and the bolts connected to the power supply and data acquisition system, the test articles are finally ready to load to the desired preload. In order to load a bolted connection, the connection is held relatively motionless during tightening. A fixture was designed and fabricated to hold the specimens in place during the application of the load. This fixture consists of two angled beams on opposite sides of the test article used to hold the square fixture stationary during torquing of the bolts. These two angled beams are bolted to a large beam fixture that can be easily held stationary while the bolts are tightened. The torquing fixture is shown in Figure 2.5. It was made from materials readily available in Crosby laboratory.

The specimens are tightened in the following manner. The first specimen is placed in the tightening fixture to hold it in place. Nickel based Locktite anti-seize is
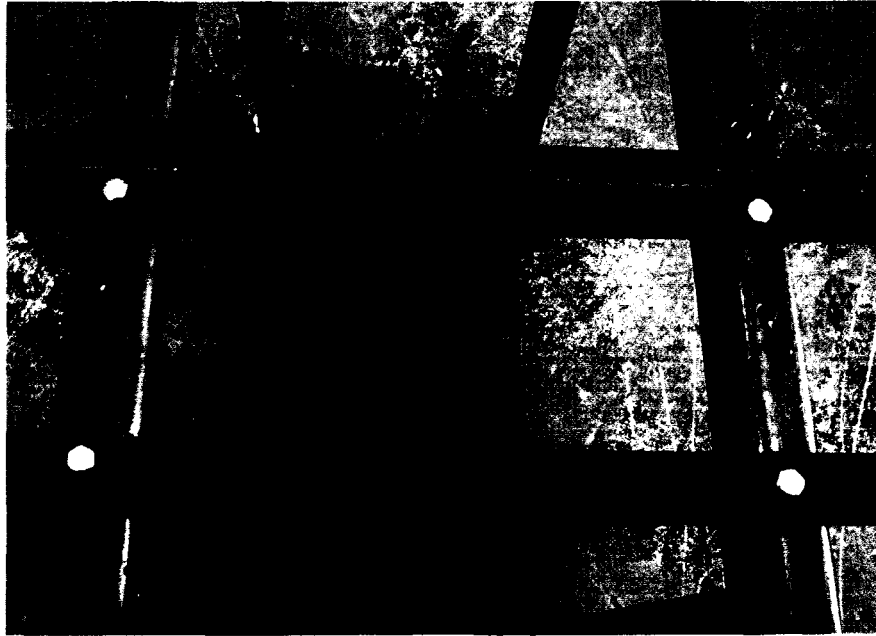
**Figure 2.5 - Pictures of Torquing Fixture**

applied lightly to the end of the bolt. The dial torque wrench is then used to apply load to the bolts. A data file is opened, and the load is monitored through the monitoring feature of the DAQFI software. Once one bolt is tightened to the desired preload, the log button is hit in the software, and a single data point is logged. This process is repeated for each test article. Once all bolts have been tightened, the run button is activated in the DAQFI software, and the computer is left to collect data at the prescribed increments.

The test procedure includes periodic retorquing of the bolts according to Table 2.3, in the same manner they were initially tightened. The computer program is stopped before the reloading process is started, and the load monitoring section of the program is activated before any reloading is started. A single data point is then logged after reloading by activating the log button in the program. This same process is repeated for any other connections that need to be reloaded.

Once all bolts have been reloaded and data points have been logged for each, the run button is activated and the software is left to automatically collect data. The software is written to append the new data set to the previous data set, unless the program is completely shut down and restarted.

At the end of the 3 month period, the final data set is collected and reduced. For each single bolt connection fixture, a plot of load vs. time is made. The reloading cycle is also recorded. This data is analyzed to determine the effects of periodic reloading on the stress relaxation in the hybrid connections. The relaxation parameters are modeled according to a power curve fit to the data in Excel. This is described in details in the results, Section 3.

## 2.4. Single Tapered Head Bolt Tests

The single tapered head bolt tests are designed to study the effects of tapered bolts vs. non-tapered bolts on the stress relaxation in the bolted hybrid connections. The test fixtures used for this group of tests are the same as those used for the single bolt reloading tests. Figure 2.6 shows a side view and a top view of the tapered bolts fixture. They consist of a square plate of aluminum bolted to a square plate of the E-Glass/vinylester composite. Load washers are used in this case to output the applied load, since instrumented tapered head bolts are not available. Four test fixtures are run at once, two bolted with tapered bolts, and two bolted with non-tapered bolts.

Only one panel thickness is used for this group of tests of ¾" thick. This thickness was chosen because it is the average thickness of the test articles being studied in the reloading tests. Other thicknesses were discussed, but considering the limit on the number of data acquisition channels and the cost to get enough sensors for all three thicknesses, it was decided to use only one thickness at this time.

This group of tests utilizes ¾" load washers (Omega series LC900) to monitor the load in the connection. The biggest disadvantage of the load washers is that the lead wires are very fragile. A great deal of care and caution must be taken to avoid damaging or destroying the wires and thus the load washer.

These tests are set up in exactly the same manner as the reloading tests, presented in Section 2.3. As with the other tests, the load is applied by using the dial torque wrench. Pressure paper is used between the aluminum and the E-glass/vinylester composite, the same as in the reloading tests.

E-glass/Vinylester Composite

6061 –T6 Aluminum Plate

Omega Series LC900 Load Washers
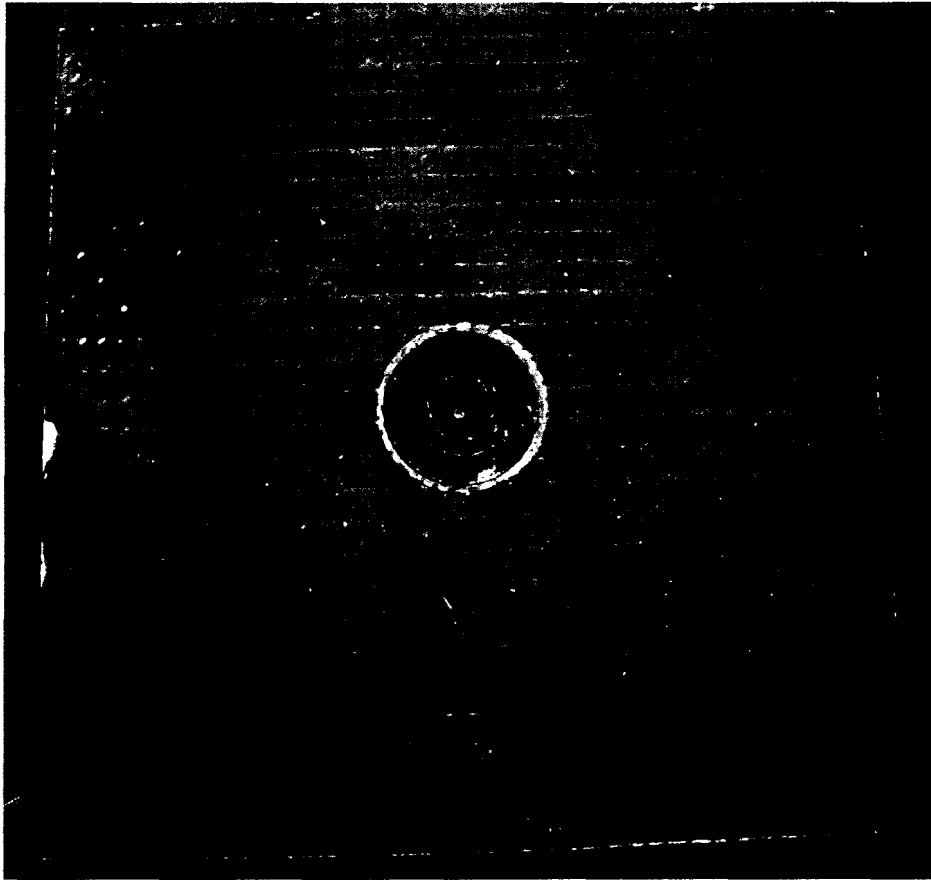
**Figure 2.6 - Tapered Bolts Fixture (Top and Side View)**

The load washers are connected to the data acquisition system, which records the applied load in the connection by multiplying the output voltage difference by the known calibration factor.

### 2.4.1. Single Tapered Head Bolt Test Article

The test article geometry for this group of tests is the very similar to that used for the single bolted, reloading test. The countersunk hole, required for the tapered bolt, has an included angle of 82 degrees, as shown in Figure 2.7. The lay-up is quasi-isotropic, as before, and material specifications are provided in Section 2.6. These test articles are also bolted to aluminum plates, with the same dimensions as the E-glass/vinylester composite plates, but without the countersunk hole.

### 2.4.2. Single Tapered Head Bolt Test Procedure

The procedure for this group of tests is very similar to that of the single bolted, reloading tests. There is no reloading of these fixtures during this series of tests. Once again, some preparation is required before the tests are run. The load washers are very similar to those used in the compression block tests. The only difference is that they are ¾" and have a larger maximum load capacity, 65000 pounds. They have the same internal 120 ohm full bridge strain gages to measure the load, thus must be connected to the data acquisition program in the same manner. The red wire from each washer is connected to a common junction point, as is the black wire. These are then connected to the power supply to provide the excitation voltage.
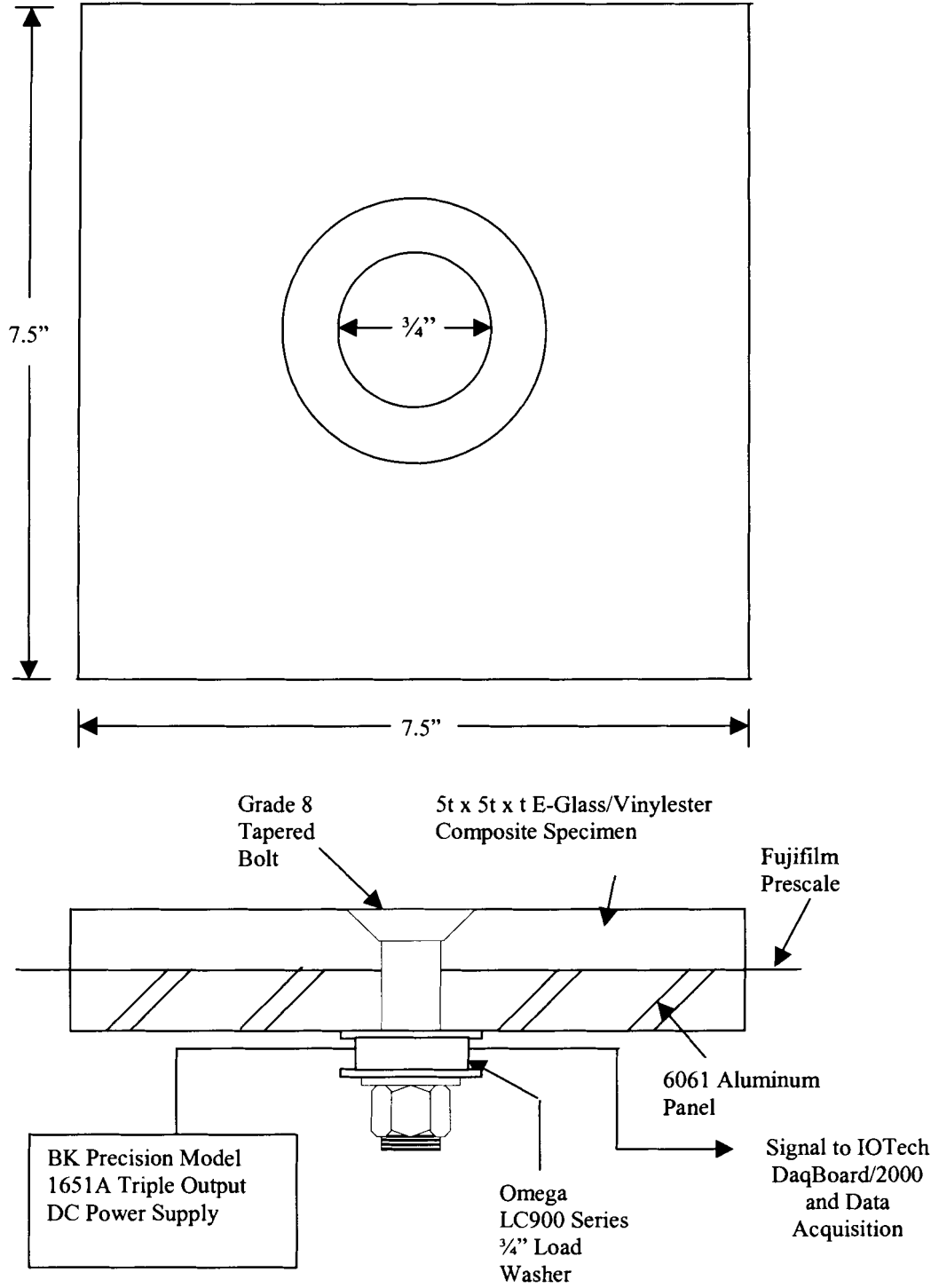
**Figure 2.7 - Tapered Bolt Test Article**

For this group of load washers, a 5 volt excitation is used. The green and white wires from each are connected to separate consecutive channels on the hub. The hub is then connected to the computer.

As with the other tests, before all of the connections are loaded, a single data point must be logged containing the voltage offsets for each load washer. This ensures that the program reads zero voltage difference when there is zero load on the load washer. Once all four load washers are connected to the power supply and the data acquisition system, the connections are ready to be assembled and loaded. The fixtures are placed together with the bolts, and pressure paper between the E-glass/vinylester composite and the aluminum. The load washers are placed at the end of the bolt, and mounted between two mounting washers so that the load applied to the washer is uniform.

The tightening fixture is used to hold the bolted connections in place while loading is being done. The load monitoring function of the DAQFI program is activated. One fixture is loaded to the desired preload and a single data point is recorded using the log button in the software. This process is repeated for each connection until all four have been loaded. At this time, the run button is activated and the DAQFI program is left to automatically collect data.

## 2.5. Environmental Testing

The environmental tests are used to study the effects of various different environmental conditions on the stress relaxation of a single bolt composite/aluminum hybrid connection. The same type of test articles used for the single bolt, reloading tests are used for the environmental tests. Only one thickness is tested, ¼" thick. The

dimensions of both the E-glass/Vinylester composite and the aluminum for these tests are 7.5 inches by 7.5 inches. A schematic and photograph of this test fixture is shown in Section 2.3, Figures 2.3 and 2.4. Internally gaged bolts are used for this series of tests.

The testing procedure is almost exactly the same as that for the single bolt reloading test procedure, described in Section 2.3.2. The only difference is that none of these test specimens are reloaded during testing. The test articles are loaded using the same loading fixture shown in Figure 2.5. This group of tests is also run for a time period of at least three months.

Various conditioning cycles are examined, as summarized in Table 2.1d. One specimen, C1, is used as a control and is held at room temperature and 50 % RH. Another specimen, C2, is conditioned for 1 month at 150 °F and 90 % RH, then tightened, then held at room temperature and 50 % RH. The third specimen in this group, C3, is conditioned for 1 month at 150 °F and 90 % RH, then tightened, and then submerged in water at room temperature. The next specimen, C4, is tightened, allowed to creep at room temperature and 50 % RH for 1 week, then submerged in water at room temperature. A fifth specimen, C5, is tightened and then submerged in water at room temperature for 1 month, then removed and held at room temperature at 50 % RH for 1 month, and then cycled. These tests are used to examine the effects of humidity on the connection, while holding temperature constant.

The final test in this group, C6, is a study of temperature effects. The test article is tightened and allowed to creep for 1 week at room temperature. The temperature is then dropped to 40 °F for half a day. It is then held at room temperature again for 1 day,

and then at 90 °F for half a day.  This whole process is done at 50 % RH.  The same test

is then run with the test article submerged in water at the same varying temperatures.

## 2.6. Material Specifications

Materials used in testing are described in this section.  The composite specimens

were made from a Dow Derakane 8084 vinylester epoxy resin reinforced with E-glass

fiber cloth.  The aluminum used was a standard grade 6061-T6.  What follows is some of

the material properties of the various materials used.

### 2.6.1. Metallic Components

The metallic plates are fabricated of aluminum Grade 6061 – T6.  The aluminum

plates are used in single bolt reloading tests, tapered bolts vs. non-tapered bolts testing,

and the environmental testing.  Table 2.4 lists some of the properties of this alloy.

**Table 2.4 – Aluminum 6061-T6 Properties (matweb.com)**

| Physical Properties | SI | US Customary |
|---|---|---|
| Density | 2.7 g/cc | 0. 0975 lb/in$^3$ |
| **Mechanical Properties** | | |
| Hardness, Brinell | 95 | 95 |
| Tensile Strength, Ultimate | 310 Mpa | 45 ksi |
| Tensile Strength, Yield | 275 Mpa | 40 ksi |
| Elongation @ break | 12% | 12% |
| Poisson's Ratio | .33 | .33 |
| Modulus of Elasticity | 69 Gpa | 10008 ksi |
| Shear Modulus | 26 Gpa | 3771 ksi |
| Shear Strength | 205 Mpa | 29,733 psi |
| Fatigue Strength | 95 Mpa | 13,779 psi |

### 2.6.2. Composite Specimens

The composite specimens used in this study were fabricated at the Crosby Laboratory, University of Maine, using a VARTM process. They consist of Dow Derakane 411, which is a two- part epoxy vinylester resin. The composite is reinforced with an E-glass cloth procured from Brunswick Technology, Inc. The cloth is either a 24 oz. 0/90 lay-up, or a 24 oz. ±45 lay-up. Properties of Dow Derakane 8084 are listed in Table 2.5, while the E-glass cloth properties are listed in Table 2.6.

The lay-up used for the test specimens is quasi-isotropic, $([(\pm45),(0/90)]_n)_s$, E-glass fabric, where n varies according to the panel thickness. N is either 4 for the ½" thick panels, 6 for the ¾" thick panels, or 8 for the 1" panels. The panels are fabricated with approximate dimensions of 50" x 25". Test coupons are then mapped out of each panel and cut out to specifications given in Sections 2.2, 2.3, 2.4, and 2.5. All test coupons for one series of tests are cut out of the same panel. Figures 2.8, 2.9, and 2.10 show the general panel and specimen layout for each of the three panel thicknesses used.

**Table 2.5 - Dow DERAKANE 8084 Epoxy Vinylester Resin (Dow Chemical Company)**

| Physical Properties | SI | US Customary |
|---|---|---|
| Viscosity | 350 cps | 73.1 (lbf s)/ft² |
| Specific Gravity | 1.02 | 1.02 |
| **Mechanical Properties** | | |
| Barcol Hardness | 30 | 30 |
| Tensile Modulus | 3.17 GPa | $4.6 \times 10^5$ psi |
| Tensile Strength, Yield | 69 - 76 MPa | 10 – 11,000 psi |
| Elongation @ break | 10 - 12 % | 10 - 12 % |
| Flexural Modulus | 3.03 GPa | $4.4 \times 10^5$ psi |
| Flexural Strength | 110 - 124MPa | 16 – 18,000 psi |
| Heat Distortion Temperature | 82 °C | 180 °F |

42

**Table 2.6 – E-Glass Cloth Properties Isotropic**

| Physical Properties | SI | US Customary |
|---|---|---|
| $E_1^f$ | 7.24E+10 Pa | 1.05E+07 psi |
| $G_{12}^f$ | 3.03E+10 Pa | 4.40E+06 psi |
| $\eta_{12}^f$ | 2.00E-01 | 2.00E-01 |
| $=+S_1^f$ | 1.86E+09 Pa | 2.70E+05 psi |
| $=-S_1^f$ | -1.10E+09 Pa | -1.60E+05 psi |
| $\rho^f$ | 2.55E-02 kg/ $m^2 s^2$ | 9.40E-02 lb/$in^2$ |
| End Area | 4.33E-07 $m^2$ | 6.71E-04 $in^2$ |
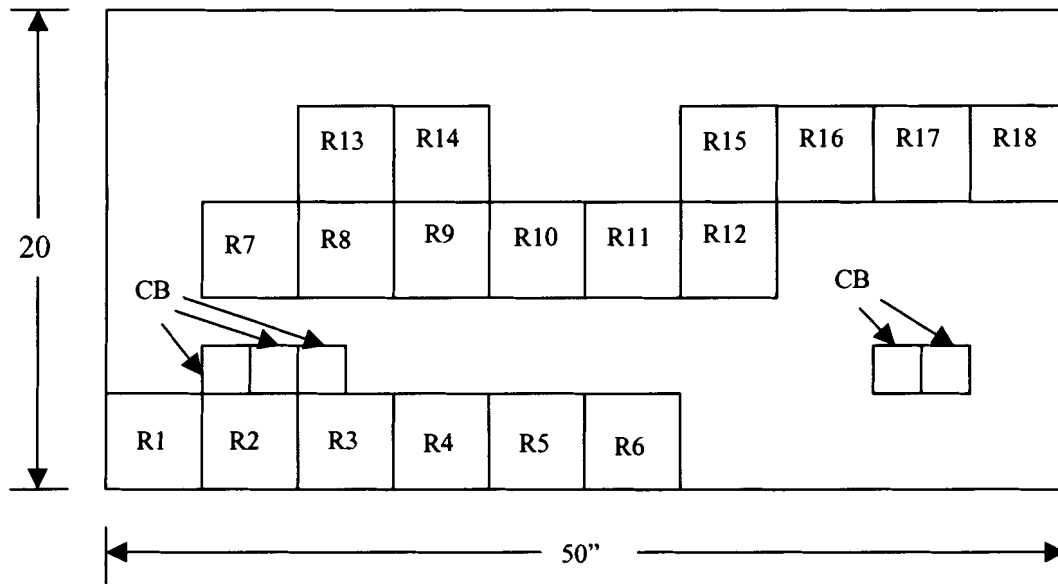


**Figure 2.8 - ½" Thick Panel Layout**
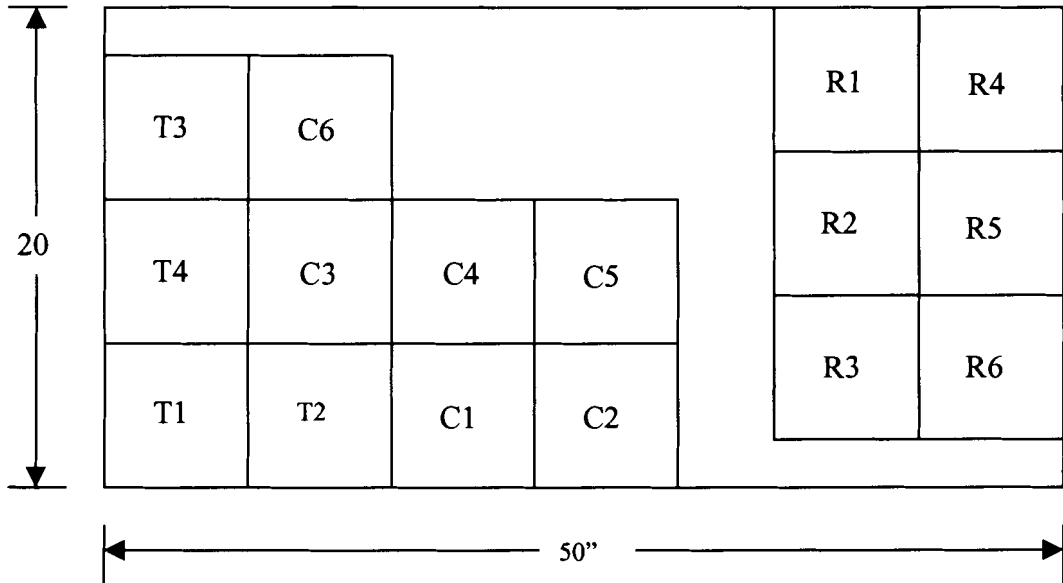
**Figure 2.9 - ¾" Thick Panel Layout**
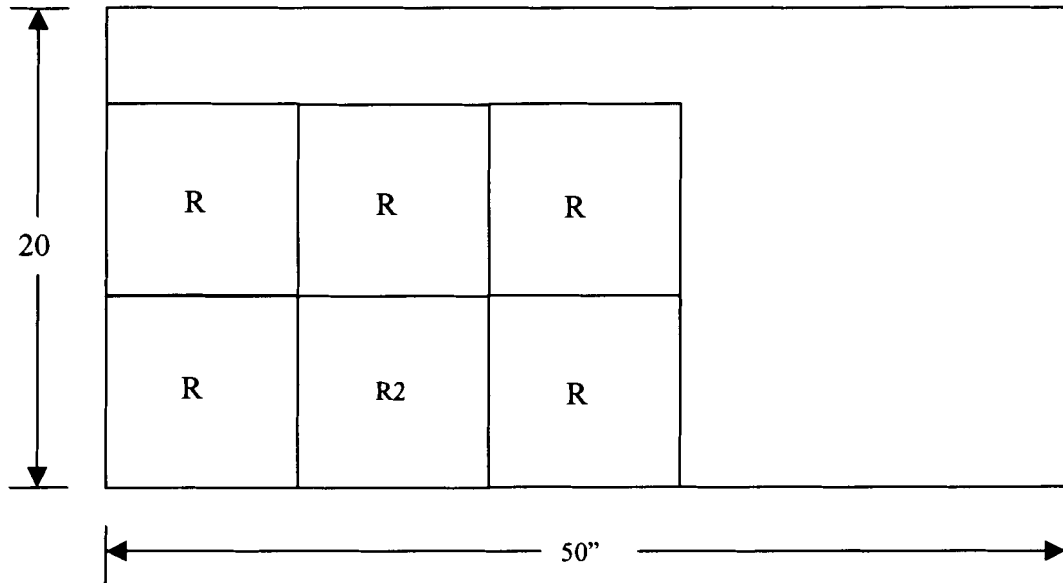


**Figure 2.10 - 1" thick Panel Layout**

44

A ½" thick panel is large enough to cut several groups of test articles from one panel. Panels labeled starting with R are for the single bolted reloading tests, while the ones marked with CB are for the compression block tests. Specimens 1 through 6 are for one group of tests, 7 through 12 for a second, and 13 through 18 for a third. The remaining material is put aside for material testing. An additional ½" thick panel was made of dimensions 40" x 20" for a fourth test.

A ¾" panel is used for several different tests. Specimens marked with an R are again used for the single bolt reloading tests, ones marked with a T are for tapered bolts versus non-tapered bolts, and ones marked with C are for environmental conditioning tests. Extra material is again set aside for material testing. A total of three panels were used to provide test specimens for all tests.

The 1" thick panel is only used for the single bolted reloading tests. A total of three 1" panels were used fabricated for this study.

## 2.7. Composite Material Tests

Verification tests are performed to quantify strength and stiffness of the composite materials used in the stress relaxation testing. These tests include:

1.  Fiber Volume Test (Burn Off) – ASTM D 2584

2.  Tension Test – ASTM D 3039

3.  Compression Test – ASTM 3410

## 2.8. Instrumentation Details

Several sensors are used during testing to monitor data such as load in the bolted connections, maximum pressure distribution in the connections, temperature, and humidity during testing. The data acquisition program is also used to monitor and record this data, in conjunction with the various sensors. What follows in this section is a description of the sensors and a description of the pertinent parts of the DAQFI data acquisition program.

### 2.8.1. Load Washers

Omega Engineering of Stamford, CT manufactures the series LC900 load washers used in these experiments. The load washers are compression load cells designed to measure the clamping force of a bolt. Two sizes of load washers are used in the testing; ½ inch, and ¾ inch. The ½ inch load washers are used in the compression block testing, while the ¾ inch load washers are used in the tapered bolts and non-tapered bolts testing. The load capacity is 30,000 lbs. and 65,000 lbs. for the ½" and the ¾" load washers, respectively.

The load washers have an internal full bridge strain gage mounted to their inner diameter. The corresponding wires from the strain gage are attached to the power supply and the data acquisition system in order to read the applied load. The power supply is applied across the red and black wires of the load washers. Since all of the load washers can use the same power supply, they are all wired and soldered to a common junction point with a female banana connection, one for the black wires, and one for the red wires.

46

From these common junction points, a banana cable connects to the power supply to provide bridge excitation. The load washers were all calibrated at 5 volts, thus this is the bridge excitation used. The power supply was a BK Precision Model 1651A Triple output DC power supply. Section 2.8.5 gives more information on this power supply.

The output voltage comes from the white and green wires of each load washer. Each load washer has its green and white wires attached to two separate consecutive channels on the hub connected to the data acquisition system. The data acquisition system, set in a differential mode, reads the voltage difference between these two wires, and multiplies this by the calibration factor to obtain the applied load in the bolt. Table 2.7 contains the calibration factors for the Omega load washers.

### 2.8.2. Internally Gaged Bolts
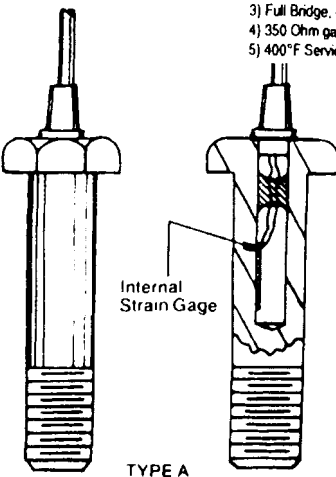
The internally gaged bolts used are model numbers ALD-BOLT-.5" X 2" LONG, ALD-BOLT-.75" X 2.5" LONG, and ALD-BOLT-1" X 3.5" LONG, depending on the bolt diameter. These bolts are designed to measure dynamic or static tension, compression or bending loads. Three sizes of bolts are used in the testing; ½ inch diameter, ¾ inch diameter, and 1-inch diameter. The ½" diameter bolts have a load capacity of 9,220 lbs, the ¾" diameter bolts have a load capacity of 21,700 lbs, and the 1" diameter bolts have a load capacity of 39,400 lbs. Figure 2.12 shows a summary of the bolt specifications. As with the load washers, the bridge excitation is connected across the red and black wires, while the green and white are connected to the data acquisition system to read the voltage difference between them, and convert this difference to load using the calibration factor.

## Table 2.7 - Load Washer Calibrations

| Washer Number | Size | Serial Number | Calibration Factor (lbs/mV) |
|---|---|---|---|
| 1 | 1/2" | 132402 | 3384.667 |
| 2 | 1/2" | 140203 | 3497.645 |
| 3 | 1/2" | 140204 | 3259.382 |
| 4 | 1/2" | 140205 | 3279.656 |
| 5 | 1/2" | 140206 | 3316.933 |
| 6 | 1/2" | 140207 | 3234.397 |
| 7 | 1/2" | 140213 | 3194.548 |
| 8 | 1/2" | 140215 | 3137.156 |
| 9 | 1/2" | 140217 | 3209.071 |
| 10 | 3/4" | 145773 | 6070.341 |
| 11 | 3/4" | 145775 | 6118.165 |
| 12 | 3/4" | 145776 | 6038.367 |
| 13 | 3/4" | 145777 | 5769.265 |
| 14 | 3/4" | 145778 | 5914.575 |
| 15 | 3/4" | 145779 | 6361.385 |



## SPECIFICATIONS:

GAGE RESISTANCE: 350 + 0.4% Ohms

TEMPERATURE COMPENSATION: Between 15°F and 150°F gage factor varies less than 0.5%

CONFIGURATION: Quarter Bridge, Double Quarter Bridge, Full Bridge

EXCITATION: 10 V Excitation

TEMPERATURE RANGE: 15°F - 150°F

OPTIONS:
1) Std. Quarter Bridge, 1 internal strain gage
2) Double Quarter Bridge, 2 internal strain gages
3) Full Bridge, 4 internal strain gages.
4) 350 Ohm gages
5) 400°F Service

Temperature range       0° - 150°F
Resistance              350 Ohms
Internal strain gages   1       Std.
                        2
                        4

| s | Bolt Dia. | Strength Lbs. | Bolt Dia. | |
|---|---|---|---|---|
| 118 | 1-4 | 2070. | 9/16 | |
| 118 | 5-16 | 3410 | 5/8 | |
| 118 | 3/8 | 5040. | 3/4 | |
| 118 | 7-16 | 6910. | 7/8 | |
| 118 | 1/2 | 9220 | 1 | |

Internal Strain Gage

TYPE A

**Figure 2.11 - Internally Gaged Bolts Spec. Sheet (aldesigninc.com)**

48

The red wires from each size bolt are connected to a common junction, and the black wires are connected to another common junction. These are then connected to the power supply using banana cables. For the bolts, a 10 volt power supply is used, since this is the excitation used during calibration. The green and white wires are both connected to successive channels on the hub, and the hub is connected to the computer through the use of a DaqBoard/2000.

Each bolt has an internal 350 ohm full bridge strain gage mounted to the inside of the bolt that is used to measure the applied tension load in the bolt. The output voltage difference is read across the green and white wires of the bolt. This difference varies depending on how much load is applied to the bolt. The voltage difference is multiplied by the calibration factor provided by A.L. Designs in order to calculate the load in the bolt. Calibration factors for each bolt are given in Table 2.8.

### 2.8.3. Humidity Sensor

Figure 2.13 shows a diagram of the chip and mounting dimensions. During testing, humidity is monitored using a HIH-3610 series sensor, manufactured by Honeywell. This sensor has a very low current draw of 200 $\mu$A when operating at 5 Vdc. It can operate on power supplies from 4 Vdc to 5.8 Vdc. For these experiments, it is operated at 5 Vdc, since this was the voltage the sensor was calibrated at. It can operate from between –40 °F to 185 °F, and between 0 and 100% RH. In that range, it is accurate to ±2% RH. The particular sensor used in these experiments has the following relationship between RH and output voltage:

**Table 2.8 - Internally Gaged Bolts Calibration Factors**

| Bolt Number | Size | Serial Number | Calibration Factor (lbs/mV) |
|---|---|---|---|
| 1 | 1/2" | 20011105 | 574.7479 |
| 2 | 1/2" | 20011106 | 427.2036 |
| 3 | 1/2" | 20011107 | 456.0101 |
| 4 | 1/2" | 20011108 | 567.0741 |
| 5 | 1/2" | 20011109 | 433.3666 |
| 6 | 1/2" | 20011110 | 443.2593 |
| 7 | 1/2" | 220642 | 455.0582 |
| 8 | 3/4" | 220109 | 1045.379 |
| 9 | 3/4" | 220110 | 1055.549 |
| 10 | 3/4" | 220111 | 1039.612 |
| 11 | 3/4" | 220112 | 1026.207 |
| 12 | 3/4" | 220113 | 1005.739 |
| 13 | 3/4" | 220114 | 1205.556 |
| 14 | 3/4" | 220643 | 1039.612 |
| 15 | 3/4" | 220644 | 1050.597 |
| 16 | 3/4" | 220645 | 1052.443 |
| 17 | 1" | 220529 | 1933.889 |
| 18 | 1" | 220530 | 1887.586 |
| 19 | 1" | 220531 | 1931.333 |
| 20 | 1" | 220532 | 1945.134 |
| 21 | 1" | 220533 | 2015.657 |
| 22 | 1" | 220534 | 1868.854 |
| 23 | 1" | 220646 | 1876.19 |
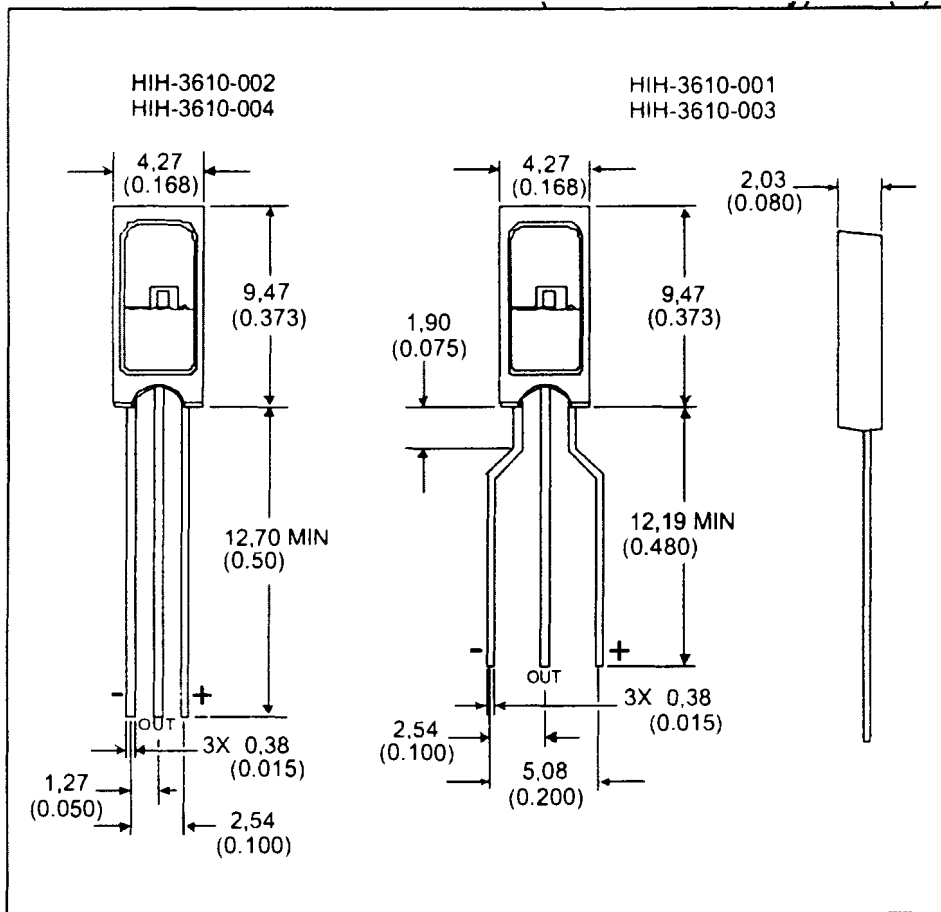
**Figure 2.12 - Diagram of HIH-3610 Series Humidity Sensor, mm (in)**

**(Honeywell.com)**

$$RH = (V_{out} - 0.781) / 0.0326, \qquad (2.1)$$

Where $V_{out}$ is the output voltage, 0.781 V is the zero offset, and 0.0326 V / %RH is the calibration factor.

### 2.8.4. Temperature Sensor

Figure 2.14 shows the overall layout and dimensions of the LM34CZ temperature sensor. The temperature sensor used to monitor room temperature during the testing is a LM34CZ chip, manufactured by National Semiconductor. It has a linear relationship between output voltage and Fahrenheit temperature, with a +10 mV/°F scale factor. It runs over a temperature range of –50 °F to 300 °F, with an accuracy of ±1 ½ °F. The sensor can operate from 5 to 30 volts, and for these tests, it is operated at 15 volts. It draws only 75 μA from its power source, thus it has a low self-heating of 0.18 °F in still air.

### 2.8.5. Environmental Chambers

Two humidity chambers are used to obtain the environmental conditions described in Section 2.5. One is a Tenney Jr. Model THJR, and the other is a PGC (Parameter Generation & Control Inc.) SS Climate-Lab. Both these chambers are located on the second floor of Crosby Laboratory at UMaine.

The Tenny Jr. is a bench top chamber capable of adjusting both humidity and temperature. It has a temperature range of between 10 and 200 °F, and has a standard wet bulb/dry bulb set up to provide the temperature and humidity.

EJECTION MARK
Ø1.6 MAX
▼0.38 MAX

5.2
4.7

5.2
4.9

14.2
12.7

0.55
0.40 TYP

1.27±0.05

2.54±0.1

2.27
2.10

4.19
3.65

SEATING PLANE

2.29 MAX
(UNCONTROLLED LEAD DIA)

0.50
0.36

DIMENSIONS ARE IN MILLIMETERS

**TO-92
Plastic Package**

+Vs    GND

Vout

BOTTOM VIEW
DS006686-2
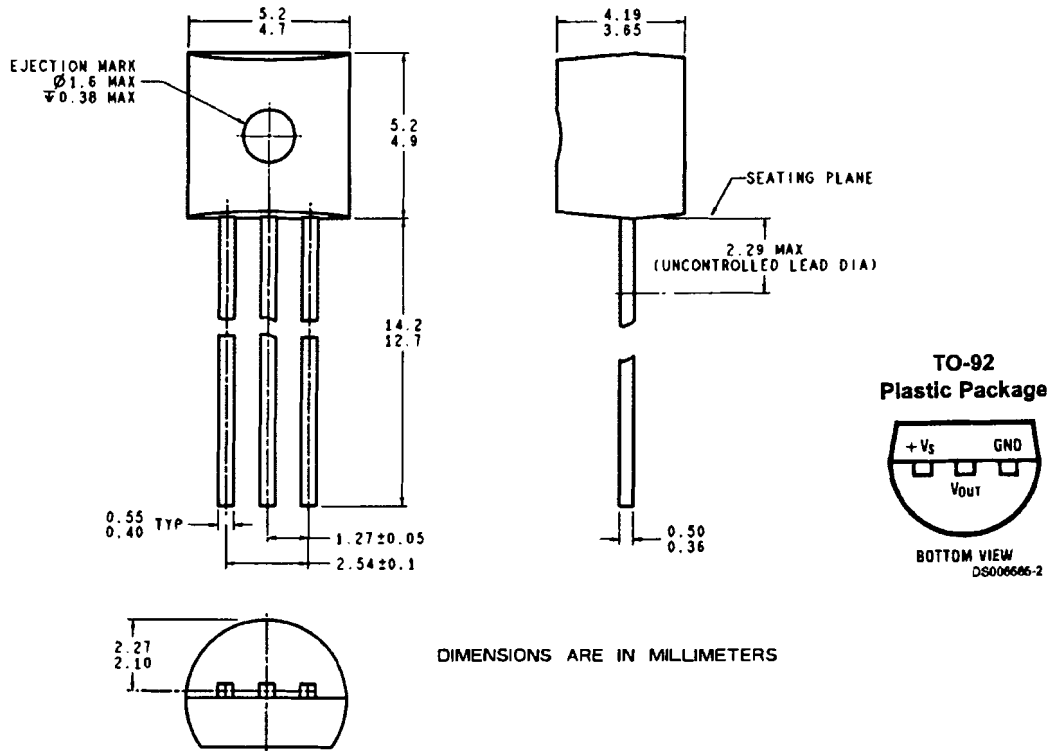
**Figure 2.13 - Dimensions of LM34 Temperature Sensor (National.com)**

It has a gravity feed system that empties the water into the heating chamber. The used water is then drained into a bucket that must be emptied every few days. The manual controls of the system are out of calibration and therefore, moisture and temperature sensors were used to set the controls. When using the chamber for the fist time, some experimentation needs to be done in order to obtain a proper setting for wet bulb and dry bulb on the device. Once these are set, the temperature and humidity remain constant throughout operation.

The PGC SS (steady state) Climate-Lab is a large floor model chamber, capable of varying both temperature and humidity. It is capable of a temperature range of 4.5 °C to 71 °C (40 °F to 160 °F), and can maintain the temperature to within ±0.2 °C, and humidity to ±0.5 % RH. This chamber does not use a wet bulb/dry bulb set up. Instead, a conditioner maintains the dry bulb temperature, while a water spray provides a mist of water to maintain the humidity. The temperature of the mist and the air temperature come to equilibrium and thus provide the desired environmental conditions. A psychometric chart is provided with the chamber in order to be able to set the controls for the appropriate temperature and humidity.

### 2.8.6. Power Supply

The power supply used in these experiments was a model number 1652, manufactured by BK Precision®. It features a triple output DC power supply, with a digital display. It has two variable power supplies, which go from 0 to 24 volts, and have a 0.5 amp current capacity. The other power supply is a fixed 5 volt supply, which has a 4 amp current capacity. The two variable power supplies can be run in constant voltage

or constant current mode. In addition, there is a series tracking feature, which allows them to be used as on 0 to 48 V, 0.5 amp supply, and a parallel tracking feature which allows them to be used as one 0 to 24 V supply, with a 1 amp current capacity. The two variable power supplies are run at a constant 10 volts, and are used as the power source for the internally gaged bolts. The fixed 5 volt supply is used for powering the load washers.

### 2.8.7. Pressure Paper

The pressure paper used in testing is made by Fujifilm and is called Prescale. This pressure paper is used to quantify the maximum pressure distribution in the single bolt connections. When pressure is applied to the Prescale, red patches appear on the film of varying color density (Density: 0.1 ~ 1.4). The varying color density corresponds to different pressure levels. The Prescale can then be analyzed using Photo Shop or a similar program. By analyzing the color density on the film, the maximum pressure distribution in the connection can be seen and quantified.

### 2.8.8. Data Acquisition System

A schematic of the data acquisition system currently employed is shown in Figure 2.15. It is based upon an IOTech Daqboard/2000 plug-in card. The 16-bit resolution, along with an ability to set an internal gain of 64, provided the necessary resolution with which to accurately read the loads in the internally gaged bolts and/or load washers.
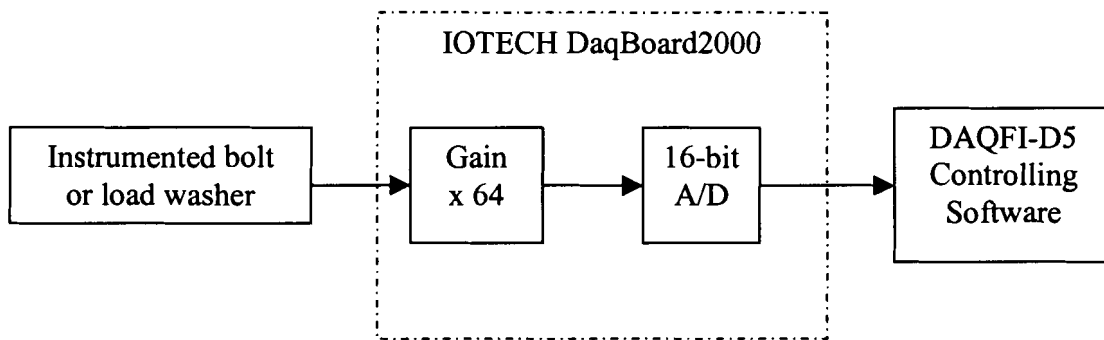
**Figure 2.14 - Data Acquisition System**

Initial tests attempted to use a Vishay 2100 strain amplifier. However, concern with drift over time lead to the use of a 16-bit A/D converter. This eliminated the need for the external amplifier, and the concern over drift of the strain amplifier.

**2.8.8.1. DaqBoard/2000.** The DaqBoard/2000, made by IOtech, is used to collect the voltage output from the hubs, and send it to the computer. The board plugs into a PCI slot on a computer, and enables 8 channels of differential data (16 if single ended) to be read per board. Two boards are connected to each computer, enabling 16 channels to be read in differential mode by each computer. The card has a 16-bit resolution, and when used at a range of ±10 V and a gain of 64, corresponds to a voltage resolution of 0.002384 mV.

**2.8.8.2. Delphi 5 Data Acquisition Program.** The DAQFI-D5 software, written at the University of Maine, controls the data acquisition system. A special dialog was written for the stress relaxation testing. The data configuration and setup screens for the

stress relaxation testing are shown in Figures 2.16 and 2.17. The screen shown in Figure

2.16 is where input data such as the number of channels being used, the number of

averages, and whether the test is being run in single ended or differential mode is

specified. This group of tests needs to be run in differential mode, as per sensor

requirements. A channel can be turned on or off at this screen. The number of averages

allows the user to gain more accurate data by allowing the program to record several

readings at one instant in time, and average them together to obtain a single data point.

Figure 2.17 shows the configuration screen for each individual sensor.

Calibration factors are entered in this section of the program. Tabulated values for these

calibrations are given in Tables 2.7 and 2.8. The second area on this screen is the voltage

offset.
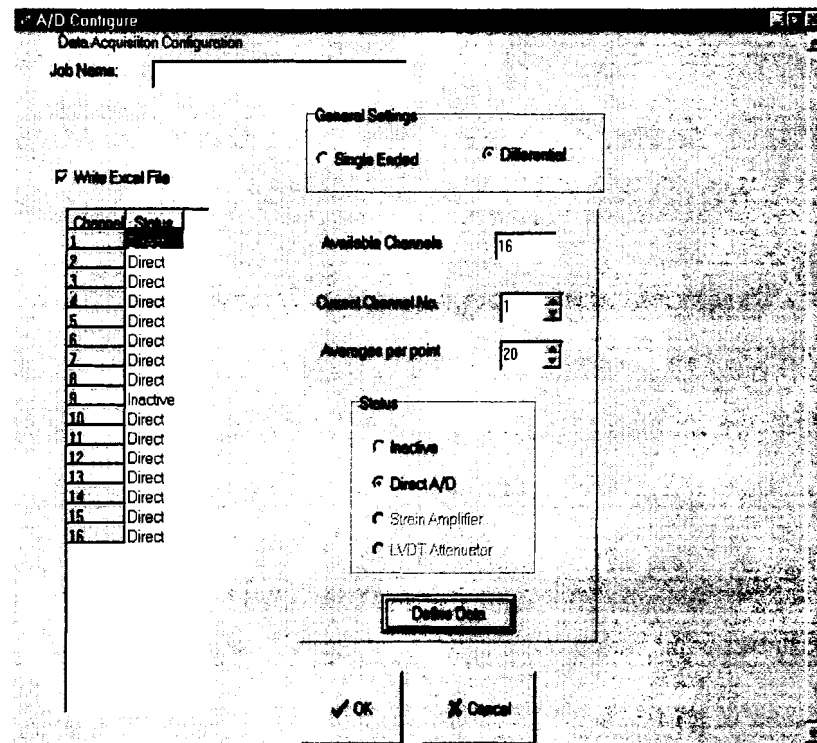


Figure 2.15 – DaqFi-D5 Configuration A
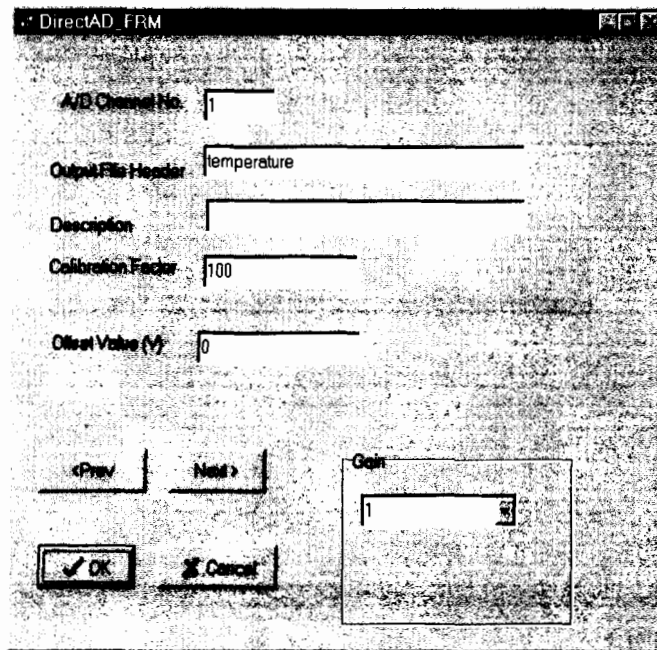
**Figure 2.16 – DaqFi-D5 configuration B**

The voltage bias, taken with no load applied to the connection, is entered into the voltage offset section of this configuration screen. Accordingly, the resulting load is:

$$(V_{in} - V_{offsett}) \cdot Calibration \qquad (2.2)$$

All other information in these two screens is headers for the data file. This is information such as a description of the data file, and a description of each channel.

Figure 2.18 shows the actual stress relaxation data recording program. The data recording schedule is shown on the left side of the screen, and is currently hard coded into the program. Below that is a place to select the name and location of the output data file. Under that is a box labeled Run Test.

58

**Stress Relaxation Data Acquisition**

| Range | Days | Sampling Interval | | | |
|---|---|---|---|---|---|
| | | Days | Hours | Minutes | Seconds |
| 1 | Start to 1 hour | | | | |
| 2 | 1 hour to 24 hours | | | | |
| 3 | 24 hours to 30 days | | | | |
| 4 | 30 days to 4 weeks | | | | |
| 5 | 4 weeks to end | | | | |

Write To File    Select File Name

C:\WINNT\Profiles\delphi\Desktop\starting points\half and three reloading 6.dat

**Monitor Load**

Refresh Rate 1

Current Increment    3

Status    Paused

Multiple Data Sets 1

Acquire    Stop    Clear

**Load Data**

| Channel | Volts | LOAD |
|---|---|---|
| 1 | 0.79086 | 7.9086E+001 |
| 2 | 0.00699 | 4.0149E+003 |
| 3 | 0.00986 | 4.2112E+003 |
| 4 | 0.01020 | 4.6532E+003 |
| 5 | 0.00738 | 4.1868E+003 |
| 6 | 0.00747 | 3.2388E+003 |
| 7 | 0.00755 | 3.3471E+003 |
| 8 | 0.00851 | 8.8912E+003 |
| 10 | 0.00954 | 9.9185E+003 |
| 11 | 0.00855 | 8.7700E+003 |
| 12 | 0.00586 | 5.8892E+003 |
| 13 | 0.00610 | 7.3538E+003 |
| 14 | 1.51519 | 4.9368E+001 |
| 15 | 0.01055 | 4.7986E+003 |
| 16 | 0.00729 | 1.3671E+004 |

**Run Test**

| Status | Running |
|---|---|
| Current Range | 3 |
| Current Increment | 35 |

Run    Abort

Figure 2.17 - DaqFi-D5 Stress Relaxation Program

This is where the program can be started or stopped. This box also dynamically lists which data taking cycle the program is currently on.

On the right side of the screen, there is a place that monitors both the output voltage for each channel, as well as the load on each channel. This is active when the program is taking data, but can also be activated in a manual mode. The refresh rate controls the data rate in manual mode. Below that is where the monitor can be turned on or off while the program is not in the run mode. The monitor allows the user to observe the load being applied to the sensors as the bolts are being tightened.

There is also a log button located on this screen. It allows the user to log a single data point, with a time stamp, during the setup phase, as the bolts are initially tightened or during reloading. Without this feature, some critical initial data would be lost, as the automated data acquisition system cannot be started until all bolts are tightened to the desired load. With this log button, one bolt can be tightened, a data point can be logged, and the initial load on every channel can be recorded, then the data acquisition can be started in the run mode when all bolts are tightened to the desired load level.

## 2.9. Pilot Test Results

The first sets of tests were relatively short-term tests that were performed to verify the testing methods. Figure 2.19 shows the results from one pilot test run using the compression block test fixture. These tests were run for approximately one week to determine any problems that might occur during testing.

Figure 2.18 – Compression Block Pilot Test Results

This group of tests was run prior to the DAQFI data acquisition program, and validated the need for an automated data taking system. It was run using an external power supply to supply the bridge excitation, and a voltmeter to record the data points.

The four bolts are labeled 1 through 4, with bolt 1 being on the opposite side from bolt 3. The top graph in Figure 2.19 shows the bolt load for each sensor and portrays the relaxation experienced by each bolt during testing. The bottom graph shows the same data normalized with respect to each bolt's initial preload. It was desired that all bolts be loaded to the same value during the tests, and this test displayed the need for procedure modification. First of all, a loading fixture is necessary to keep the compression block from rotating during loading. Without the fixture, the compression block had to be held in place as best as possible by hand, which lead to issues with being able to tighten each bolt to the same preload. Due to the geometry of the compression block, each bolt has an effect on the load in the other bolts.

Figures 2.20, 2.21, and 2.22 show results from initial pilot tests for reloading of ½", ¾", and 1" thick single bolt hybrid connections, respectively. This series of tests were run for slightly over 1 month. These tests also showed the need for a few adjustments to the testing procedures and the DAQFI program.

Once again, the need for a loading fixture to keep the specimens from rotating is seen in this group of tests. The two other adjustments made after this series of tests were to the DAQFI program. The jaggedness in the curves is due to the inability, in part, to adjust the gain in the program. A selectable gain was added to the program to reduce fluctuation in the readings.

1/2 reloading test
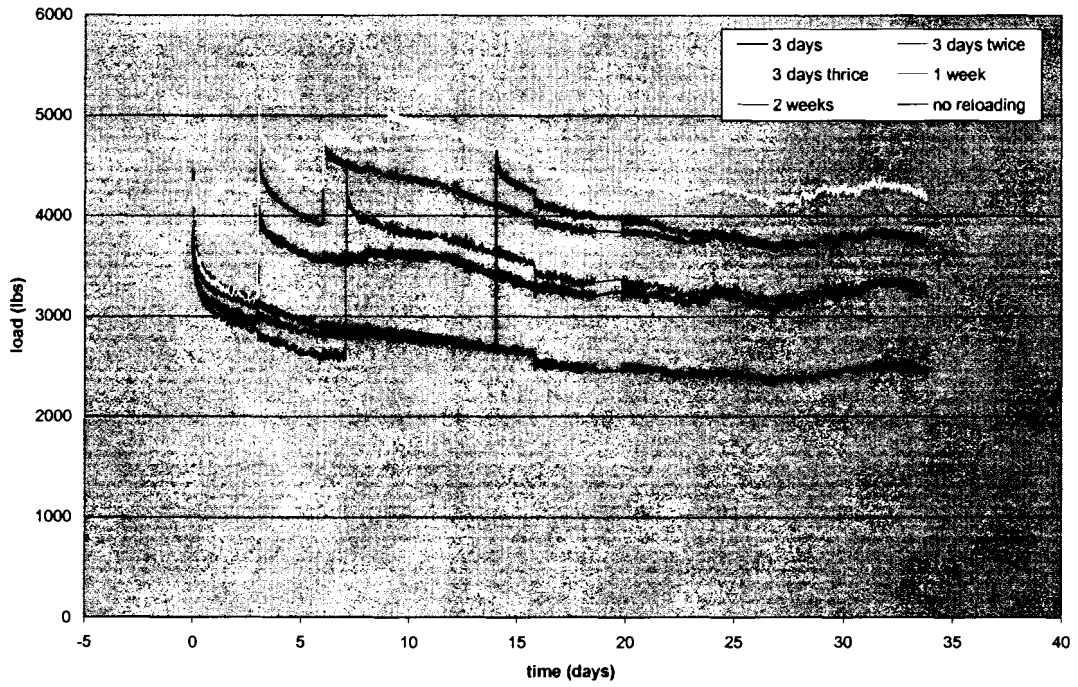
**Figure 2.19 – ½" Reloading Pilot Test**



3/4 inch reloading

**Figure 2.20 – ¾" Reloading Pilot Test**

63
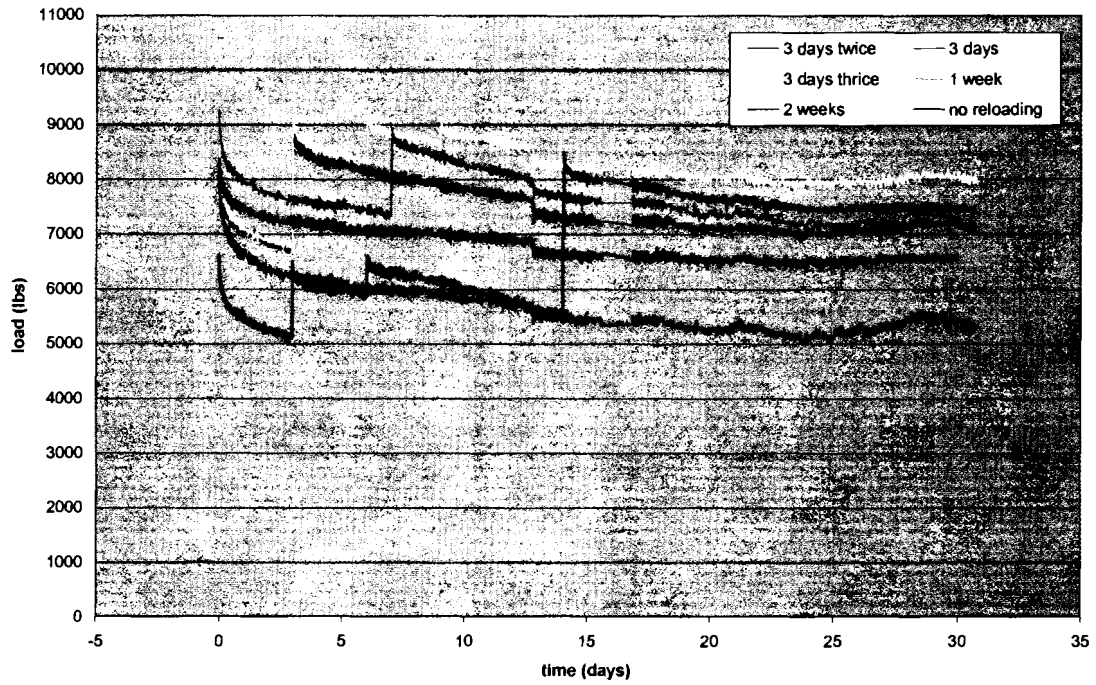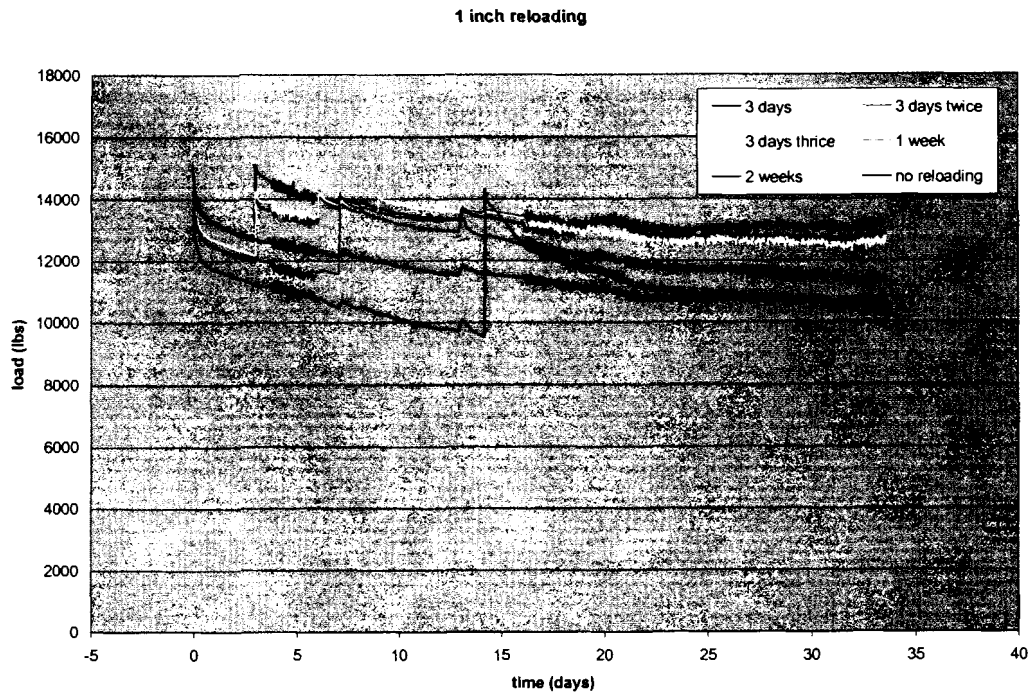
**Figure 2.21 – 1" Reloading Pilot Test**

The other feature that was added to the software at this stage in experimentation was the manual log button. This was done to insure that a data point was logged for each bolt exactly when initial preload was reached.

## 3.  TEST RESULTS

### 3.1. Compression Block Test Results

Figure 3.1 shows the results from a compression block test loaded to an initial preload of 10,000 pounds. Great effort was made to get each bolt loaded as close as possible to the initial preload goal of 10,000 pounds. However, due to the geometry of the fixture, it is difficult to load each bolt to the same preload. The actual preload on each bolt was 10,480 lbs. for bolt #1, 10,120 lbs. for bolt #2, 10,740 lbs. for bolt #3, and 10,000 lbs. for bolt #4. As stated in section 2.2, the geometry of the fixture is set up so that bolt numbers 1 and 3 are opposite of each other, and bolt numbers 2 and 4 are also opposite of each other.

All four bolts show a reduction in the initial preload that occurs at roughly the same rate. Each bolt lost roughly 15 % of its initial preload over the time period of 110 days. Final loads for all four bolts were 8,320 lbs for bolt #1, 8,660 lbs for bolt #2, 9,510 lbs for bolt #3, and 8,490 lbs for bolt #4.

Figure 3.2 shows a second compression block test loaded to an initial preload of approximately 5,000 pounds. Actual initial preloads were 5010 lbs. for bolt 1, 5000 lbs. for bolt 2, 5,000 lbs. for bolt 3, and 5,020 lbs. for bolt 4. Final loads for each bolt after the 115 day period were 4,550 lbs. for bolt 1, 4470 lbs. for bolt 2, 4,380 lbs. for bolt 3, and 3,730 lbs. for bolt 4. Bolts 1, 2, and 3 all lost roughly 10 % of their initial preloads,
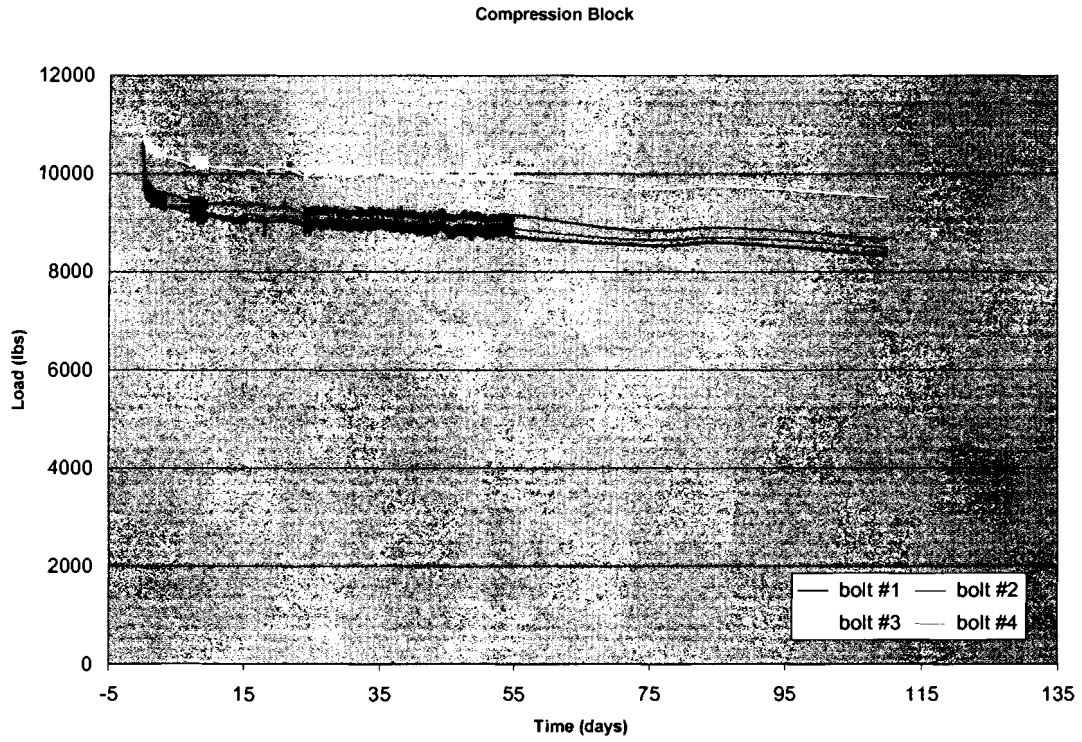
**Figure 3.1 – Compression Block Test Results with a Preload of 10,000 lbs.**
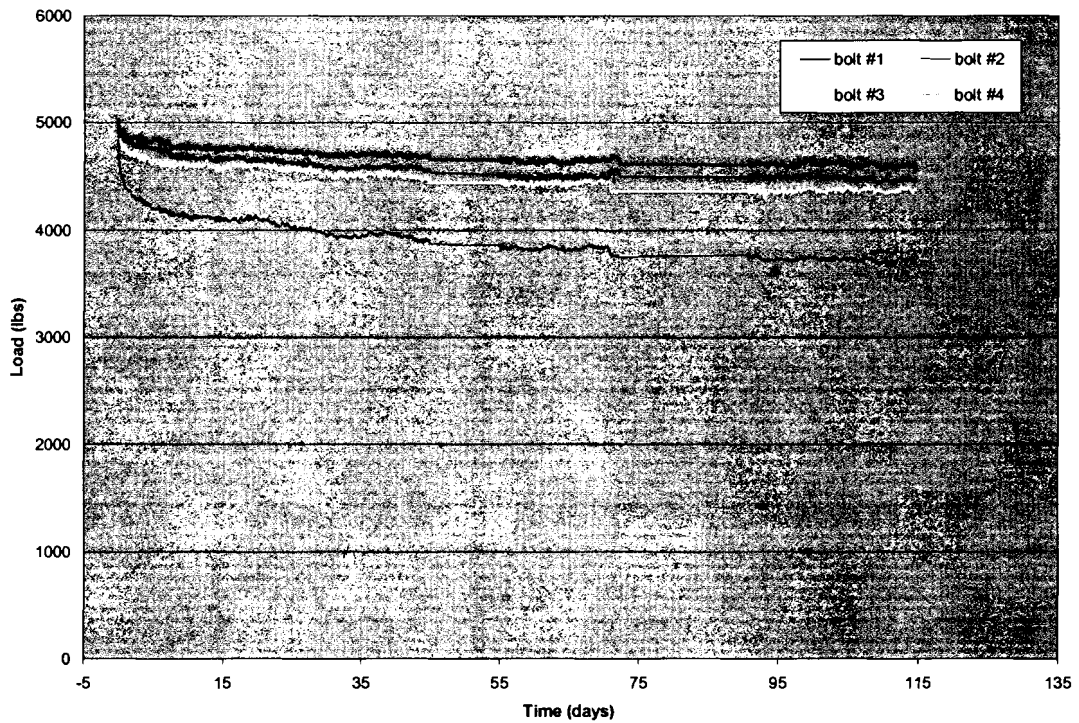


**Figure 3.2 – Compression Block Test Results with a Preload of 5,000 lbs.**

while bolt 4 lost roughly 25 % of its initial preload. It is unknown at this time why bolt 4 lost so much of the initial preload.

## 3.2. Single Bolt, Reloading Hybrid Connection Test Results

Figures 3.3, 3.4 and 3.5 show results from three groups of ½" thick single bolted reloading test specimens. All three of these tests were run for a time period of slightly over 90 days. Each specimen in Figure 3.3 was preloaded to 2,500 lbs, while the specimens in Figures 3.4 and 3.5 were preloaded to 5,000 lbs, with a variance of ±1%. When reloading specimens, they were also loaded to their initial preloads. Temperature and humidity are displayed at the bottom of the graphs in Figures 3.4 and 3.5, on a separate y-axis, with temperature in degrees Fahrenheit, and humidity in %RH, while temperature alone is displayed at the bottom of Figure 3.3.

Figures 3.3 and 3.4 seem to show a large temperature dependence on the stress relaxation of the reloaded bolted connections. The specimens in Figure 3.3 underwent short temperature shifts of between 5 and 20 degrees Fahrenheit, and these shifts show in the results. In Figure 3.4, there are two places on the graph where this temperature dependence is best shown. In general, temperature in the room was around 80 °F for this series of tests. Around day 31, however, there was a small temperature drop to about 75 °F. Corresponding to this drop, there is a drop in the load that each specimen is maintaining. Between days 46 and 60, there is a prolonged temperature increase of roughly 5 °F, from about 80 °F to 85 °F. This increase corresponds to a sharp increase in the stress relaxation of the specimens, especially those reloaded multiple times.
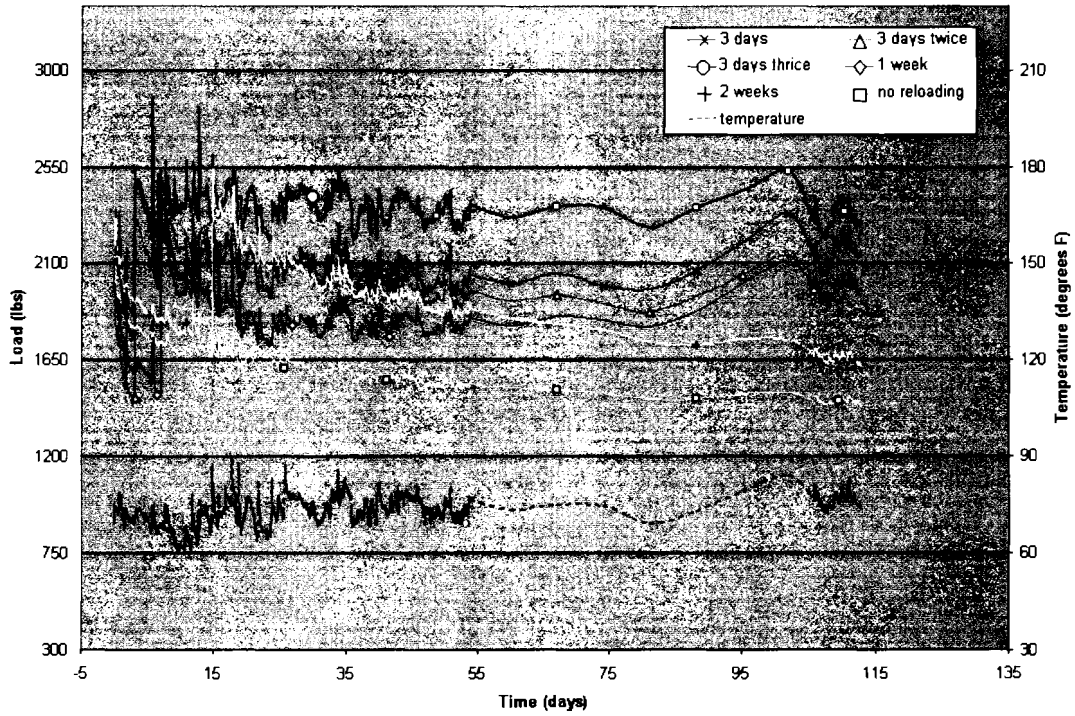
**Figure 3.3 - ½" Reloading Tests with a Preload of 2,500 lbs.**
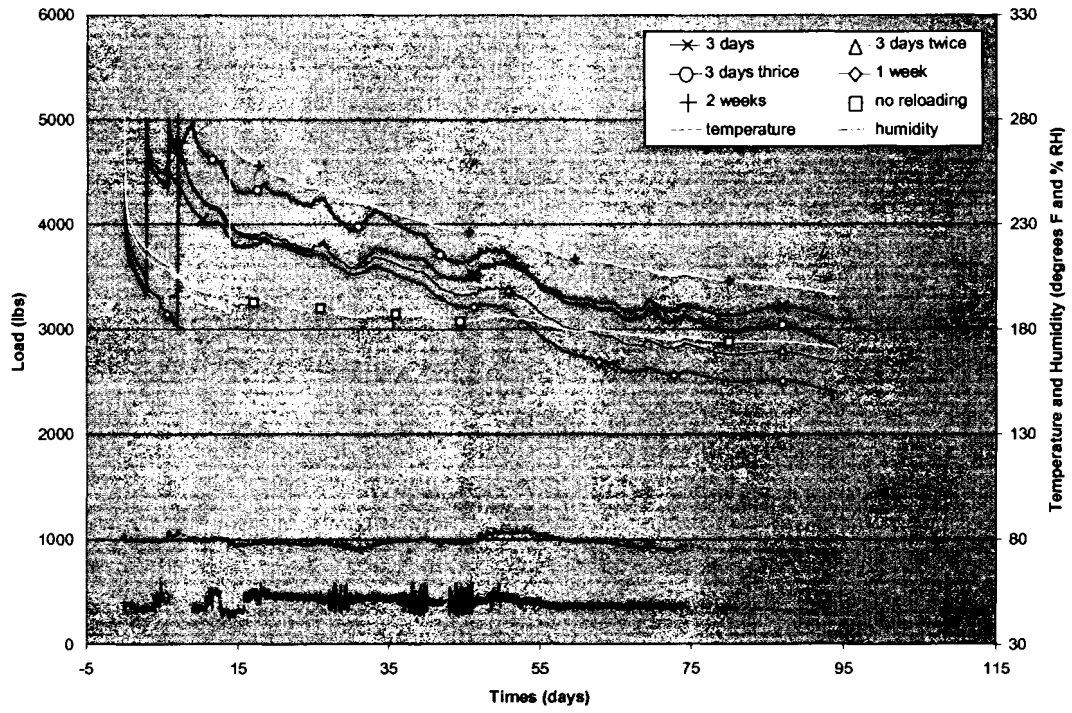


**Figure 3.4 – 1ˢᵗ ½" Reloading Test with a Preload of 5,000 lbs.**
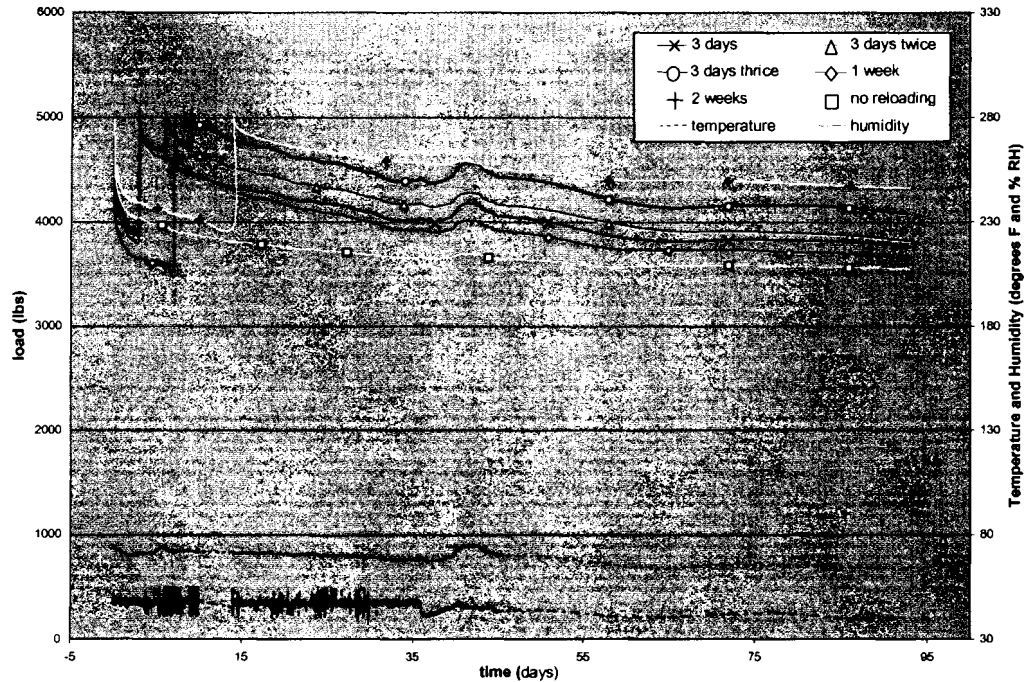
**Figure 3.5 – 2<sup>nd</sup> ½" Reloading Test with a Preload of 5,000 lbs.**

This is also evident on the graph in Figure 3.5, though to a much less degree.
The room temperature when running these tests was roughly 10 °F lower than the
previous tests. Between days 40 and 45 of this group of tests, there was a temperature
increase of about 5 °F. During this time, the load in the connections increases slightly.
This increase is more prominent in the connections that have been reloaded multiple
times. The loads in the connections return to what is expected after the temperature has
returned to normal. In general, the reloaded connections seem to be very sensitive to
temperature fluctuations, particularly extended periods of temperature changes, even
relatively small changes.

Figures 3.6 and 3.7 are results from two reloading tests performed using the ¾"
diameter bolts.
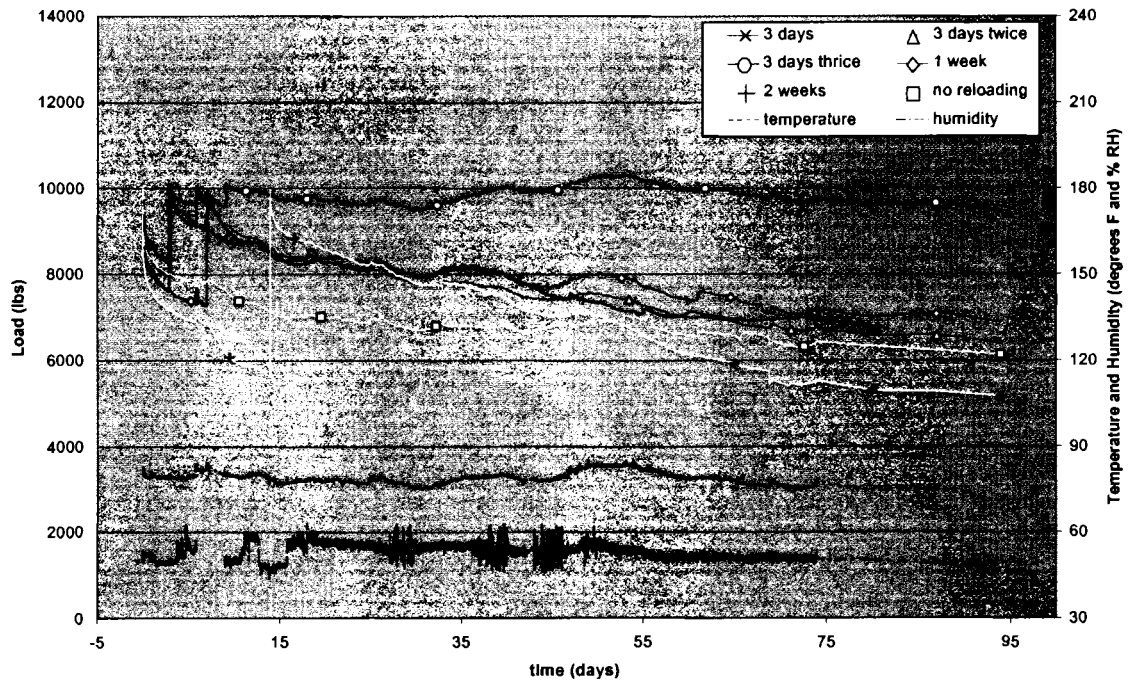
**Figure 3.6 - 7/8" Reloading Tests with a Preload of 10,000 lbs.**



**Figure 3.7 – ¾" Reloading Tests with a Preload of 10,000 lbs.**

70
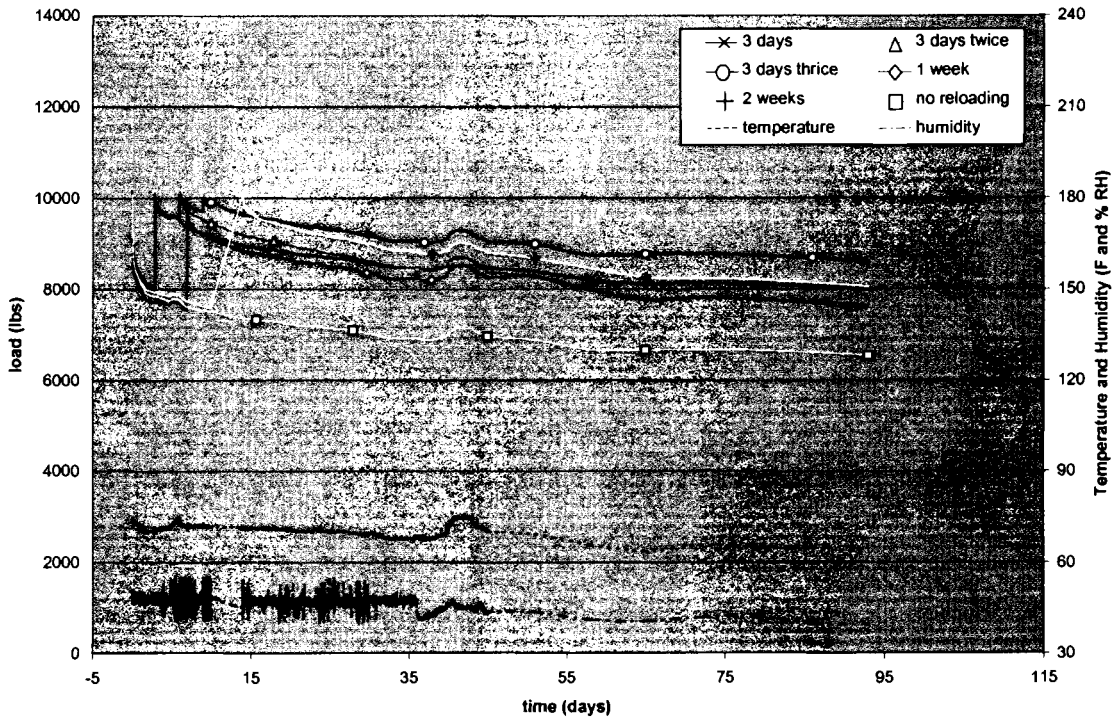
Results in Figure 3.6 show results from 7/8" thick composite specimens bolted to ¾" thick aluminum plates with the ¾" bolts. A ¾" panel was not prepared to be tested at the time this trial was run, so the decision was made to use a 7/8" panel. Figure 3.7 shows the results from test run using ¾" thick composite samples. Both of these tests were also run for a time period of just over 90 days. Each of the test specimens were loaded to 10,000 lbs, ±1%. In addition, reloading was done to 10,000 lbs, ±1%. Again, temperature (degrees Fahrenheit) and humidity (%RH) are at the bottom of each graph.

These tests show the same temperature effects that the ½" thick tests show. The tests shown in Figure 3.6 were run at the same time as those in Figure 3.4, while the tests in Figure 3.7 were run at the same time as those in Figure 3.5. The graph in Figure 3.6 shows similar changes in stress relaxation over the same time periods as the graph in Figure 3.5. Figure 3.7 shows a similar load increase as the data in Figure 3.5, which corresponds to the temperature spike at day 40.

Figure 3.8 shows the results of reloading tests performed on 1 inch thick panels, using the 1" diameter bolts. Each bolt was loaded to 15000 lbs, ±1% for this series, and reloading was also done to the same value. This series of tests was run during the same time period as the tests in Figures 3.5 and 3.7. It has the same temperature spike around day 40, and experiences brief load increases on all channels corresponding to that temperature shift. The load levels return mostly to normal after the temperature has dropped back to its previous level. Figure 3.9 shows results of tests performed on 1 inch thick panels again using the 1" diameter bolts. For this group of tests, the bolts were only loaded to 7,500 lbs, ±1 %.
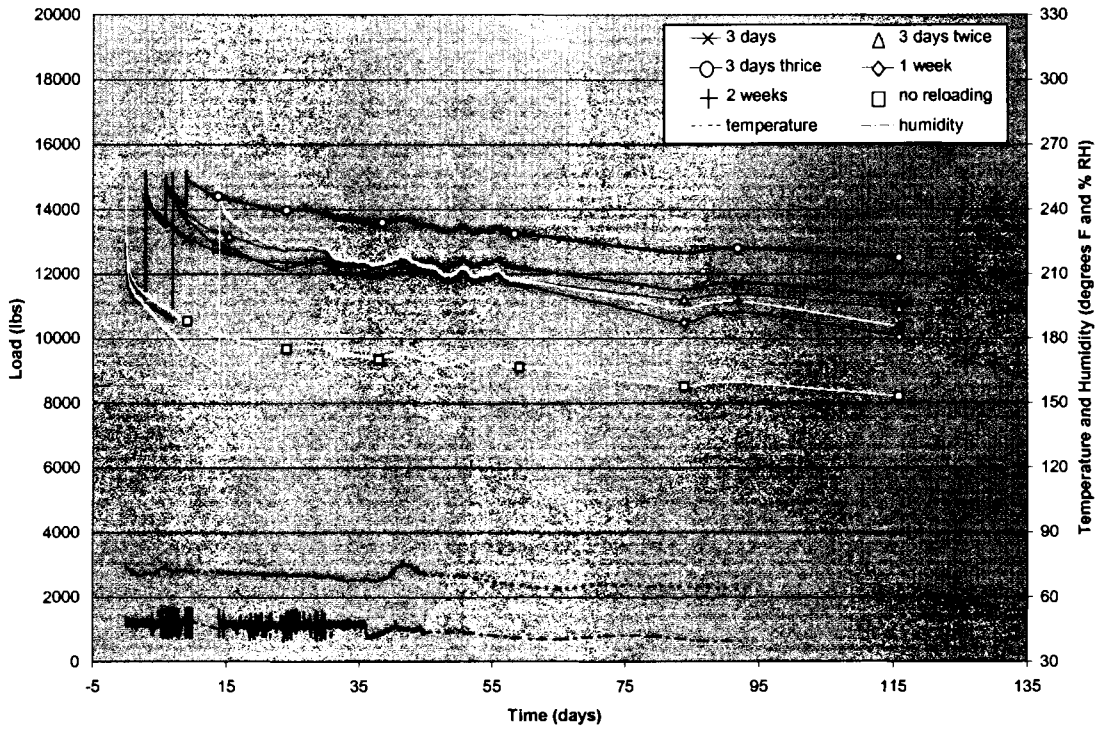
**Figure 3.8 – 1" Reloading Tests with a Preload of 15,000 lbs.**
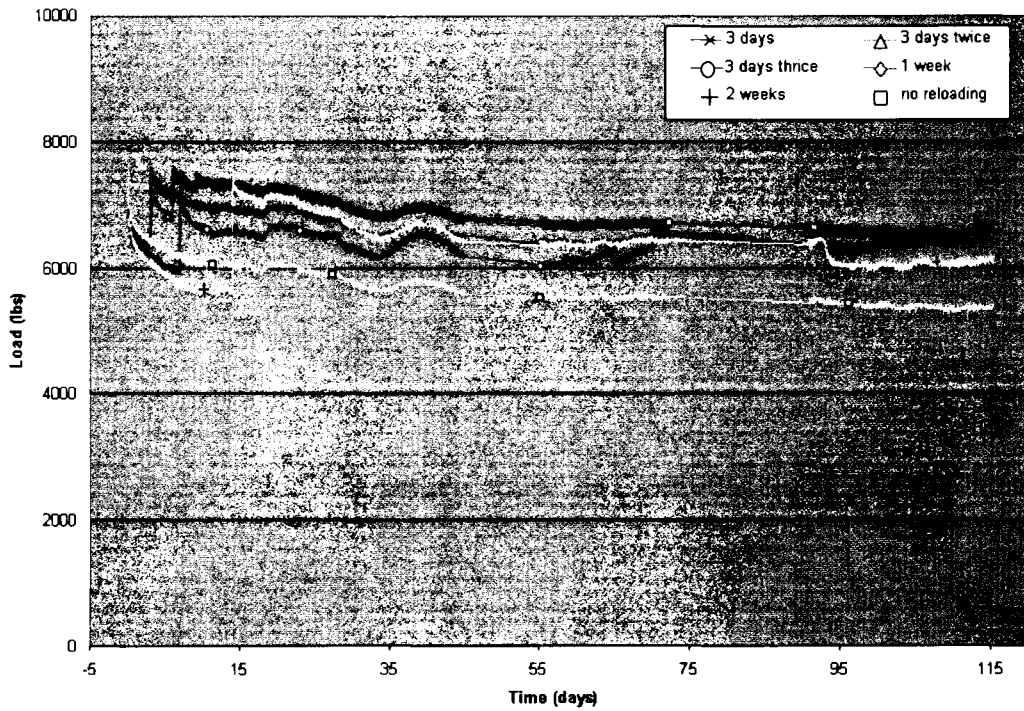


**Figure 3.9 – 1" Reloading Tests with a Preload of 7,500 lbs.**

No temperature or humidity data were recorded for this group of tests, since the second computer that was reading the temperature and humidity were moved during the time this group of tests was run.

### 3.3. Single Tapered Head vs. Non-Tapered Head Bolt Test Results

Figure 3.10 shows results from both tapered and non-tapered head bolts when loaded to 10000 lbs, ± 1 %. This group of four test specimens was run during the same time period. The tests were run in a room that had standard room temperatures and humidity. No temperature or humidity data were recorded for this group of tests, since there seems to be very little effect from small changes at ambient temperature when there is no reloading in the connection. There was no reloading done on this group of tests, since these tests were designed solely to study if using tapered head bolts changed the rate of stress relaxation when compared to non-tapered head bolts. For this group of tests, three tapered head bolts and one non-tapered head bolt were used. The results show no significant difference in stress relaxation rate between the connections with tapered head bolts and the connection with the non-tapered head bolt.

The next group of tests, shown in Figure 3.11, shows results from tapered and non-tapered head bolts loaded to an initial preload of 5000 lbs, ±1 %. Again, no reloading was done on this series of tests. No humidity or temperature data were recorded, since the tests were running at ambient temperature. This group of tests used two tapered head bolts, and two non-tapered head bolts. Again, no significant difference is seen between the stress relaxation rate of the tapered head bolts and the stress relaxation rate of the non-tapered head bolts.
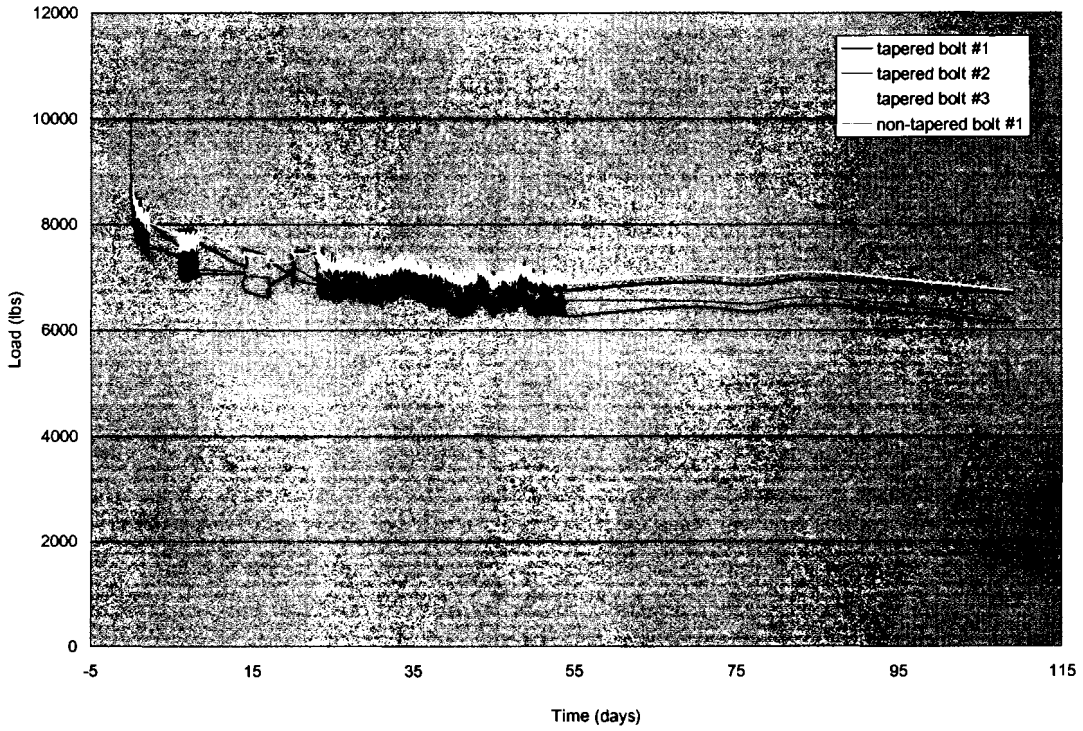
**Figure 3.10 – Tapered and Non-Tapered Head Bolt Test Results at 10,000 lbs.**
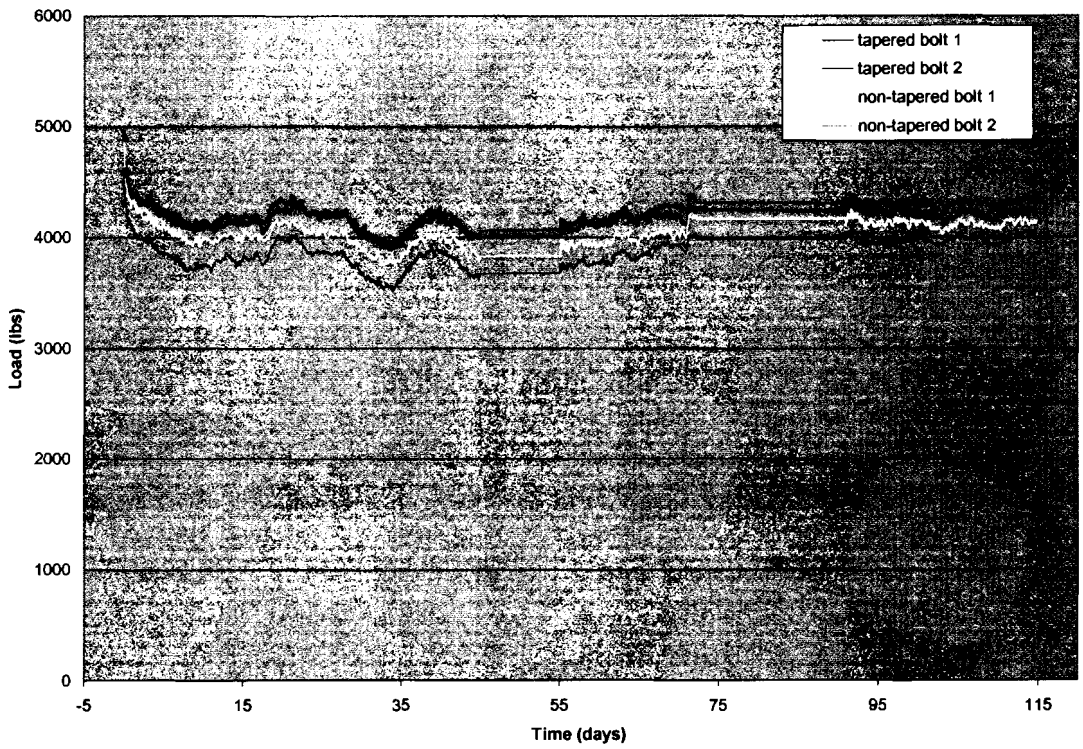


**Figure 3.11 – Tapered and Non-Tapered Head Bolt Test Results at 5,000 lbs.**

## 3.4. Pressure Distributions

Pressure distributions were measured for several of the single bolted tests using the Prescale pressure paper from FujiFilm. The pressure paper was used in both the reloading tests and the tapered head vs. non-tapered head bolts tests. Since the pressure paper used only shows the maximum pressure distribution in the connection, reloading the connection to the same initial preload does very little to the pressure distribution. For this reason, the pressure distributions in the reloading tests do not change significantly between tests done with different loading cycles. Figure 3.12 shows a chart that shows the pressure corresponding to the colors in each pressure distribution. When analyzing the pressure distribution, there was not a clear separation between the different stress levels when one stress level changes to another. Thus the chart shows a gradual change in colors from one stress level to another.

Figures 3.13, 3.14, and 3.15, show pressure distributions from three of the control tests done with no reloading in the connections. Figure 3.13 is the pressure distribution between the composite and aluminum from one of the one inch tests specimens loaded with an initial preload of 15,000 lbs. Very little of the pressure applied to the connection by the bolt actually makes it to the center of the connection, as compared to the other thicknesses. This is likely due to the increase in thickness of the composite. Due to the greater thickness, the composite deflects less, and thus leaves less of a pressure distribution on the pressure paper. Figure 3.14 shows the pressure distribution from one of the ¾" thick test specimens loaded to 10,000 lbs. Being a thinner specimen, the pressure distribution shows better in this figure. It is applied over a larger area than that of the ½ inch thick specimens, but due to the stiffness, the magnitude at the center is not

| | |
|---|---|
| | Greater than 7.83 ksi |
| | 7.83 ksi |
| | 6.16 ksi |
| | 5.08 ksi |
| | 4.21 ksi |
| | 3.19 ksi |
| | 2.03 ksi |
| | Less than 2.03 ksi |
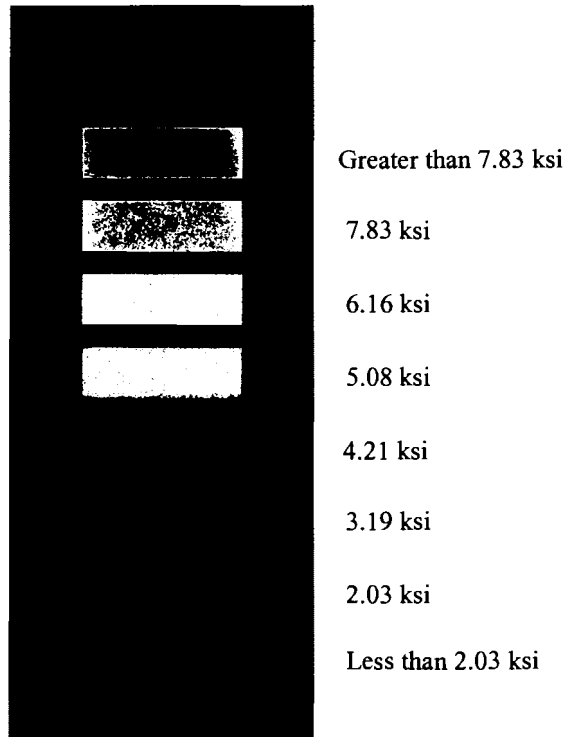
**Figure 3.12 – Pressure Distribution Color Chart**
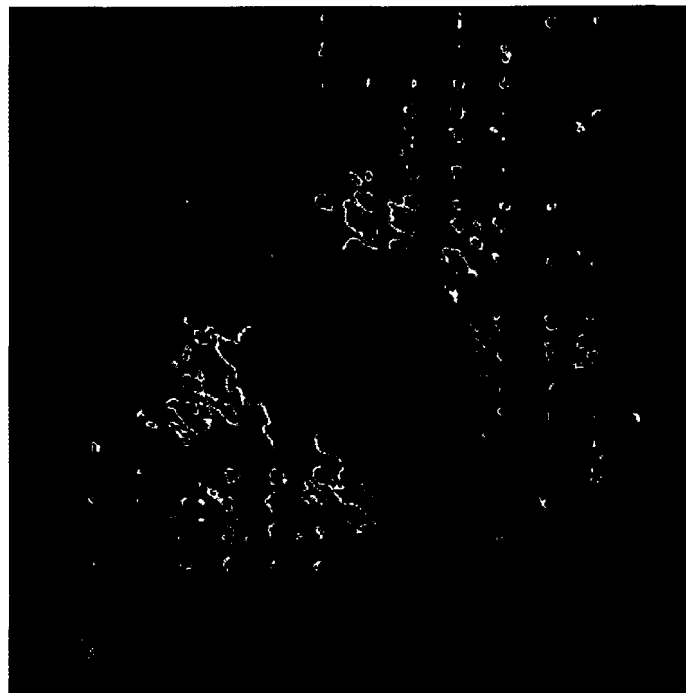


**Figure 3.13 – Pressure Distribution for 1" Thick Specimen Loaded to 15,000 lbs.**

Figure 3.14 – Pressure Distribution for ¾" Thick Specimen Loaded to 10,000 lbs.
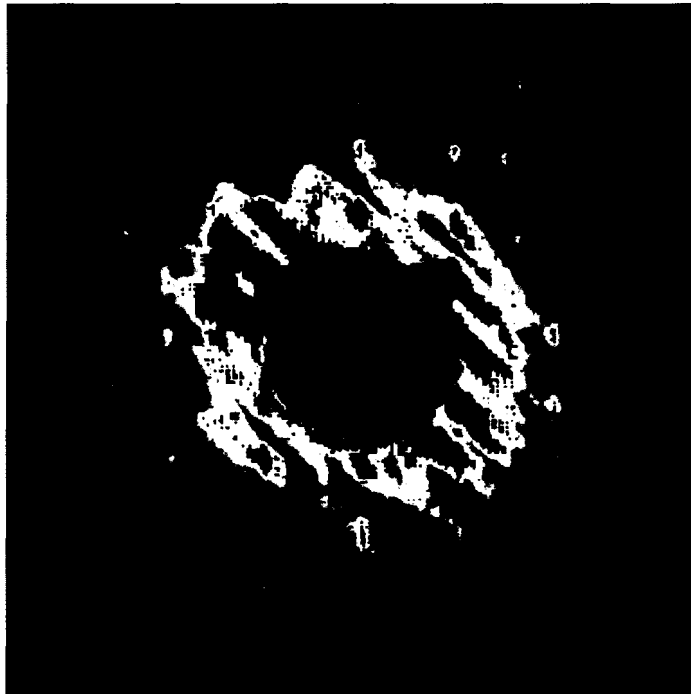


Figure 3.15 – Pressure Distribution for ½" Thick Specimen Loaded to 5,000 lbs.

as great. Figure 3.15 shows the distribution from one of the ½" thick test specimens loaded initially to 5,000 lbs. This shows pressure in this size connection is more evenly distributed, though it is applied over a much smaller area. The pressure at the center is also at the limit of what the pressure paper can detect.

Figures 3.16 and 3.17 show the pressure distribution of one of the tapered head bolt connections and one of the non-tapered bolt connections, respectively. Both test specimens were ¾" thick, and were loaded to 10,000 lbs. The pressures from these two tests are very similar to each other. Both are fairly evenly distributed over the central area of the connection. The only slightly noticeable difference between the two is that the tapered head bolt seems to be applying the pressure much or evenly over the connection than the non-tapered head bolt.

## 3.5. Quantifying the Effects of Stress Relaxation on the E-Glass/Vinylester Composite

The general effects that stress relaxation has on the composite used in testing in the transverse direction can be seen in the results of the compression block tests, shown in section 3.1. Under relatively uniform loading, a great deal of the stress relaxation occurs over the first week after tightening. After a period of between 2 and 3 weeks, the load starts to level off, and is not dropping so rapidly. There is not much difference in the applied load between week 3 and the end of the 3-month time period.

The rate that the composite looses load over time most closely fits a power law curve, as follows:

$$P_t = \beta P_I t^\alpha \qquad\qquad (3.1).$$
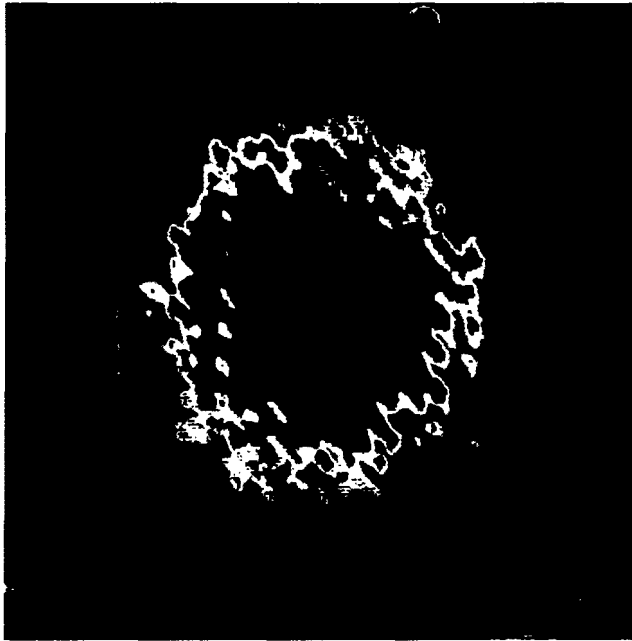
**Figure 3.16 – Pressure Distribution for Tapered Head Bolt Test Loaded to**

**10,000 lbs.**



**Figure 3.17 – Pressure Distribution for Non-tapered Head Bolt Test Loaded to**

**10,000 lbs.**

In this equation, $P_t$ is the load at a given time, in pounds, $\beta$ is a constant dependent on pressure distribution and reloading cycle, $P_1$ is the preload, t is the time in days, and $\alpha$ is a constant which seems to be based on specimen thickness, initial preload, and material properties of the composite. The constant, $\beta$, seems to be roughly 1 with a relatively uniform pressure distribution and no reloading. It is below 1 when there is no uniform loading, and if the connection is reloaded. More testing needs to be done to determine what relationship $\alpha$ has to material properties, thickness, and preload.

Based on a power law fit to the curves, equations were developed for the load in each bolt over time in the compression block tests. These equations are shown in Tables 3.1 and 3.2 for two different load levels. Table 3.3 gives the values of $\beta$ for each bolt, as well as an average value, while Table 3.4 gives the values of $\alpha$. As seen in Table 3.3, the constant $\beta$ is approximately 0.95 in each bolt, since the constant in front of the equations is very close to the initial preload. In addition to the individual load equations for each bolt, a general equation is shown based on average values of $\beta$ and $\alpha$. These equations apply only to the cases where the specimen is ½" thick and the applied preload is either 10,000 or 5,000 pounds respectively. The equations developed fit the data very closely, with little error.

Tables 3.5 and 3.6 show estimates of the load in each bolt at different times, based on the power law equations from Tables 3.1 and 3.2. The actual data at 1, 2, and 3 month matches these estimates very closely. From these estimates, an average load in the composite at the given times was calculated, which is given at the bottom of the table.

**Table 3.1 – Equations for Uniformly Compressed ½" Thick Specimen Loaded to**

**10,000 lbs.**

| bolt number | Equation |
|---|---|
| 1 | $P = 9544t^{-0.0201}$ |
| 2 | $P = 9629t^{-0.0133}$ |
| 3 | $P = 10439t^{-0.0121}$ |
| 4 | $P = 9434t^{-0.0147}$ |
| average | $P = 9761t^{-.0151}$ |

**Table 3.2 – Equations for Uniformly Compressed ½" Thick Specimen Loaded to**

**5,000 lbs.**

| bolt number | Equation |
|---|---|
| 1 | $P = 4890t^{-0.0117}$ |
| 2 | $P = 4845t^{-0.0158}$ |
| 3 | $P = 4758t^{-0.0168}$ |
| 4 | $P = 4453t^{-0.0353}$ |
| average | $P = 4737t^{-0.0199}$ |

**Table 3.3 - β Values for Compression Block Tests**

| 1/2 inch thick, 10000 lbs | | | 1/2 inch thick, 5000 lbs. | | |
|---|---|---|---|---|---|
| | bolt # | beta | | bolt # | beta |
| | 1 | 0.91 | | 1 | 0.98 |
| | 2 | 0.95 | | 2 | 0.97 |
| Test 1 | 3 | 0.97 | test 2 | 3 | 0.95 |
| | 4 | 0.94 | | 4 | 0.89 |
| | average | 0.95 | | average | 0.95 |

## Table 3.4 - α Values for Compression Block Tests

| 5000 lbs. | |
|---|---|
| bolt number | Equation |
| 1 | 0.012 |
| 2 | 0.016 |
| 3 | 0.017 |
| 4 | 0.035 |
| average | 0.020 |

| 10000 lbs. | |
|---|---|
| bolt number | Equation |
| 1 | 0.020 |
| 2 | 0.013 |
| 3 | 0.012 |
| 4 | 0.015 |
| average | 0.015 |

## Table 3.5 – Load Predictions for a Uniformly Loaded ½" Thick Composite Specimen Loaded to 10,000 lbs.

| bolt # | Load Estimates using Power Law Equations (lbs) | | | | | | |
|---|---|---|---|---|---|---|---|
| | 1month | 2 months | 3 months | 6 months | 1 year | 5 years | 10 years |
| 1 | 8913 | 8790 | 8719 | 8598 | 8479 | 8209 | 8096 |
| 2 | 9203 | 9118 | 9069 | 8986 | 8904 | 8715 | 8635 |
| 3 | 10018 | 9934 | 9886 | 9803 | 9721 | 9534 | 9454 |
| 4 | 8973 | 8882 | 8830 | 8740 | 8652 | 8449 | 8364 |
| | | | | | | | |
| Averages | 9277 | 9181 | 9126 | 9032 | 8939 | 8727 | 8637 |

## Table 3.6 – Load Predictions for a Uniformly Loaded ½" Thick Composite Specimen Loaded to 5,000 lbs.

| bolt # | Load Estimates using Power Law Equations (lbs) | | | | | | |
|---|---|---|---|---|---|---|---|
| | 1month | 2 months | 3 months | 6 months | 1 year | 5 years | 10 years |
| 1 | 4699 | 4661 | 4639 | 4602 | 4565 | 4479 | 4443 |
| 2 | 4592 | 4542 | 4513 | 4464 | 4415 | 4304 | 4257 |
| 3 | 4494 | 4442 | 4412 | 4360 | 4310 | 4195 | 4146 |
| 4 | 3949 | 3854 | 3799 | 3707 | 3618 | 3418 | 3335 |
| | | | | | | | |
| Averages | 4434 | 4375 | 4341 | 4283 | 4227 | 4099 | 4046 |

## 3.6. Effects of Reloading on Stress Relaxation

In general, reloading the bolted hybrid connections seems to decrease the rate of stress relaxation. There is a definite correlation between temperature shifts and the stress relaxation rate in specimens that have been reloaded, however. Based on the graphs in Section 3.2, it seems the more a connection is reloaded, the greater effect temperature changes will have. As shown in those graphs, even small temperature changes of 5 to 10 degrees can cause a rapid increase in the stress relaxation rate, especially on the connections reloaded multiple times.

There also seems to be a correlation between how long a temperature shift lasts and how much the stress relaxation rate increases. Figure 3.3 shows the stress relaxation being effected by temperature shifts quite frequently during testing. Figures 3.4, and 3.6, show the stress relaxation rates increases rapidly after an extended temperature change. In Figures 3.5, 3.7, and 3.8, there is not much change in stress relaxation rate, since the temperature shift occurs in a relatively short time period. Once the temperature returns to normal, the stress relaxation rate returns fairly close to what it was before the temperature change. There seems to be a trade off between reloading and extended temperature changes. Reloading helps to maintain the load in the connections, with varying success, depending on how many times the connection is reloaded, but reloaded specimens are much more sensitive to temperature changes that occur over extended time periods. It also seems that the more a specimen is reloaded, the more sensitive it is to those temperature changes.

Table 3.7 gives the power law equation for each test specimen from the tests shown in Figures 3.3, 3.4, 3.5, 3.6, 3.7, 3.8, and 3.9. These are based on taking the

starting time on each curve to be when the connection was loaded for the final time, since this is the curve the data should follow once no more reloading is done. These equations apply only for the specific preloads used during those tests. The preloads for these tests were 2,500 and 5,000 pounds for the ½" thick specimens, 10000 pounds for the ¾" thick specimens, and 7,500 and 15,000 pounds for the 1" thick specimens. These equations slightly overestimate the actual load curves, but in general representative up to the 3 month test period. The equation for the 7/8" thick specimen loaded to 10,000 pound shows that there was a problem with that channel during testing, since it is virtually a straight line.

**Table 3.7 – Equations for the Reloading Tests**

| thickness | Load (lbs) | 3 days | 3 days twice | 3 days thrice | 1 week | 2 weeks | no reloading |
|---|---|---|---|---|---|---|---|
| | | | | Reloading Cycle | | | |
| 1/2 inch | 2500 | $P = 2272t^{-0.0244}$ | $P = 2295t^{-0.0347}$ | $P = 2414t^{-0.0081}$ | $P = 2061t^{-0.0282}$ | $p = 2314t^{-0.0571}$ | $P = 1928t^{-0.055}$ |
| 1/2 inch | 5000 | $P = 4483t^{-0.0649}$ | $P = 4621t^{-0.0683}$ | $P = 4764t^{-0.0746}$ | $P = 4522t^{-0.0078}$ | $P = 4659t^{-0.0513}$ | $P = 3877t^{-0.0608}$ |
| 1/2 inch | 5000 | $P = 4656t^{-0.0345}$ | $P = 4703t^{-0.029}$ | $P = 4802t^{-0.0199}$ | $P = 4467t^{-0.0324}$ | $P = 4800t^{-0.0143}$ | $P = 4145t^{-0.0327}$ |
| 3/4 inch | 10000 | $P = 9507t^{-0.0271}$ | $P = 9569t^{-0.0288}$ | $P = 9686t^{-0.0153}$ | $P = 9172t^{-0.0259}$ | $P = 9500t^{-0.019}$ | $P = 8163t^{-0.0408}$ |
| 7/8 inch | 10000 | $P = 9217t^{-0.0473}$ | $P = 9444t^{-0.0642}$ | $P = 9866t^{0.00002}$ | $P = 9123t^{-0.0443}$ | $P = 9148t^{-0.0839}$ | $P = 8312t^{-0.0544}$ |
| 1 inch | 7500 | $P = 7272t^{-0.0272}$ | $P = 7502t^{-0.0282}$ | $P = 7420t^{-0.0235}$ | $P = 6773t^{-0.0166}$ | $P = 7207t^{-0.0322}$ | $P = 6711t^{-0.045}$ |
| 1 inch | 15000 | $P = 13709t^{-0.0288}$ | $P = 14035t^{-0.0375}$ | $P = 14478t^{-0.0188}$ | $P = 13551t^{-0.0344}$ | $P = 13458t^{-0.0282}$ | $P = 11786t^{-0.0584}$ |

Table 3.8 shows values of $\beta$ for each test shown in Figures 3.3, 3.4, 3.5, 3.6, 3.7, 3.8, and 3.9, while Table 3.9 shows the values of $\alpha$. The value of $\beta$ seems to be dependent on both the number of times the connection is reloaded and the reloading cycle. It does not seem to be based on specimen thickness, since it does not seem to change much between the different thicknesses of each of the reloading tests. The constant $\alpha$ seems to be based on more than just the reloading cycle and preload.

**Table 3.8 – Values of the Constant β for the Reloading Tests**

| thickness | Load (lbs) | Reloading Cycle | | | | | |
|---|---|---|---|---|---|---|---|
| | | 3 days | 3 days twice | 3 days thrice | 1 week | 2 weeks | no reloading |
| 1/2 inch | 2500 | 0.91 | 0.92 | 0.97 | 0.82 | 0.93 | 0.77 |
| 1/2 inch | 5000 | 0.93 | 0.94 | 0.96 | 0.89 | 0.96 | 0.83 |
| 1/2 inch | 5000 | 0.90 | 0.92 | 0.95 | 0.90 | 0.93 | 0.78 |
| 3/4 inch | 10000 | 0.95 | 0.96 | 0.97 | 0.92 | 0.95 | 0.82 |
| 7/8 inch | 10000 | 0.92 | 0.94 | 0.99 | 0.91 | 0.91 | 0.83 |
| 1 inch | 7500 | 0.97 | 1.00 | 0.99 | 0.90 | 0.96 | 0.89 |
| 1 inch | 15000 | 0.92 | 0.94 | 0.97 | 0.90 | 0.90 | 0.79 |
| | | | | | | | |
| Averages | | 0.93 | 0.95 | 0.97 | 0.91 | 0.94 | 0.82 |

**Table 3.9 – Values of the Constant α for the Reloading Tests**

| thickness | Load (lbs) | Reloading Cycle | | | | | |
|---|---|---|---|---|---|---|---|
| | | 3 days | 3 days twice | 3 days thrice | 1 week | 2 weeks | no reloading |
| 1/2 inch | 2500 | 0.024 | 0.035 | 0.008 | 0.028 | 0.057 | 0.055 |
| 1/2 inch | 5000 | 0.065 | 0.088 | 0.075 | 0.099 | 0.051 | 0.061 |
| 1/2 inch | 5000 | 0.035 | 0.029 | 0.020 | 0.032 | 0.014 | 0.033 |
| 3/4 inch | 10000 | 0.027 | 0.029 | 0.015 | 0.026 | 0.019 | 0.041 |
| 7/8 inch | 10000 | 0.047 | 0.064 | 0.000 | 0.044 | 0.084 | 0.054 |
| 1 inch | 7500 | 0.027 | 0.028 | 0.024 | 0.017 | 0.032 | 0.045 |
| 1 inch | 15000 | 0.029 | 0.038 | 0.019 | 0.034 | 0.028 | 0.058 |

Based on these equations, predictions can be made for the loads at different times. Tables 3.10, 3.11, 3.12, 3.13, 3.14, 3.15, and 3.16 show load predictions for the tests shown in Figures 3.3, 3.4, 3.5, 3.6, 3.7, 3.8, and 3.9, respectively. Again, predictions overestimate the actual load in the connection after 3 month by 2 – 8 %, depending on the reloading cycle, but are still fairly accurate.

**Table 3.10 – Load Predictions for ½" Thick Specimens Shown in Figure 3.3**

| loading cycle | Load Estimates using Power Law Equations (lbs) | | | | | | |
|---|---|---|---|---|---|---|---|
| | 1month | 2 months | 3 months | 6 months | 1 year | 5 years | 10 years |
| 3 days | 2091 | 2056 | 2035 | 2001 | 1968 | 1892 | 1860 |
| 3 days twice | 2039 | 1991 | 1963 | 1916 | 1871 | 1769 | 1727 |
| 3 days thrice | 2348 | 2335 | 2327 | 2314 | 2301 | 2272 | 2259 |
| 1 week | 1873 | 1836 | 1816 | 1780 | 1746 | 1668 | 1636 |
| 2 weeks | 1905 | 1831 | 1789 | 1720 | 1653 | 1508 | 1450 |
| no reloading | 1599 | 1539 | 1505 | 1449 | 1395 | 1277 | 1229 |

**Table 3.11 – Load Predictions for ½" Thick Specimens Shown in Figure 3.4**

| loading cycle | Load Estimates using Power Law Equations (lbs) | | | | | | |
|---|---|---|---|---|---|---|---|
| | 1month | 2 months | 3 months | 6 months | 1 year | 5 years | 10 years |
| 3 days | 3595 | 3437 | 3348 | 3201 | 3060 | 2756 | 2635 |
| 3 days twice | 3422 | 3219 | 3106 | 2921 | 2748 | 2384 | 2242 |
| 3 days thrice | 3696 | 3510 | 3405 | 3234 | 3071 | 2723 | 2586 |
| 1 week | 3242 | 3030 | 2912 | 2721 | 2543 | 2173 | 2030 |
| 2 weeks | 3913 | 3776 | 3698 | 3569 | 3445 | 3172 | 3061 |
| no reloading | 3152 | 3022 | 2949 | 2827 | 2710 | 2458 | 2356 |

**Table 3.12 – Load Predictions for ½" Thick Specimens Shown in Figure 3.5**

| loading cycle | Load Estimates using Power Law Equations (lbs) | | | | | | |
|---|---|---|---|---|---|---|---|
| | 1month | 2 months | 3 months | 6 months | 1 year | 5 years | 10 years |
| 3 days | 4140 | 4042 | 3986 | 3892 | 3800 | 3595 | 3510 |
| 3 days twice | 4261 | 4176 | 4127 | 4045 | 3965 | 3784 | 3709 |
| 3 days thrice | 4488 | 4427 | 4391 | 4331 | 4271 | 4137 | 4080 |
| 1 week | 4001 | 3912 | 3861 | 3775 | 3691 | 3504 | 3426 |
| 2 weeks | 4572 | 4527 | 4501 | 4456 | 4412 | 4312 | 4270 |
| no reloading | 3708 | 3625 | 3577 | 3497 | 3419 | 3244 | 3171 |

**Table 3.13 – Load Predictions for 7/8" Thick Specimens Shown in Figure 3.6**

| loading cycle | Load Estimates using Power Law Equations (lbs) | | | | | | |
|---|---|---|---|---|---|---|---|
| | 1month | 2 months | 3 months | 6 months | 1 year | 5 years | 10 years |
| 3 days | 7848 | 7594 | 7450 | 7210 | 6977 | 6466 | 6257 |
| 3 days twice | 7592 | 7261 | 7075 | 6767 | 6472 | 5837 | 5583 |
| 3 days thrice | 9867 | 9867 | 9867 | 9867 | 9867 | 9867 | 9868 |
| 1 week | 7847 | 7610 | 7474 | 7248 | 7029 | 6546 | 6348 |
| 2 weeks | 6877 | 6489 | 6272 | 5917 | 5583 | 4878 | 4602 |
| no reloading | 6908 | 6652 | 6507 | 6266 | 6034 | 5528 | 5324 |

**Table 3.14 – Load Predictions for ¾" Thick Specimens Shown in Figure 3.7**

| loading cycle | Load Estimates using Power Law Equations (lbs) | | | | | | |
|---|---|---|---|---|---|---|---|
| | 1month | 2 months | 3 months | 6 months | 1 year | 5 years | 10 years |
| 3 days | 8670 | 8509 | 8416 | 8259 | 8106 | 7760 | 7615 |
| 3 days twice | 8676 | 8505 | 8406 | 8240 | 8077 | 7711 | 7559 |
| 3 days thrice | 9195 | 9098 | 9041 | 8946 | 8852 | 8636 | 8545 |
| 1 week | 8399 | 8249 | 8163 | 8018 | 7875 | 7554 | 7419 |
| 2 weeks | 8905 | 8789 | 8721 | 8607 | 8495 | 8239 | 8131 |
| no reloading | 7106 | 6907 | 6794 | 6605 | 6420 | 6012 | 5845 |

**Table 3.15 – Load Predictions for 1" Thick Specimens Shown in Figure 3.8**

| loading cycle | Load Estimates using Power Law Equations (lbs) | | | | | | |
|---|---|---|---|---|---|---|---|
| | 1month | 2 months | 3 months | 6 months | 1 year | 5 years | 10 years |
| 3 days | 6630 | 6506 | 6434 | 6314 | 6196 | 5931 | 5820 |
| 3 days twice | 6816 | 6684 | 6608 | 6480 | 6355 | 6073 | 5955 |
| 3 days thrice | 6850 | 6739 | 6675 | 6567 | 6461 | 6221 | 6121 |
| 1 week | 6401 | 6328 | 6285 | 6213 | 6142 | 5980 | 5912 |
| 2 weeks | 6459 | 6316 | 6235 | 6097 | 5962 | 5661 | 5536 |
| no reloading | 5759 | 5582 | 5481 | 5313 | 5150 | 4790 | 4643 |

**Table 3.16 – Load Predictions for 1" Thick Specimens Shown in Figure 3.9**

| loading cycle | Load Estimates using Power Law Equations (lbs) | | | | | | |
|---|---|---|---|---|---|---|---|
| | 1month | 2 months | 3 months | 6 months | 1 year | 5 years | 10 years |
| 3 days | 12430 | 12184 | 12043 | 11805 | 11571 | 11047 | 10829 |
| 3 days twice | 12354 | 12037 | 11856 | 11552 | 11255 | 10596 | 10324 |
| 3 days thrice | 13581 | 13405 | 13304 | 13131 | 12961 | 12575 | 12412 |
| 1 week | 12055 | 11771 | 11608 | 11334 | 11067 | 10471 | 10224 |
| 2 weeks | 12227 | 11990 | 11854 | 11625 | 11400 | 10894 | 10683 |
| no reloading | 9663 | 9279 | 9062 | 8703 | 8358 | 7608 | 7306 |

## 3.7. Effects of Tapered vs. Non-Tapered Bolts

Based upon current results, there seems to be little difference in stress relaxation when using tapered head bolts as opposed to non-tapered head bolts. There seems to be a slight difference in the pressure distributions of the tapered and non-tapered head bolts, but there seems to be little to no effect on the rate of stress relaxation. The lines on the graphs in Figures 3.10 and 3.11 are virtually on top of one another. Tapered head bolts are better at making the pressure distribution in the connection more even, but beyond that, there seems to be no advantage to using tapered bolts over non-tapered ones.

These tests also closely follow a power law fit to the curves, as shown in equation 3.1. Based upon this, equations were generated that best fit each curve. Tables 3.17 and 3.18 show the equations for each of the bolted connections shown in Figures 3.10, and 3.11, as well as an equation which uses an average value of the constants β and α. The Equations from Table 3.18 closely resemble the equation for the reloading tests done on the ¾" thick specimen with no reloading in the connection and a preload of 10,000 lbs, as they should, since no reloading was done to any of the tapered vs. non-tapered test connections, and all connections were loaded to 10,000 pounds preload.

**Table 3.17 – Equations for ¾" Tapered and Non-Tapered Head Bolt Tests When**

**Loaded to 5,000 lbs.**

| bolt number | Equation |
|---|---|
| tapered bolt 1 | $P = 4309t^{-0.0098}$ |
| tapered bolt 2 | $P = 4315t^{-0.0067}$ |
| non-tapered bolt 1 | $P = 4183t^{-0.0103}$ |
| non-tapered bolt 2 | $P = 3944t^{-0.0057}$ |
| **avergage tapered** | $P = 4312t^{-0.0083}$ |
| **average non** | $P = 4064t^{-0.008}$ |

**Table 3.18 – Equations for ¾" Tapered and Non-Tapered Head Bolt Tests When**

**Loaded to 10,000 lbs.**

| bolt number | Equation |
|---|---|
| tapered bolt 1 | $P = 8138t^{-0.0407}$ |
| tapered bolt 2 | $P = 7693t^{-0.042}$ |
| tapered bolt 3 | $P = 8194t^{-0.0388}$ |
| non-tapered bolt 1 | $P = 7806t^{-0.0415}$ |
| **avergage tapered** | $P = 8008t^{-0.0345}$ |

Values for the constant $\beta$ are shown in Table 3.19, while the constant, $\alpha$, is shown in

Table 3.20. The values of $\alpha$ and $\beta$ for the case where the initial preload was 10,000 lbs

are very close to those of the ¾" thick specimen with no reloading and an initial preload

of 10,000 lbs shown in Tables 3.8 and 3.9.

Future predictions were made with these tests, based on the equations for each

connection. These predictions closely match the actual loads in each bolt for the

corresponding 1-month, 2 months, and 3 months time periods. Tables 3.21 and 3.22

show the predictions, as well as an average predictions of load both the tapered and non-

tapered head bolt based on the average predictions of the load in each of the connections.

**Table 3.19 – Values of β for Tapered vs. Non-Tapered Bolt Tests**

| | load (lbs) | beta |
|---|---|---|
| Tapered Bolts | 5000 | 0.86 |
| | 5000 | 0.88 |
| | 10000 | 0.81 |
| | 10000 | 0.76 |
| | 10000 | 0.83 |
| | average | 0.83 |
| Non-Tapered Bolts | 5000 | 0.84 |
| | 5000 | 0.81 |
| | 10000 | 0.78 |
| | average | 0.81 |

**Table 3.20 – Values of α for Tapered vs. Non-Tapered Head Bolt Tests**

| 5000 lbs | |
|---|---|
| | |
| bolt number | alpha |
| tapered bolt 1 | 0.0098 |
| tapered bolt 2 | 0.0067 |
| non-tapered bolt 1 | 0.0103 |
| non-tapered bolt 2 | 0.0057 |
| **avergage tapered** | 0.0083 |
| **average non** | 0.0080 |

| 10000 lbs. | |
|---|---|
| | |
| bolt number | alpha |
| tapered bolt 1 | 0.0407 |
| tapered bolt 2 | 0.0420 |
| tapered bolt 3 | 0.0388 |
| non-tapered bolt 1 | 0.0415 |
| **avergage tapered** | 0.0345 |

**Table 3.21 – Load Predictions for ¾" Tapered and Non-Tapered Head Bolt Tests**

**Loaded to 5,000 lbs.**

| Estimates of Load over time | | | | | | | |
|---|---|---|---|---|---|---|---|
| bolt number | 1month | 2 months | 3 months | 6 months | 1 year | 5 years | 10 years |
| tapered bolt 1 | 4168 | 4140 | 4123 | 4095 | 4068 | 4004 | 3977 |
| tapered bolt 2 | 4218 | 4198 | 4187 | 4167 | 4148 | 4104 | 4085 |
| non-tapered bolt 1 | 4039 | 4010 | 3994 | 3965 | 3937 | 3872 | 3845 |
| non-tapered bolt 2 | 3868 | 3853 | 3844 | 3829 | 3814 | 3779 | 3764 |
| | | | | | | | |
| average tapered | 4193 | 4169 | 4155 | 4131 | 4108 | 4054 | 4031 |
| | | | | | | | |
| average non-tapered | 3954 | 3932 | 3919 | 3897 | 3875 | 3826 | 3804 |

**Table 3.22 - Load Predictions for ¾" Tapered and Non-Tapered Head Bolt Tests**

**Loaded to 10,000 lbs.**

| bolt number | Load Estimates using Power Law Equations (lbs) |
|---|---|---|---|---|---|---|---|
| | 1month | 2 months | 3 months | 6 months | 1 year | 5 years | 10 years |
| tapered bolt 1 | 7086 | 6889 | 6776 | 6588 | 6405 | 5999 | 5832 |
| tapered bolt 2 | 6669 | 6477 | 6368 | 6185 | 6008 | 5615 | 5454 |
| tapered bolt 3 | 7181 | 6990 | 6881 | 6699 | 6521 | 6126 | 5964 |
| non-tapered bolt 1 | 6779 | 6587 | 6477 | 6293 | 6115 | 5719 | 5557 |
| | | | | | | | |
| averages of tapered | 6979 | 6786 | 6675 | 6491 | 6311 | 5913 | 5750 |

The results from Table 3.22 closely match the predictions made for the ¾" thick no reloading test loaded to 10,000 lbs. shown in Table 3.14.

## 3.8. Environmental Tests Results

A full set of environmental tests has not yet been conducted, though they have been started. This is due to a few factors. The initial proposed environmental tests involved running several of the tests at 150 °F and 90-95 % RH. It was determined, however, that these were not the best conditions to run the tests in, due to thermal expansion effects from both the composite and the aluminum. It would have been very hard to separate those thermal expansion effects from the creep and stress relaxation effect. Thus, late in the project, the testing was revised to the current proposed study given in the test matrix in Table 2.1 and the procedure given in section 2.5. It was felt that these conditions would best simulate both underwater applications and dry dock conditions.

Other factors delayed testing during the preconditioning of some of the samples. Several samples were to be preconditioned at approximately 150 °F and 90 % RH, prior to loading of the connections. These specimens need to be conditioned for at least 1 month, thus delaying testing for at least that one month time period.

The other major factor that delayed environmental testing was issues getting the two environmental chambers running at the same time, both of which are required to simulate the various desired environmental conditions. While specimens were being conditioned in the small Tenney Jr. chamber, the larger SS-Climate Lab was not yet ready for long-term operation. It has been only about 1 or 2 weeks since both chambers have been operational and ready to be used at the same time.

The first series of environmental tests have been started. The results after a five day period are presented in Figure 3.18. The temperature study, has not yet been started, since a temperature controlled room has not yet been set up to run the test in. Each bolt in this series of tests was initially loaded to 10,000 lbs. Specimen C1 will be held at 70 °F and 50 % RH. Specimen C2 was preconditioned at 150 °F and 90 % RH for 2-3 months and is now being submerged in water at 70 °F. Specimen C3 was preconditioned at 150 °F and 90 % RH for 2-3 months, and is now being held at 70 °F and 50 % RH. Specimen C4 was loaded and held at 70 °F and 50 % RH for one week, and will then be submerged in waster at 70 °F. Specimen C5 was submerged in water at 70 °F after loading, and will be cycled in and out of water at a one month interval.
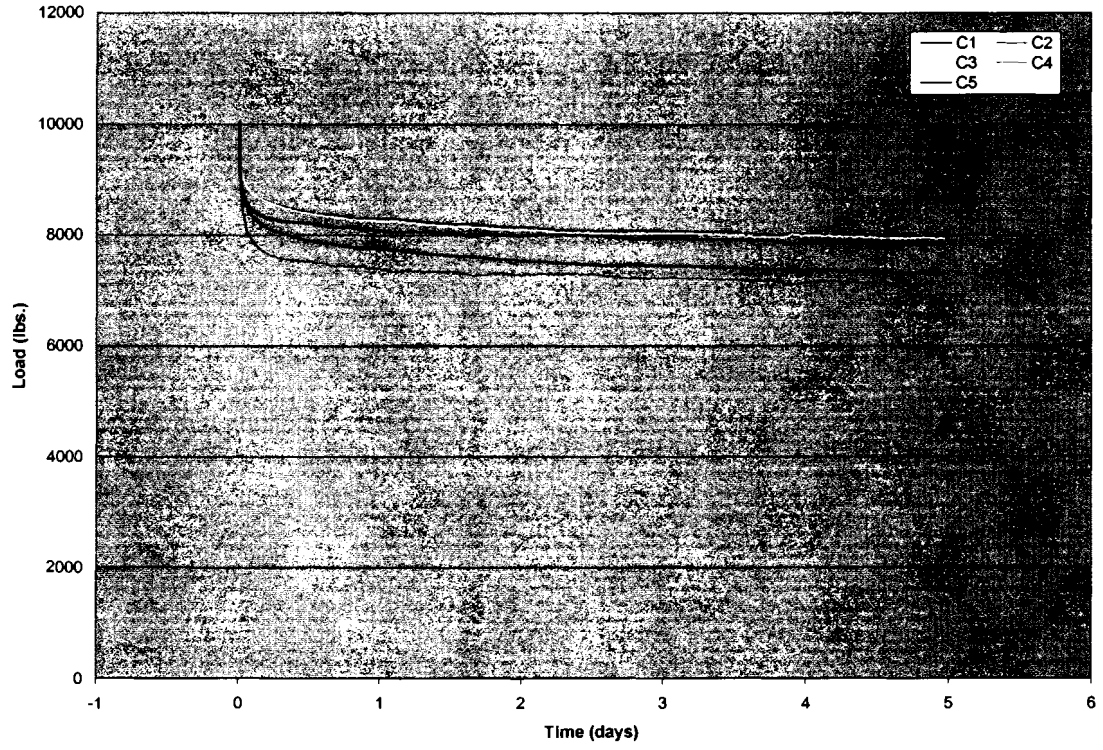
**Figure 3.18 - Initial 5 Day Environmental Test Results Loaded to 10,000 lbs.**

**Chapter 4**

## 4. SUMMARY, CONCLUSIONS, AND RECOMMENDATIONS

The load with respect to time in the transverse direction of the E-Glass/Vinylester

composite takes the form of the power law equation (), The constant, $\beta$, depends

primarily on the pressure distribution in the connection. If the composite is compressed

relatively uniformly, such as in the compression block tests, then this constant is roughly

equal to 0.95. In the bolted connects, $\beta$ is smaller due to the non-uniform stress

distribution, but can be increased if the connection is reloaded. Table 3.* shows values

for $\beta$ for various preloads, thicknesses, and loading cycles. This table shows that in

general, the connections that are reloaded more frequently have higher values of $\beta$. There

seems to be little effect on $\beta$ when using tapered bolts. Table 3.* shows that the average

value for $\beta$ in the non-tapered tests was 0.81, while the average value for tapered bolts

was 0.83. The difference is minor.

The constant $\alpha$ seems to be dependent on more factors than the stress distribution,

such as initial preload, specimen thickness, and material properties. The $\alpha$ values given

in Tables, 3.*, 3.*, and 3.* seem to vary a lot between one another, and even seem to be

dependent on temperature and temperature changes. In order to determine the

dependence of $\alpha$ on thickness, temperature variations, and initial preload, more testing

needs to be done, including tests at the same initial preload on different specimen

thicknesses, and tests at different preloads using the same specimen thickness.

Reloading the bolted hybrid connections in general seems to allow the connection to retain more of the initial preload. In particular, the connections reloaded multiple times retain more of their initial preload. There does seem to be a trade-off between reloading and temperature effects, however. It seems that the reloaded specimens are more sensitive to changes in temperature, even minor changes. In particular, temperature shifts that occur for extended time periods seem to have a greater effect on the rate of stress relaxation. Figures 3.4 and 3.6 show this effect. The temperature increases 5 to 10 degrees, and remains there for about 2 weeks, and then drops to the previous temperature. Once the temperature returns to its previous value, the rate of the stress relaxation seems to increase in the reloaded specimens, while having little effect on the specimens that were not reloaded. The other reloading tests also show temperature effects, but to a much smaller degree. Figure 3.3 shows the specimens being effected by temperature shifts as great as 20 degrees. The other tests shown in Chapter 3.2 shown a minor temperature shift for a period of roughly 5 days. This small shift for a relatively short time period does not seem to have a very large effect on the final results of these curves.

The tapered vs. non-tapered head bolt tests show very little advantage to using tapered bolts in the connections. The average calculated value of the constant $\beta$ for the tapered bolt connections is 0.83, vs. 0.81 for the non-tapered bolt connections. The individual calculations for $\beta$ vary around these averages, so there is some variations in those values. There also seems to be minor differences in the pressure distributions at the center of the tapered connections vs. those of the non-tapered head bolt connections, but they are also minor. More testing should be done between the two connections, but, from

the results obtain thus far, there seems to be no advantage to using tapered bolt connections over non-tapered head bolt connections.

Environmental testing of the connections has just been started, after the delays described in Section 3.8. The pilot tests have been inconclusive in determining any real environmental factors. Thermal expansion effects are indistinguishable from the stress relaxation effect, and some damage may have occurred to the gaged bolts. Prior to testing the three bolts used for the environmental testing had voltage offsets of -4.16, -3.28, and –8.28 millivolts. After testing, the three bolts had offsets of 23.02, 1.98, and 20.22 millivolts, respectively. The two sensors showing high voltage offsets need to be recalibrated before being used again. Once the current set of environmental tests are complete, it is recommended that multiple tests be performed at various load level. Testing should also be done using the different thicknesses of the composite.

It is not recommended at this time to use just bolted connections for the hybrid joints. As stated, current results seem promising that reloading the connections helps to maintain the initial preload, however, the temperature effects seem to cause an increase in the stress relaxation rate. From current results, this causes connections that were reloaded multiple times to lose initial preload at a greater rate after a temperature shift occurs. If the temperature can be held relatively constant, then the connections reloaded multiple time do seem to retain more of the initial preload, however. More testing should be completed to isolate this temperature effect from the reloading effects.

# REFERENCES

A.L. Design, Inc. – Designers and Manufactures of Custom and Standard Load Cells, A.L. Design, Inc., www.aldesigninc.com, copyright 1999-2002

ASTM Designation D 2990-01 [2001], "Standard Test Method for Tensile, Compressive, and Flexural Creep and Creep-Rupture of Plastics," Vol. 8.02, 202-221

ASTM Designation E 328-86 [1986], "Standard Test Method for Stress Relaxation for Materials and Structures," Vol. 3.01, 379-390

ASTM Designation F 1276-99 [1999], "Standard Test Method for Creep Relaxation of Laminated Composite Gasket materials," Vol. 9.02, 414-418

Chen, H. –S. and Kung H. K. [2002], "A Hygrothermal Sensitivity Evaluation on the Clamp Torque of Bolted Composite Joint," 17th Annual Technical Conference American Society for Composites, October 21-23, 2002

"Derakane Epoxy Vinyl Ester Resins," Form no. 125-00016-396X SMG, March 1996, The Dow Chemical Company, 16-17

Findley, W. N., James, L. S. and Onaran, K. [1976], Creep and Relaxation of Nonlinear Viscoelastic Materials, Dover Publications, Inc., New York

Guedes, R. M., Morais, J. J.L., Marques, A. T., and Cardon, A.H.[2000], "Prediction of Long-Term Behavior of Composite Materials, Computers and Structures, vol. 76, 183-194

Honeywell Home, Honeywell International Inc., www.honeywell.com, copyright 2003

Kim, K. T. and McMeeking R. M. [1994], "Power Law Creep with Interface Slip and Diffusion in a Composite Material," Mechanics of Materials, vol. 20, 153-164

Kim, W. and Sun C. T. [2002], "Modeling Relaxation of a Polymeric Composite During Loading and Unloading," Journal of Composite Materials, vol. 36, no. 06, 745-755

Maksimov, R. D. and Plume E. [2001], "Long-Term Creep of Hybrid Aramid/Glass-Fiber-Reinforced Plastics," Mechanics of Composite Materials, vol. 37, no. 4, 271-280

MatWeb – Online Material Data Sheet, Automation Creations, Inc., www.matweb.com, Copyright 1996-2003

National Semiconductor, The Sight and Sound of Information, National Semiconductor Corperation, www.national.com, copyright 2003

Pang, F. and Wang C. H. [1999], "Activation Theory for Creep of Woven Composites," Composites: Part B, vol. 30, 613-620

Raghavan, J. and Meshii M. [1997], "Creep of Polymer Composites," Composites Science and Technology, vol. 57, 1673-1688

Scott, D. W. and Zureick A. [1998], "Compression Creep of a Pultruded E-Glass/Vinylester Composite," Composites Science and Technology, vol. 57, 1361-1369

Shen, W., Smith, S. M., Ye, H., Jones, F., and Jacobs, P. B. [1998], "Real Time Observation of Viscoelastic Creep of a Polymer Coating by Scanning Probe Microscope," Tribology Letters, vol. 5, 75-79

Weerth, D. E. and C. R. Ortloff [1986], "Creep Considerations in Reinforced Plastic Laminate Bolted Connections," Army Symposium on Solid Mechanics - Lightening the Force, Oct 1986, 137-154

## Appendix A.  Material Properties of the E-Glass/Vinylester Composite

Tension (ASTM 3094) and compression (ASTM 3410) tests were performed on ½"

thick specimens cut from the E-Glass/Vinylester composite used the stress relaxation

studies.  Table A.1 gives the material properties found from this testing.  Fiber volume

(burn-off) tests were performed on the specific panels used in the stress relaxation tests.

The fiber volumes are listed in Table A.2 for each panel.  Panels 21 and 22 were used in

the pilot tests.  In addition, panel 21 was also used in the compression block tests shown

in Figures 3.1 and 3.2, as well as the reloading tests shown in Figures 3.4 and 3.5, while

panel 22 was also used for the tapered vs. non-tapered head bolt tests shown in Figure

3.10.  Panel 54 was used in the reloading tests shown in Figure 3.3, while panel 45 is

being used for the environmental tests.  Panel 24 was used for the reloading tests shown

in Figure 3.6, while panel 34 was used for the reloading tests shown in Figure 3.7, and

the tapered vs. non-tapered tests shown in Figure 3.11.  Finally, panel 36 was used for the

reloading tests shown in Figure 3.8, while panel 44 was used for the tests shown in Figure

3.9.

### Table A.1 – Tensile and Compressive Properties of the E-Glass/Vinylester Composite

| | |
|---|---|
| Tensile Strength | 39,000 psi |
| Tensile Modulus | 2.0 Msi |
| Compressive Strength | 40,250 psi |
| Compressive Modulus | 2.7 Msi |

**Table A.2 – Fiber Volume Percents in Each Panel Used During Testing**

| Panel # | panel thickness | Fiber Volume (%) |
|---------|-----------------|------------------|
| 21 | 1/2" | 51.4 |
| 54 | | not yet tested |
| | | |
| 22 | 3/4" | 53 |
| 34 | | 50 |
| 45 | | not yet tested |
| 24 | 7/8" | 46.9 |
| | | |
| 36 | 1" | 52.1 |
| 44 | | 47.6 |

# Appendix B. Addition Pressure Distribution Scans

Additional pressure distributions were scanned and are included in this appendix. Figure B.1 shows two additional pressure distributions from the ½" thick reloading specimens loaded to 5,000 lbs. The pressure distributions shown in Figure B.2 are from two ¾" thick reloading test specimens loaded to 10,000 lbs. Finally, Figure B.3 show two additional pressure distributions from the tapered head bolt test specimens loaded to 10,000 lbs.
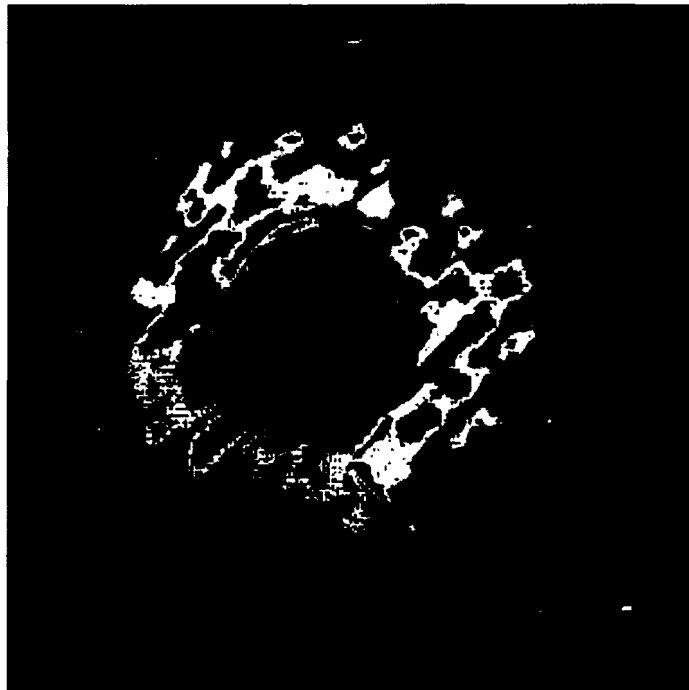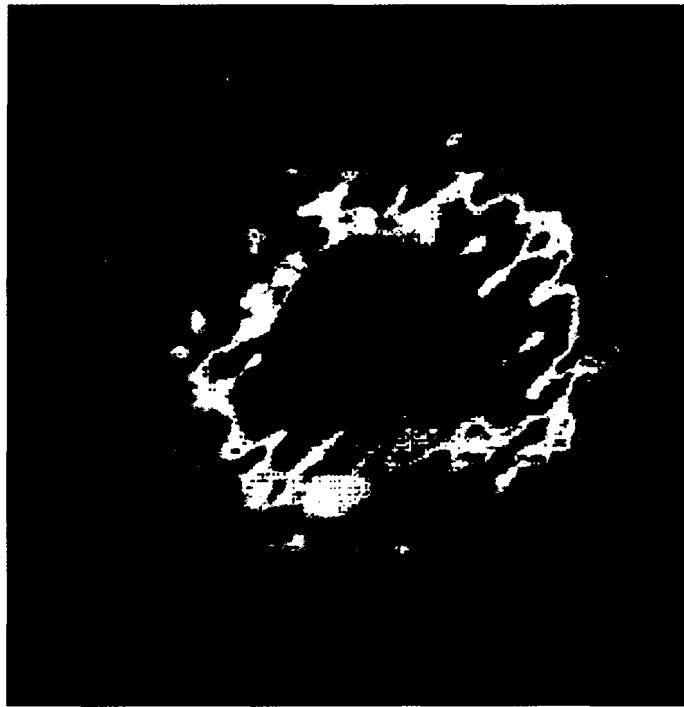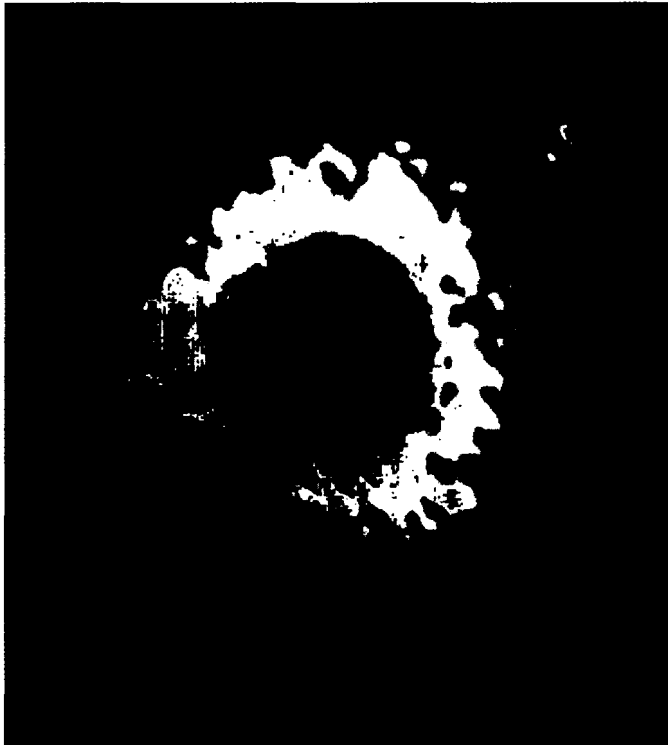
**Figure B.1 – Two Additional Pressure Distributions from ½" Thick Specimens Loaded to 5,000 lbs.**

**Figure B.2 – Two Additional Pressure Distributions from ¾" Thick Specimens**
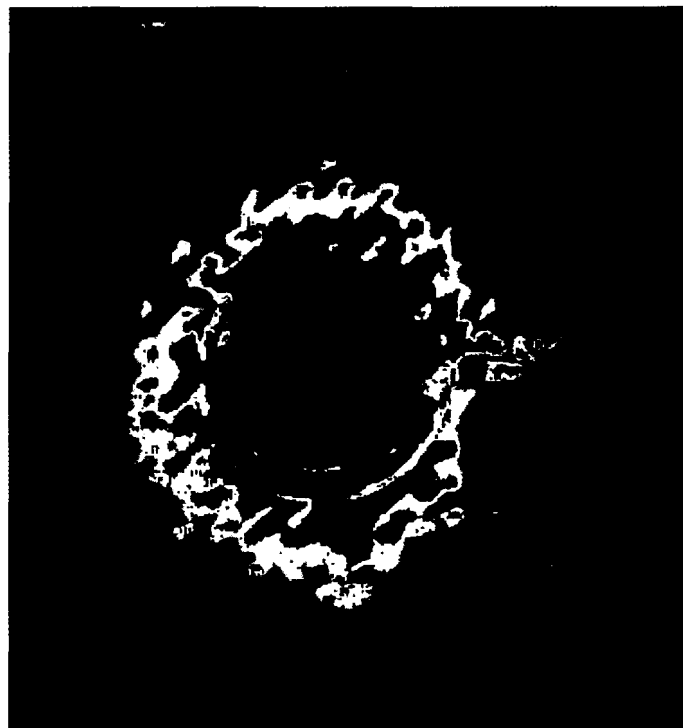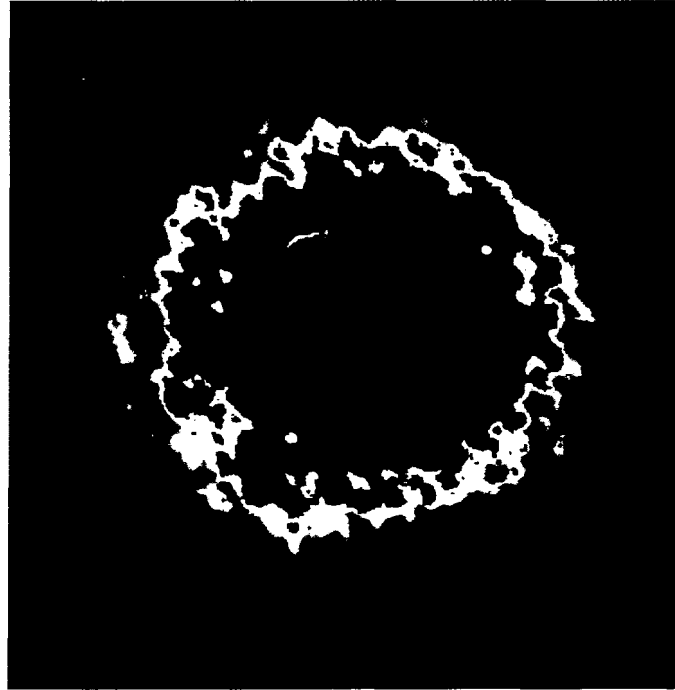
**Loaded to 10,000 lbs.**

**Figure B.3 – Two Additional Pressure Distributions from Tapered Head Bolt Tests**

**Loaded to 10,000 lbs.**

# Appendix C. Single Bolt Aluminum Tests

During testing, a few aluminum specimens were tested with no composite to examine whether there was any relaxation occurring in the bolt sensor. Figures C.1, C.2, and C.3 show the three bolted aluminum tests that have been run. Two bolt sizes were used, ½" and 1". For the ½" diameter bolt, a ½" by 5" by 5" specimen was used, while for the 1" diameter bolt, a 1" by 10" by 10" specimen was used. Figures C.1 and C.2 used the same bolt and the same piece of aluminum during two separate time periods. These show no relaxation in the sensors, but they do show possible drift in the sensors.

Using a statically indeterminent model based on thermal expansion for the tests in Figures C.1 and C.3, load changes based on a few of the temperature changes were calculated. These are shown in Table C.1, along with actual load changes. The actual changes from Figure C.3 vary slightly from theoretical most likely due to the simplified model used and drift in the sensor. A variation of a couple hundred pounds isn't uncommon when the 1" bolts are loaded to 15,000 lbs.

The first load change in Figure C.1 actually matches closely to the theoretical value. The second load change doesn't compare as well, however. The load goes up by about 400 pounds, but does not drop when the temperature does. This could very well indicate a sensor issue with that specific load bolt that carried over into the test shown in Figure C.2. No calculations were done on the test shown in Figure C.2, since it is apparent based on previous calculations that the load increase is not due to thermal expansion of the system. It is most likely due to a problem that occurred with that sensor. A sample calculation is shown on page 108.
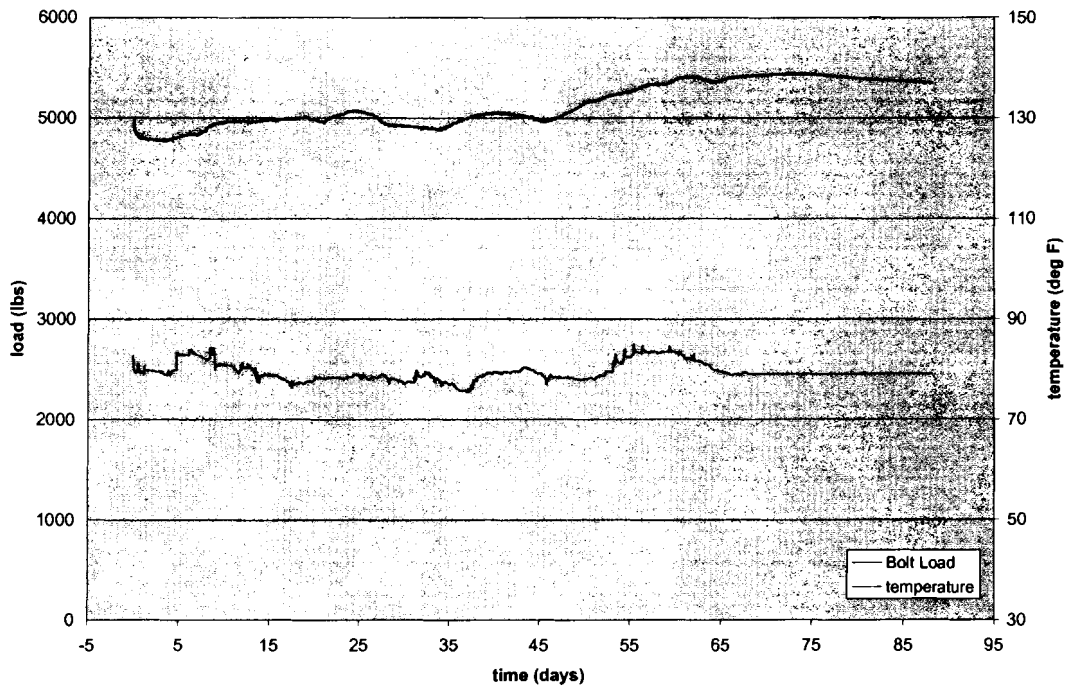
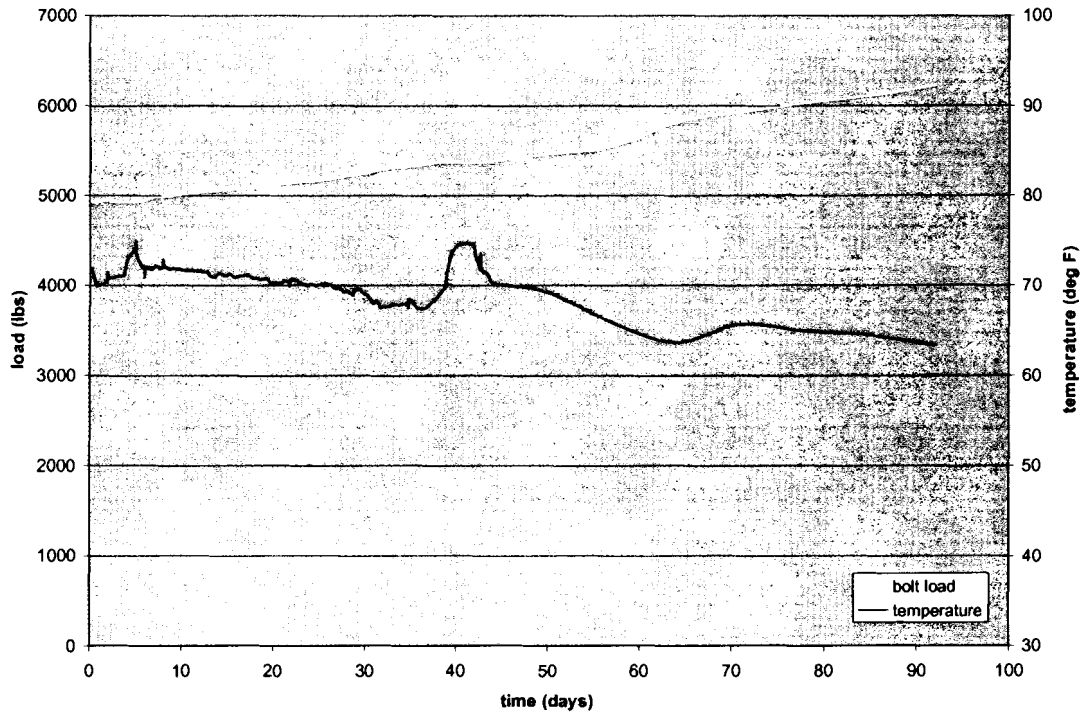**Figure C.1 - ½" Bolted Aluminum Specimen Test 1**



**Figure C.2 – ½" Bolted Aluminum Specimen Test 2**
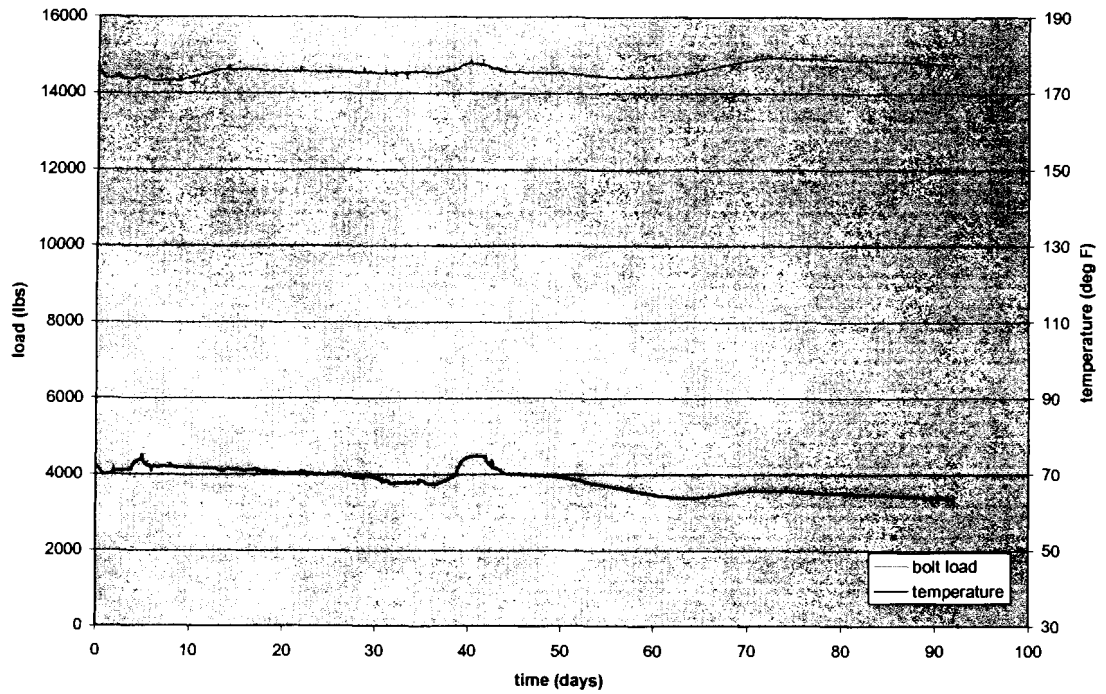
106

**Figure C.3 –1" Bolted Aluminum Specimen Test**

**Table C.1 – Theoretical vs. Experimental Load Changes Due to Thermal Expansion**

| Aluminum Test Specimen | Time Period Of Temperature Change | Temperature Change (deg F) | Theoretical Load Change (lbs) | Experimental Load Change |
|---|---|---|---|---|
| Figure C.1 | day 38 to 44 | 4 | 102 | 130 |
| | day 51 to 58 | 5.3 | 135 | 410 |
| Figure C.3 | day 37 to 41 | 6.7 | 683 | 300 |
| | day 60 to 70 | 2 | 204 | 500 |

## Statically Indeterminate System

### Known Values:

$$E_{bolt} := 30 \cdot 10^6 \qquad E_{aluminum} := 10 \cdot 10^6$$

$$\alpha_{bolt} := 6.5 \cdot 10^{-6} \qquad \alpha_{aluminum} := 12.8 \cdot 10^{-6}$$

$$D_{bolt} := .5 \qquad ID_{washer} := .5 \qquad OD_{washer} := 1.375 \qquad delT := 5.$$

### Cross-sectional Areas:

$$A_{aluminum} := \frac{\pi}{4} \cdot \left(1.375^2 - .5^2\right) \qquad A_{bolt} := \frac{\pi}{4} \cdot \left(.5^2\right)$$

$$A_{aluminum} = 1.289 \qquad A_{bolt} = 0.196$$

### Load Increase or Decrease Due to Temperature:

$$F_{washer} = F_{bolt} = F$$

$$F \cdot \left( \frac{1}{A_{bolt} \cdot E_{bolt}} + \frac{1}{A_{aluminum} \cdot E_{aluminum}} \right) = \left( \alpha_{aluminum} - \alpha_{bolt} \right) \cdot delT$$

$$F := \frac{\left( \alpha_{aluminum} - \alpha_{bolt} \right) \cdot delT}{\left( \dfrac{1}{A_{bolt} \cdot E_{bolt}} + \dfrac{1}{A_{aluminum} \cdot E_{aluminum}} \right)}$$

$$F = 134.979$$

# BIOGRAPHY OF THE AUTHOR

Keith Pelletier was born in Augusta, Maine on March 14, 1976. He was raised in Sidney, Maine, and graduated from Messalonskee High School in Oakland, Maine in 1994. He attended the University of Maine, and graduated in 1998 with a Bachelor's Degree in Engineering Physics, with a minor in Mathematics. He returned to The University of Maine in the fall of 2000 and entered the Mechanical Engineering graduate program. Keith is a candidate for the Master of Science degree in Mechanical Engineering from The University of Maine in December 2003.